DETERMINATION OF THE KINETIC ROLES OF THE MEMBRANE IN THE CATALYSIS OF RASGEFS BY USING AN ENGINEERED MODEL PROTEIN

By

Hanh My Hoang

DISSERTATION

Submitted to the Faculty of the Graduate School of The University of Texas at Arlington

in partial fulfillment of the requirements for the degree of

DOCTOR OF PHILOSOPHY

THE UNIVERSITY OF TEXAS AT ARLINGTON

August 2021

Supervising Committee:

Dr. Jongyun Heo, Supervising Professor

Dr. Subhrangsu S. Mandal

Dr. He Dong

Dr. Frank W. Foss

ACKNOWLEDGMENTS

First, I would like to thank my supervising professor, Dr. Jongyun Heo for unendingly supporting my research. I am grateful for his patience to correct my writing. I appreciate all the knowledge in enzyme kinetics and lab skills he has imparted to me. I thank Dr. Heo for helping me become a creative and independent person in the lab. I've been honored to have the opportunity to work with him during my Ph.D. program.

I would like to extend my sincere appreciation to thank my committee members, Dr. Subhrangsu S. Mandal, Dr. He Dong, and Dr. Frank W. Foss for providing me valuable feedbacks that help me understand the weaknesses in my research study. Furthermore, I thank Dr. Mandal for trusting and granting me access to his lab to use important lab instruments.

Next, I would like to thank the staff members in the department of Chemistry and Biochemistry – Jill Howard and Debbie Cooke for guiding me to complete department's duties, Dr. Roy McDougald for training me how to use lab instruments and quickly troubleshooting machinery problems, and Natalie Croy and Elizabeth Klimek for helping me placing orders for the lab.

I am truly fortunate to have had amazing colleagues – Dr. Michael Wey, Dr. Hope Umutesi, Dr. Monira Obaid, and Hope Johnson – for their support, feedback, and friendship.

Last, I would like to say a big thank to my amazing parents and sister for encouraging me to pursue my dream.

LIST OF FIGURES

LIST OF TABLES

LIST OF ABBREVIATIONS

1-palmitoyl-2-arachidonoyl-sn-phosphatidylcholine .....PAPC

1-Palmitoyl-2-pyrenedecanoyl Phosphatidylcholine 10-Pyrene-PC

2'-(or-3')-O-(N-Methylanthraniloyl) Guanosine 5'-Diphosphate ..... mant-GDP

2-nitro-5-thiobenzoic acid .....TNB^-

3- phosphoinositide-dependent protein kinase-1 .....PDK1

5,5'-dithiobis(2-nitrobenzoic acid) .....DTNB

Adipose-PLA_2 .....$AdPLA_2$

Calcium-independent PLA_2 ..... $iPLA_2$

Catalytic domain REM-Cdc25 of RasGRP1 .....$RasGRP1^{cat}$

Catalytic turnover rate ..... k_{cat}

Catechol-O-methyltransferase .....COMT

Cell division cycle 25 .....Cdc25

Coiled coil motif CC

CTP:phosphocholine cytidylyltransferase ..... CT

Cytochrome P450 .....CYP

Cytosolic PLA_2 ..... $cPLA_2$

Dbl homology ..... DH

Diacylglycerol-binding domain C1

Diacylglycerols .....DAGs

Dissociation constant ..... K_D

EF hands .....EF

Elongation factor Tu ..... EF-Tu

Emission wavelength ..... λ_{em}

Endoplasmic reticulum ..... ER

Eps homology ..... EH

Excitation wavelength ..... λ_{ex}

Extracellular signal-regulated kinase ..... ERK

G protein-coupled receptors ..... GPCRs

Growth factor receptor-bound protein 2 ..... Grb2

GTP hydrolases ..... G proteins

GTPase activating proteins ..... GAPs

Guanine nucleotide exchange factors ..... GEFs

Guanine nucleotide-binding domain ..... G domain

Harvey Ras ..... HRas

Histone-like domain ..... H

Hypervariable ..... HVR

Ilimaquinone motif ..... IQ

Initial rate ..... v_0

Isopropyl-β-D-thiogalactopyranoside ..... IPTG

Kirsten Ras ..... KRas

Linker for activation of T Cells ..... LAT

Lipid binding domain C2

Lysogeny broth ..... LB

Lysosomal PLA_2 ..... $LPLA_2$

Maltose-binding protein ..... MBP

Mammalian target of rapamycin ..... mTOR

MAPK/ERK kinase ..... MEK

Maximal reaction velocity ..... V_{max}

Mechanistic target of rapamycin complex 2 ..... mTORC2

Membrane-bound COMT ..... MB-COMT

Michaelis constant ..... K_m

Mitogen-activated protein kinase ..... MAPK

Neuroblastoma Ras ..... NRas

Non-reduced ..... NR

Optical density at 600 nm ..... OD_{600}

Partner of RalBP1 ..... POB1

Phosphatidic acid ..... PA

Phosphatidyl inositol-dependent kinase 1 ..... PDK1

Phosphatidylcholine ..... PC

Phosphatidylethanolamine ..... PE

Phosphatidylglycerol ..... PG

Phosphatidylinositol ..... PI

Phosphatidylinositol 3-kinase PI3K

Phosphatidylserine ..... PS

Phosphoinositide (3,4,5) trisphosphate ..... PIP_3

Phosphoinositide (4,5) bisphosphate ..... PIP_2

Phospholipase A_2 ..... PLA_2

Phospholipase C ..... PLC

Phospholipase Cγ ..... PLC-γ

Platelet-activating factor acetylhydrolase ..... PAF-AH

Pleckstrin homology ..... PH

Proliferating cell nuclear antigen ..... PCNA

Proline-rich ..... PR

Protein Data Bank ..... PDB

Protein kinase B ..... AKT

Protein kinase B ..... PKB

Protein kinase C ..... PKC

Ral binding protein 1 ..... RalBP1

Ral guanine nucleotide dissociation stimulator ..... RalGDS

RalBP1- associated EH domain protein 1 ..... Reps1

Rapidly Accelerated Fibrosarcoma ..... Raf

Ras association domain family member ..... RASSF

Ras Association ..... RA

Ras exchange motif – Cdc25 homology domain REM-Cdc25

Ras exchanger motif ..... REM

Ras Guanine Exchange factors ..... RasGEFs

Ras Guanine Nucleotide Releasing Factor ..... RasGRF

Ras Guanine Nucleotide Releasing Protein ..... RasGRP

Ras-like ..... Ral

Receptor tyrosine kinase ..... RTK

Reduced ..... R

Relative catalytic efficiency ..... k_{cat}/K_m

Rhodamine B ..... RB

Rod outer segments ..... ROS

S-adenosyl methionine ..... ADOMET

S-adenosylmethionine ..... SAM

Secreted PLA_2 ..... $sPLA_2$

Small monomeric G proteins ..... Small GTPases

Soluble COMT ..... S-COMT

Son of Sevenless ..... SOS

Sphingomyelin ..... SM

Substrate binding rate constant ..... k_1

Substrate dissociation rate constant ..... k_{-1}

Wild type ..... wt

α subunits ..... G_α

ABSTRACT

Hanh My Hoang, Ph.D.

The University of Texas at Arlington, 2021

Supervising Professor: Dr. Jongyun Heo

Ras guanine nucleotide exchange factors (RasGEFs), which include Son of Sevenless (SOS), Ras Guanine Nucleotide Releasing Protein (RasGRP), and Ras Guanine Nucleotide Releasing Factor (RasGRF), catalyze nucleotide exchange of Ras upon activating signals. Crystal structure analyses suggest that catalytic cavities of RasGEFs are not deep enough to uphold their substrates. Given that RasGEFs are all membrane binding proteins, a novel “membrane supplement hypothesis” is proposed that RasGEFs in cytoplasm are catalytically unformed; and RasGEFs on membrane are catalytically competent. The reason RasGEFs are catalytically unformed without the support of membrane is because the catalytic sites of RasGEFs are not sufficiently deep to hold their substrates within their catalytic sites for their catalysis. It was shown that the catalytic function of SOS, one of RasGEFs, is enhanced upon its binding to membrane, supporting this membrane supplement hypothesis.

To examine the membrane supplement hypothesis, an engineered RasGRP is designed, in which a catalytically unformed RasGRP is fused with a foreign protein that mimics the plasma membrane. Comparative kinetic analyses of the catalytically unformed RasGRP with the engineered RasGRP showed that the fused-foreign protein of engineered RasGRP functioned to hold and precisely orientate the substrate Ras

within the catalytic site of engineered RasGRP, thereby making the engineered RasGRP become catalytically efficient.

RasGEFs are classified as amphitropic enzymes, which adapt a compact conformation in the cytosol and are fully activated when recruited to membrane. The catalytic sites of many amphitropic proteins, including RasGEFs, are brought proximally toward the membrane interface after membrane binding event, and furthermore, the catalysis of these amphitropic enzymes is enhanced upon their membrane binding. However, the role of the membrane in the kinetic action of these amphitropic enzymes has not been previously proposed. The membrane supplement hypothesis in this study provides a rationalization that these amphitropic enzymes also possess a shallow pocket at their catalytic sites, challenging them to hold the bulky substrates. Therefore, locating the catalytic site of these amphitropic enzymes close to the membrane interface strengthens their substrate binding interactions, thereby facilitating their catalytic functions.

TABLE OF CONTENTS

CHAPTER 1

FUNCTION AND REGULATION OF RAS SUBFAMILY PROTEINS

Introduction

Superfamily of regulatory GTP hydrolases (G proteins) functions as cellular switches that alternate between a GDP-bound off state and a GTP-bound on state to regulate the cell signaling pathways.[1-2] G proteins are classified into three groups: G proteins involved in protein synthesis, such as elongation factor Tu (EF-Tu); the α subunits (G_α) of heterotrimeric G proteins; and small monomeric G proteins (small GTPases).[2-3] The recognition site for guanine nucleotides is conserved in G protein superfamily.[3] GTP-bound form of EF-Tu plays important role in recognizing, binding, and delivering aminoacyl-tRNA to the ribosome.[4] The G_α of heterotrimeric G proteins are activated by the G protein-coupled receptors (GPCRs). Binding of hormone to GPCRs stimulates the exchange of GTP for GDP on G_α.[3-4] When bound to GTP, G_α can initiate many cellular processes including activation of phospholipases C and A_2; transmembrane channels for K^+, Na^+, and Ca^{2+}; adenyl cyclase; and cyclic GMP phosphodiesterase.[3-4]

Small GTPases play important roles in cell growth, divisions, and proliferation in higher organisms.[4] They are classified into five principal subfamilies: Ras, Rho, Rab, Arf, and Ran families.[5] Various functions of small GTPases in cellular processes are known, for example, Ras and Rho subfamilies regulate gene expression, Rho subfamily modulates cytoskeletal reorganization, Rab and Arf subfamilies check intracellular vesicle trafficking, and Ran subfamily regulates nucleocytoplasmic transport and microtubule organization of the cell cycle.[6]

G proteins play key roles in many hormonal and transducing processes by carrying signals from cell-surface receptors to intracellular effector proteins.[7] G proteins

are synthesized in the cytosol on free polysomes.[8] To transduce signals, G proteins must associate with the cytoplasmic face of the plasma membrane.[9] Membrane receptors are integral membrane glycoproteins which induce conformational change through an external signal.[10] The activated receptors trigger the activation of G proteins by recruiting them to the cytosolic face of the plasma membrane.[8] However, mechanism for the membrane-binding effect on G protein activation is still unclear. This chapter will mainly focus on the role of membrane interactions in the activation of Ras subfamily, one of the most widely studied small GTPases.

Ras subfamily

Classification

The Ras subfamily consists of more than 39 protein members.[11] Of these, Harvey Ras (HRas), Kirsten Ras (KRas) and Neuroblastoma Ras (NRas) are the most characterized members which play essential roles in the regulation of important cellular functions.[11] H-Ras and N-Ras contain 189 amino acids, whereas K-Ras contains 188 amino acids. The three members are > 90% identical in the first 165 amino acids (Figure 1.1).[12] The diversity of Ras isoforms comes from the C-terminal 24 amino acids where the sequence identity is less than 15%.[13-14] Although the Ras isoforms show high degree of sequence homology, they mostly differ in their post-translational modifications, subcellular localization, and involvement in diseases.[15]

Structure

Structure of Ras subfamily can be divided into three domains: N-terminal Guanine nucleotide-binding domain (G domain), hypervariable region (HVR) domain, and C-terminal anchor region.[13] G domain (residues 1-165), the core of all G proteins,

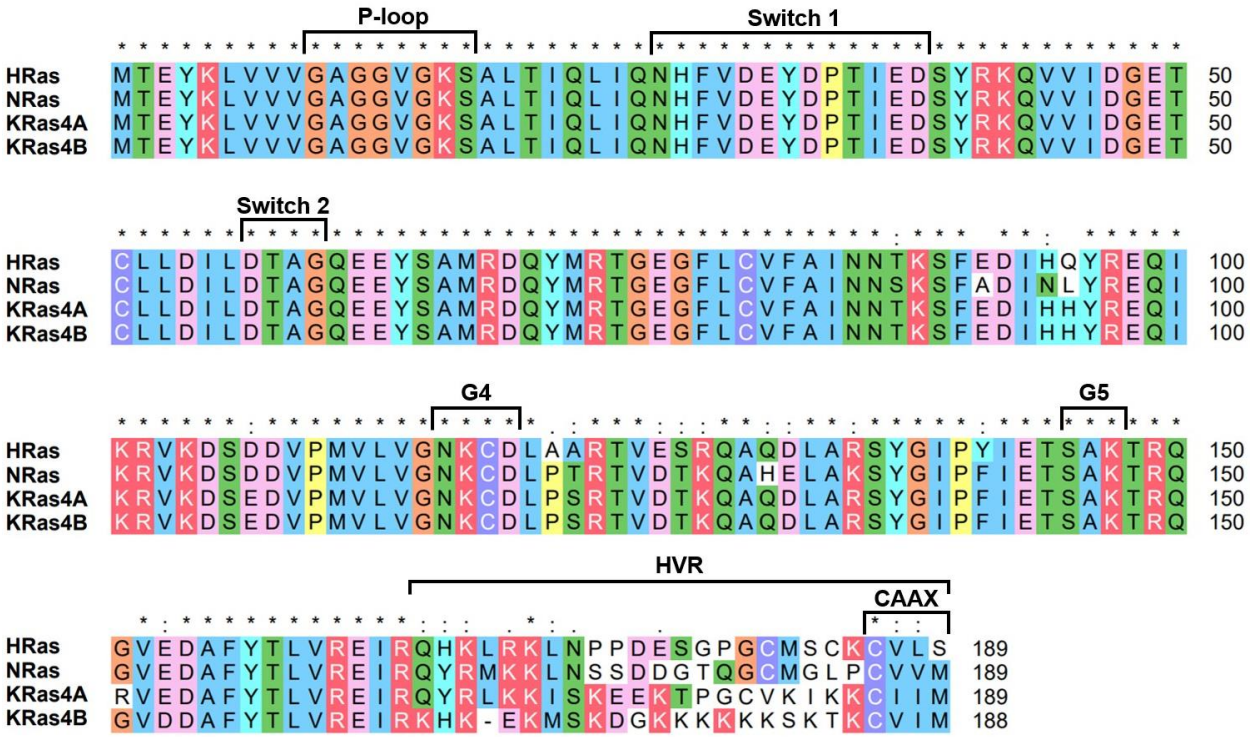

Figure 1.1. Protein sequence alignment of Ras isoforms.

Ras subfamily consists of three domains: G domain (residues 1-165), hypervariable region (HVR) domain (residues 166-189), and C-terminal CAAX region. The first 165 amino acids in G domain of Ras isoforms are > 90% identical. The diversity of Ras isoforms comes from the C-terminal HVR domain where the sequence identity is less than 15%. The CAAX sequence directs the post-translational modification required for Ras activation and signaling. The NCBI Reference Sequence numbers of HRas, NRas, KRas4A, and KRas4B are, respectively, NP_005334.1, NP_002515.1, NP_001356716.1, and NP_203524.1. The figure was created using ClustalW and BioEdit.

contains a central six-stranded β-sheet surrounded by five α-helices.[3, 8] These β-strands and α-helices are connected by 10 polypeptide loops. Five of these loops (named G1 through G5) are directly involved in the binding of guanine nucleotide. The β1 strand and the α1 helix are connected by G1 (residues 10-17), which contains the consensus sequence GXXXXGK(S/T), also known as P-loop or Walker A motif.[3] P-loop wraps around and interacts with the β- and γ-phosphates of the guanine nucleotide.[16] In addition, the hydroxyl group of the serine or threonine interacts with the magnesium ion.[16] The α1 helix and the β2 strand are connected by G2 (residues 26-38) which contains a conserved threonine residue involving in Mg^{2+} coordination and sensing the presence of γ-phosphate of the guanine nucleotide.[3, 16] Besides, the purine ring of guanine nucleotide is stabilized by the support of phenylalanine residue on G2 region.[3, 17] G3 sequence (residues 57-60) with a DXXG motif, also known Walker B motif, locates between the α2 helix and the β3 strand, and involves in the binding of Mg^{2+} and the γ-phosphate of the guanine nucleotide.[3, 16] The conserved NKXD sequence of G4 (residues 116-119), which links the β5 strand and the α4 helix, recognizes the guanine base.[3] The asparagine and aspartate of G4 form hydrogen bonds with nitrogen and oxygen atoms of the purine.[16] The amino group of lysine also forms part of binding pocket of the guanine base by interacting with the oxygen of the ribose ring.[16] G5 sequence (residues 145-147), which locates between the β6 strand and the α5 helix contains the weakly conserved SAK motif.[3] The main chain NH of alanine binds to the oxygen of the purine, and the serine side chain helps to stabilize the aspartate of the adjacent loop G4.[16, 18] The G2 and G3 regions (switch I and switch II, respectively) change conformation upon the GTP- and GDP-bound states of Ras (Figure 1.2).[19]

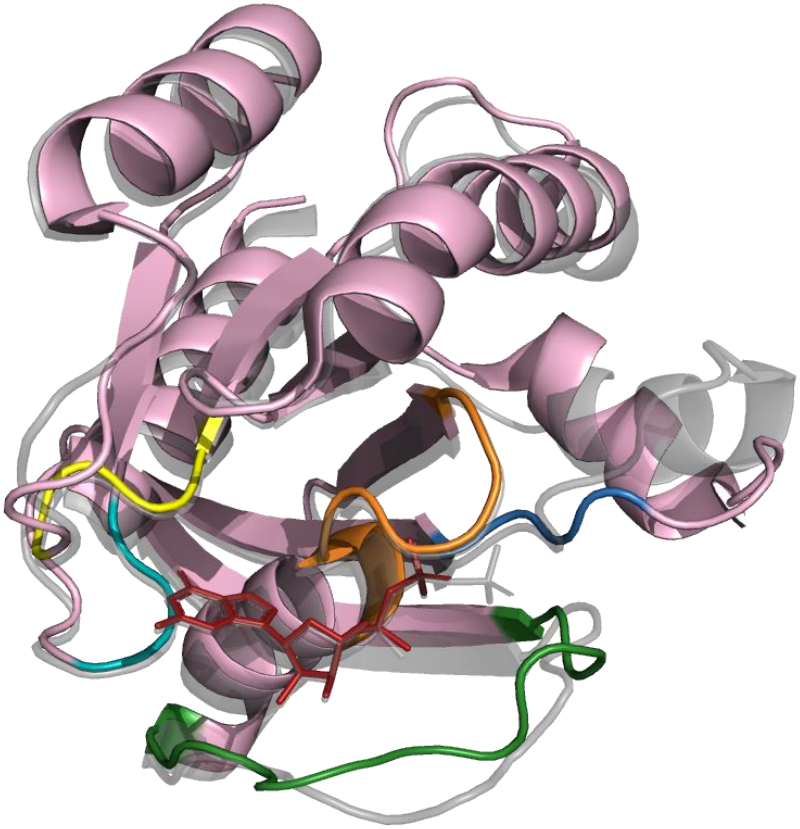

Figure 1.2. Superimposition of GDP- and GTP-bound HRas structure.

GDP-bound HRas structure (PDB 2CE2) is shown in pink. The P-loop, switch 1, switch 2, G4, and G5 regions of GDP-bound HRas are, respectively, indicated in orange, green, blue, yellow, and cyan. GTP-bound HRas structure (PDB 2CL7) is highlighted in gray. Switches I and II change their conformation upon the binding of guanine nucleotide GTP- and GDP to Ras. The image was created using PyMOL. Side chains of important residues that are involved in the guanine nucleotide binding are shown in Figure A-1.

When the γ-phosphate of the guanine nucleotide is cleaved off, the switch regions become mobile since the interactions of the γ-phosphate with the side chain hydroxyl group of threonine in switch I and the main chain nitrogen of glycine in switch II are lost.[20]

The HVR domain contains 24 amino acids which undergo direct post-translational modification.[21] Ras isoforms are not intrinsic membrane proteins because they lack signal sequences and hydrophobic trans-membrane regions.[22] Ras isoforms are originally synthesized in the cytosol on free polysomes and then targeted to cellular membranes as the consequence of post-translational modification.[23] Therefore, this 24 amino acid sequence plays essential role in in anchoring Ras to the plasma membrane and trafficking of newly synthesized and processed Ras from endoplasmic reticulum (ER) to the inner surface of the plasma membrane.[13]

The C-terminal anchor region contains CAAX motif, where C is cysteine, but not always, an aliphatic amino acid and X is any amino acid.[24] The CAAX sequence directs the post-translational modification required for Ras activation and signaling.[25] Modification process begins with the attachment a farnesyl extension through stable thioether linkage to the cysteine by protein farnesyltransferase.[14] The final three amino acids AAX are then cleaved by the endoprotease at in the endoplasmic reticulum. This is followed by S-adenosylmethionine (SAM)-dependent methylation of the COOH terminus by isoprenylcysteine carboxylmethyltransferase.[26] After transferring to Golgi membrane, HRas, NRas and KRas4A are further modified on other cysteine residues near the C-terminus by adding one or two palmitic acids upstream of the site of farnesylation.[13] The fully lipidated HRas, NRas and KRas4A then direct to the plasma

membrane via conventional vesicle transport.[27] Other Ras isoform, KRas4B, possesses a polybasic region (KKKKKKKSKTK) (Figure 1.1) which is believed to interact with the negatively charged head groups of membrane.[28] After K-Ras4B is released from the endoplasmic reticulum, it binds the the membrane surface through electrostatic interactions.[29]

Regulation

Multiple hydrogen bond interactions between Ras and guanine nucleotides in complex with Mg^{2+} (e.g., Mg^{2+}•GDP and Mg^{2+}•GTP) predominantly contribute to high affinity of Ras with Mg^{2+}•GDP or Mg^{2+}•GTP.[17] In addition to the high affinity of Ras with Mg^{2+}•GDP or Mg^{2+}•GTP, Ras also possesses slow intrinsic guanine nucleotide exchange and GTPase activity.[30-31] The dissociation rates are on the order of 10^{-4} and 10^{-5} s^{-1} for GDP and GTP, respectively, in the presence of Mg^{2+}.[3] These very slow reactions require catalysis by guanine nucleotide exchange factors (GEFs) and GTPase activating proteins (GAPs) which are controlled by upstream signals (Figure 1.3).[3]

In the presence of GEF, the nucleotide release is promoted by sterically displacing the magnesium ion and weakening the nucleotide-biding site that facilitates the release of bound nucleotide and then promotes the binding of a new nucleotide in solution.[32] GEF first perturbs switch I of nucleotide-binding site by steric hindrance. Second, GEF remodels switch II which in turn inserts alanine near the Mg^{2+}-binding site and orients glutamate to form stable salt bridge with lysine (P-loop).[33] The remodeling of switch II competes with the Mg^{2+}•GDP interaction, thereby enhancing the release of Mg^{2+}•GDP from Ras.[17] Ras does not distinguish between GDP and GTP, the result of nucleotide exchange thus depends on the availability of GDP and GTP.[34] In most cases,

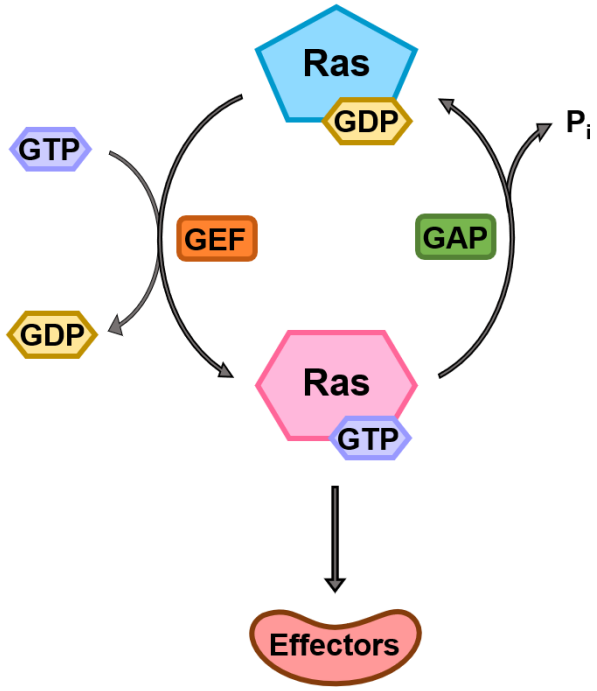

Figure 1.3. Ras activation cycle.

Ras has two interconvertible conformations: inactive GDP-bound and active GTP-bound form. Ras activation occurs through an intrinsic dissociation of the Ras-bound GDP followed by association of GTP to produce GTP-bound Ras. Ras inactivation occurs through an intrinsic hydrolysis of the Ras-bound GTP to produce a Ras-bound GDP and free P_i. However, the rates of these intrinsic processes are too slow to account for the activation and inactivation of Ras in biological processes. These reactions are therefore enhanced by regulator proteins GEFs and GAPs. GEFs promote dissociation of the bound GDP that allows association of free GTP to produce GTP-bound GTPase, whereas GAPs facilitate the hydrolysis of the bound GTP to produce GDP and P_i. Ras in the active GTP-bound state can interact with downstream effectors including Rapidly Accelerated Fibrosarcoma (Raf), Phosphatidylinositol 3-kinase (PI3K), Ral guanine nucleotide dissociation stimulator (RalGDS), and Ras association domain family member RASSF) (see Figure 1.4).

the active state Ras-GTP will be formed because the GTP level is 10-50 folds higher than GDP level in cells.[35] GTP hydrolysis requiring the action of GAP is critical for inactivation from Ras-GTP to Ras-GDP. GAP first interacts with Ras residues Tyr32, Pro34, and Ile36 in the switch I region that overlap with the Ras effector-binding region.[17] GAP-catalyzed GTP hydrolysis begins with the interaction of Glu61 in Ras and arginine finger (FLR motif) of GAP.[36] The oxygen of the carbonyl group in the backbone of the arginine interacts with water molecule in the active site thus creating a bridge between the amine group of Ras Glu61 and the γ-phosphate of the guanine nucleotide.[17, 37] Thus, the arginine finger in GAP plays crucial role in generating the nucleophile as well as stabilizing the transition state of the GTPase hydrolysis reaction.[37] The structural modification of Ras associated to the binding of GDP decreases affinity of GAP to Ras and cause switch I of Ras to become inaccessible to Ras downstream effectors, thus leading to an inactive conformation state.[33, 38]

Downstream effectors

Signal transduction of Ras subfamily proteins is maintained by the association of Ras with downstream effectors (Figure 1.4). Among 60 effectors interacting with Ras proteins, Rapidly Accelerated Fibrosarcoma (Raf) kinases are the best-characterized Ras effectors. Raf kinases phosphorylate mitogen-activated protein kinase (MAPK)/extracellular signal-regulated kinase (ERK) kinase (MEK), which sequentially phosphorylates ERK kinases and triggers their translocation from the cytoplasm into the nucleus where they activate transcription factors that induce transcription of genes required for entry into S phase of the cell cycle.[15, 20, 39] Phosphoinositide 3-kinase (PI3K) is also the well-known Ras effector which phosphorylates phosphoinositide (4,5)

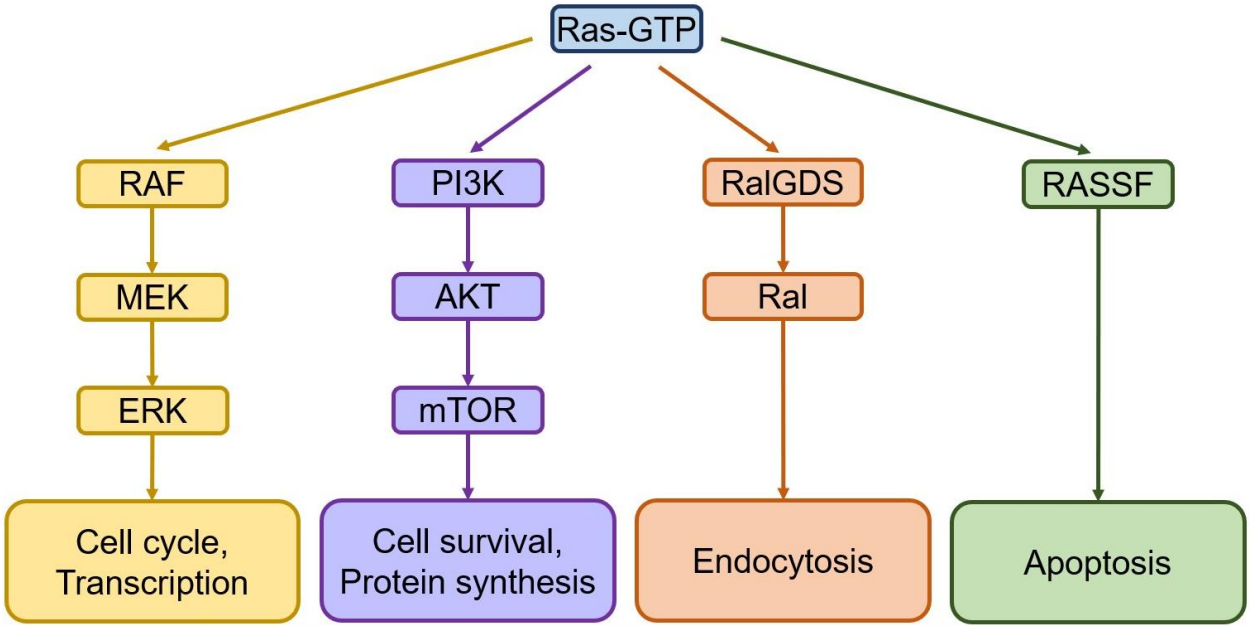

Figure 1.4. Downstream effectors of GTP-bound Ras and their cellular effects.

The best characterized Ras downstream effectors and their roles in cell signaling pathway are shown above. Raf/MEK/ERK pathway controls cell cycle and transcription. PI3K/AKT/mTOR pathway plays an essential role in regulating cell survival and protein synthesis. RalGDS/Ral pathway modulates cell endocytosis. RASSF pathway involves in cell apoptosis; MARK, Mitogen-activated protein kinase; ERK, extracellular signal-regulated kinase; MEK, MARK/ERK kinase; AKT, Protein kinase B; mTOR, mammalian target of rapamycin; Ral, Ras-like.

bisphosphate (PIP_2) and produces the second messenger phosphoinositide (3,4,5) trisphosphate (PIP_3).[40] PIP_3 recruits Protein kinase B (AKT) to the plasma membrane, where it is activated by the phosphorylation of phosphatidyl inositol-dependent kinase 1 (PDK1) and mechanistic target of rapamycin complex 2 (mTORC2).[41] When activated, AKT can stimulate many downstream effectors including mTOR which is involved in controlling cell survival and protein synthesis.[42-44] Other Ras effector, Ral guanine nucleotide dissociation stimulator (RalGDS) is also widely studied. Ras-like (Ral) GTPases are 46%-51% identical with RasGTPases.[45] RalGDS, a member of RalGEF family, shares sequence homology REM-Cdc25 with RasGEF, but RalGDS shows high affinity to RalA and RalB instead of Ras.[46] Activated Ras binds RalGDS which in turn activate RalA and RalB. GTP-bound form of RalA and RalB directly interacts with many downstream effectors such as Ral binding protein 1 (RalBP1) which then form complexes with RalBP1- associated Eps homology (EH) domain protein 1 (Reps1) and Reps2/ partner of RalBP1 (POB1) proteins that are involved in endocytosis.[15, 43, 46] Another well-studied downstream effector of Ras is Ras association domain family member (RASSF), which contain conserved Ras Association (RA) domains.[47] RASSF proteins are identified as the main Ras death effectors which are able to stimulate apoptosis.[15, 43, 47]

Regulation of Ras by three classes of RasGEFs

There are 30 RasGEFs found in human genome.[37] Of these, Son of Sevenless (SOS), Ras Guanine Nucleotide Releasing Protein (RasGRP), and Ras Guanine Nucleotide Releasing Factor (RasGRF) are the major and best characterized RasGEFs. Although three members possess similar catalytic core, they have distinct regulatory

domains (Figure 1.5.A). Each RasGEF member is stimulated by different upstream signals and exhibits distinct cellular processes.[15]

SOS

SOS gene, which functions downstream of the Drosophila epidermal growth factor receptor, was first identified in Drosophila melanogaster.[48-49] SOS proteins are expressed ubiquitously.[8] The central segment of SOS contains an extensive homology called Ras exchange motif – Cdc25 homology domain (REM-Cdc25), also termed catalytic domain. N-terminal segment of SOS includes the Histone-like domain (H), the Dbl homology (DH) domain, and the Pleckstrin homology (PH) domain. The H and PH domains are responsible for the interaction with plasma membrane, while the DH homology domain regulates the nucleotide exchange of RhoGEFs, which regulate cell morphology and the cytoskeleton via their connections with actin filaments.[32] The C-terminal segment of SOS consists of proline-rich (PR) domain which contains multiple PR motifs that bind SH3 domain-containing proteins such as growth factor receptor-bound protein 2 (Grb2).[8] The C-terminal PR domain is the first membrane anchor site that translocates SOS to the membrane through the interaction with SH3 domain of Grb2.[50] The positively charged H domain is the second membrane anchor site of SOS through the interaction with PIP_2 or phosphatidic acid (PA).[51] The third membrane anchor site of SOS is PH domain which can bind membrane lipids such as PIP_2 or PA with high affinity.[32] SOS has two binding site for Ras, the active site where the empty Ras is bound and processes the nucleotide exchange, and the allosteric site which is occupied by the nucleotide-loaded Ras.[52] The interaction of SOS with nucleotide-loaded Ras at allosteric site is considered as the fourth anchor site that stabilizes the

membrane localization of SOS.[53] In the cytosol, SOS is inactive due to the DH domain which blocks the allosteric binding site of Ras (Figure1.5.D). Upon membrane-dependent signal integration, adapter protein Gbr2 directly binds phosphotyrosine site of an activated receptor tyrosine kinase (RTK) that recruits SOS to the membrane.[32] Interaction of PH domain with PIP_2 or PA leads to rearrangement of PH-DH domains and allows the nucleotide-loaded Ras to bind the allosteric site of SOS (Figure1.5.D).[53] The binding of Ras-GTP to the allosteric site causes the conformational change at the active site and stimulates the nucleotide exchange activity of SOS.[32, 53]

RasGRP

There are four isomers of RasGRP (RasGRP1 through RasGRP4), but most research studies have been performed on RasGRP1 which is used as a framework for the other RasGRPs to study the protein domain structures. RasGRP1 is expressed in the brain, in primary keratinocytes, and in T cells which originate in bone marrow and travel to thymus to mature.[8, 54] Starting from N-terminus, RasGRP1 consists of a catalytic domain REM-Cdc25 ($RasGRP1^{cat}$) following by an EF hands domain, a diacylglycerol-binding (C1) domain, and a coiled-coil (CC) domain which is unique in RasGRP1 and absent in other RasGRP proteins. The CC domain which contains leucine zipper motif is possible to mediate and stabilize RasGRP1 dimer.[52, 55] EF-hands domain includes EF-hand 1 and EF-hand 2, but only EF-hand 1 can bind calcium ion.[52] EF-hand 1 of RasGRP1 contains the helix-loop-helix motif observed in structure of calmodulin. In contrast, EF-hand 2 of RasGRP1 is missing the entering helix which is instead replaced by a connector sequence.[52] The exact mechanism of calcium ions regulating RasGRP1 is not well known. Previous studies showed that EF-hand 1 is

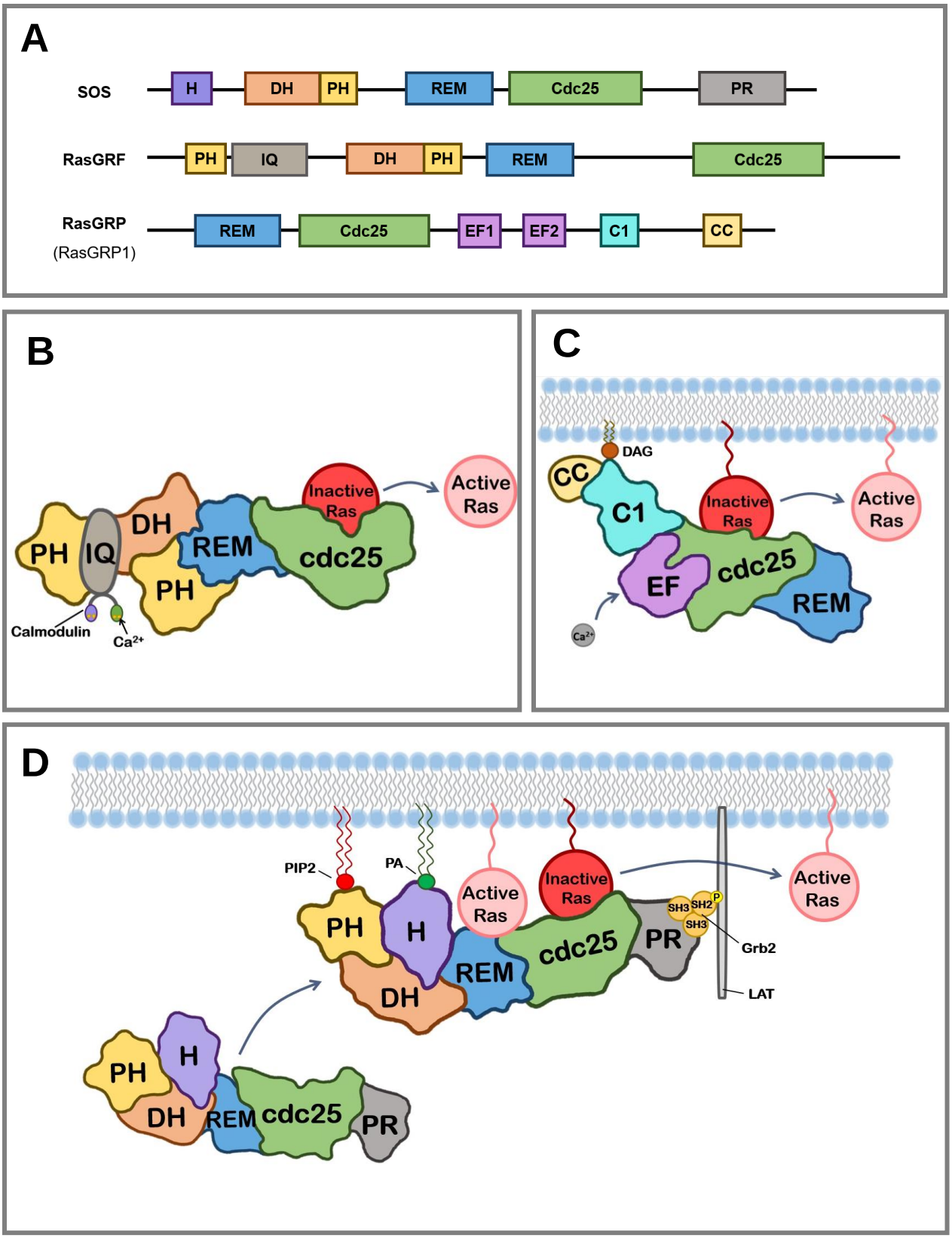

Figure 1.5. Mechanisms of the activation of various RasGEFs.

Figure 1.5. Mechanisms of the activation of various RasGEFs.

(A) Domain architectures of RasGEF family. Although RasGEF members – RasGRP, RasGRF, and SOS – share an extensive homology called REM-Cdc25 domains, but their regulatory domains differ from one another. C1, Diacylglycerol-binding domain; CC, coiled coil motif; Cdc25, Cell division cycle 25; DH, Dbl homology domain; EF, EF hands; H, Histone-like domain; IQ, Ilimaquinone motif; PH, Pleckstrin homology domain; PR, Proline-rich domain; REM, Ras exchanger motif. **(B)** Mechanism of RasGRF activation. RasGRF is activated in response to the increment of the intracellular Ca^{2+} concentration. Activation is mediated by the binding of calmodulin to the IQ motif in the RasGRF structure. **(C)** Mechanism of RasGRP1 activation. The increase in diacylglycerol (DAG) levels on the membrane recruits RasGRP1 through the C1 domain to the membrane where RasGRP1 can target and activate Ras. Moreover, Ca^{2+}-binding RasGRP1 which induces the conformational changes in RasGRP1 also contributes to the membrane localization of RasGRP1. **(D)** Mechanism of SOS activation. SOS has two binding sites for Ras, the active site where the empty Ras is bound and processes the nucleotide exchange of Ras, and the allosteric site which is occupied by the nucleotide-loaded Ras. In the cytosol, SOS is inactive due to the DH domain blocking the allosteric binding site of Ras. SOS activation begins with the recruitment of SOS to membrane through the interaction with phosphorylated linker for activation of T Cells (LAT). Interaction of PH domain with PIP_2 leads to rearrangement of PH-DH domains and allows the nucleotide-loaded Ras to bind the allosteric site of SOS. The binding of Ras-GTP to the allosteric site causes the conformational change at the active site and stimulates the nucleotide exchange activity of SOS.

important for membrane localization of RasGRP1.[56] C1 domain of RasGRP1 also plays essential role in membrane translocation. This domain has two zinc ion coordination sites that maintain proper folding and form compact structure.[57] Upon T cell receptor stimulation, tyrosine phosphorylation of the adapter molecule recruits phospholipase Cγ (PLC-γ) to the membrane.[32] The activation of PLC-γ cleaves PIP_2 into IP_3 and DAG which trigger the two second messenger pathways, Ca^{2+} and DAG.[32] The increase in diacylglycerols (DAGs) level in the membrane recruits RasGRP1 through its C1 domain, thus facilitating the binding of Ras to the active site of $RasGRP1^{cat}$ (Figure 1.5.C).[32] The critical difference in the catalytic domain of SOS and RasGRP1 is that RasGRP1 regulation does not depend on the allosteric control of REM domain.[52]

RasGRF

RasGRF family is made of RasGRF1 and RasGRF2 which contain multiple domains: REM-Cdc25 domain, two PH domains, DH domains, ilimaquinone (IQ) domain, and CC domain (Figure 1.5.B). RasGRF1 and RsGRF2 are expressed at high level in the brain, but RasGRF2 shows more widespread distribution.[50] One PH domain (PH1) locates at N-terminus, and the other PH domain (PH2) forms a tandem DH-PH domain which is similar to that of SOS protein.[32, 38] In addition to Ras activation, RasGRF proteins are able to activate Rac GTPase family through their DH domain.[58] The IQ domain allows interaction with calmodulin that activates RasGRFs in response to increases of intracellular calcium ions concentration (Figure 1.5.B).[50] Unlike SOS and RasGRP1, Cdc25 domain is the only one that is responsible for the guanine nucleotide exchange activity in RasGRF.[59]

Membrane-protein interaction

Membrane classification

Plasma membranes are key components of all cells that serve as the boundaries to isolate the interior of cells from the surrounding.[4, 60-61] Prokaryotic cells, which have no intracellular organelles, carry out biological processes at the plasma membrane and cytoplasm itself. Unlike prokaryotic cells, eukaryotic cells include various intracellular organelles such as nucleus, mitochondria, Endoplasmic Reticulum (ER), and the Golgi apparatus. Therefore, eukaryotic cells have not only plasma membranes surround the whole cells, but also intracellular membranes that surround these intracellular organelles. Intracellular membranes are usually thinner than plasma membranes.[60] Both types of membrane contain the same major components which are lipid and protein; however, the concentrations of these components vary between membranes and depend on functional needs.[4, 62]

Membrane compositions

Lipids are major components of membranes.[4, 60-61] The three major lipid components of eukaryotic membrane include glycerophospholipids, sphingolipids, and cholesterol.[60] Glycerophospholipids, the most abundant lipids of membrane, are amphipathic, and made of glycerol molecule with a phosphate group esterified at α-carbon and two long-chain fatty acids esterified at the 1- and 2-positions.[60] Phosphatidic acid (PA), the parent compound of glycerophospholipids, is the intermediate to synthesize other glycerophospholipids such as phosphatidylcholine (PC), phosphatidylethanolamine (PE), phosphatidylserine (PS), phosphatidylglycerol (PG), and phosphatidylinositol(PI).[4] Another principal class of lipids, sphingolipids such as

sphingomyelin (SM) and glycosphingolipids, are amino alcohols which are frequently found in membrane.[4] Cholesterol is also essential component of membrane which functions to alter the fluidity and permeability of membrane.[60]

In addition to lipids, proteins are also fundamental components of membranes. Membrane proteins include integral proteins (intrinsic proteins), peripheral proteins (extrinsic proteins), and lipid-anchored proteins.[4, 60, 63] Integral proteins can insert themselves partially into the membrane or all the way cross the membrane.[4] In contrast, peripheral proteins associate with membrane surface through non-covalent interaction such as electrostatic and hydrogen bond interactions at the membrane interface.[4, 64] Lipid-anchored proteins interact with membrane through various covalently linked anchors.[4, 60]

Membrane structures

There are several forms of membrane structures including monolayers, bilayers, micelles, unilamellar vesicle, and multilamellar vesicle.[4] Of these, phospholipid bilayers are the fundamental structures of biological membrane.[60, 65] The polar head groups of phospholipid bilayers interact with aqueous environment, whereas hydrophobic lipid tails are buried between the bilayers.[66] The two monolayers of biological membrane have different lipid and protein compositions which cause asymmetric structure of lipid bilayer.[65] The acidic and amine-containing phospholipids such as PS, PA, PG, and PI mainly distribute in the cytoplasmic leaflet of the plasma membrane, whereas SM and PC are predominant in the out leaflet.[4] Phospholipid bilayer is a fluid matrix which allows lipids and proteins to laterally diffuse or transversely move between bilayers of membrane.[4, 60, 66]

Key features of membrane interactions

This chapter will solely focus on the proteins which bind reversibly to membranes; therefore, the integral proteins will not be discussed here. The best-characterized reversible membrane interactions consist of membrane-targeting domains, covalent lipid anchors, amphipathic α-helices, and hydrophobic core (Figure A-2).

The first class of reversible membrane interactions is membrane-targeting domains which possess a binding pocket for specific phospholipid head group.[63] Examples of this interaction include C1 domain, Ca^{2+} and lipid binding domain (C2), and PH domain. C1 domain interacts with DAG and phorbol esters to recruit proteins to membrane.[67] C1 motif can be found in many signaling enzyme such as RasGRP, Raf, and protein kinase C (PKC).[52, 67-68] Binding of C2 domain with Ca^{2+} induces more positive charges around the C2 domain, thus allowing C2 domain to interact with anionic membrane.[67] C2 domain is present in many enzymes such as PKC β, cytosolic PLA_2 ($cPLA_2$), and phospholipase C (PLC).[69-71] The third motif of membrane-targeting domains is PH domain whose structure contains up to 10 basic residues that allow PH domain to bind phosphoinositides such as PIP_2 or PIP_3 with high affinity.[67] PH domain has been widely recognized in SOS, RasGRF, protein kinase B (PKB), and 3-phosphoinositide-dependent protein kinase-1 (PDK1).[32, 72-73]

The second class of reversible membrane interactions is covalent lipid anchor inserted into bilayer membrane. Example of this interaction can be found in some members of Ras Subfamily whose C-terminal CAAX sequence undergoes post-translational modification that results in a thioether-linked farnesyl group.[27] Another

example is recoverin which is anchored to membrane through its N-terminal myristoyl group.[74]

The third class of reversible membrane interactions involves amphipathic α-helices which arrange polar residues at one face, and hydrophobic residues at the opposite face.[75] This structure lies parallel to the membrane surface so that the polar face of helix contacts with aqueous environment, and the other transmembrane hydrophobic face interacts with the hydrophobic environment within the bilayer.[76] Some examples of proteins which are recruited to membrane by amphipathic α-helices are ADP-ribosylation factor (Arf), CTP:phosphocholine cytidylyltransferase (CT), and vinculin.[77-79]

The last class of reversible membrane interactions is hydrophobic cores which are present in proteins that only interact superficially with the polar head group of membrane.[80] The insertion of transmembrane hydrophobic α-helices or hydrophobic loops allows these proteins to interact with membrane surface. Examples of this case can be found in cytochrome P450 (CYP) and membrane-bound catechol-O-methyltransferase (MB-COMT).[81-82]

Biological roles of membrane

Membranes serve as barriers that separate the cytoplasm from surrounding.[80] These barriers control the traffic of molecules or ions which move across the bilayer membrane to supplement the metabolic and physiological demands for cells.[4] The transport process can be proceeded through specific diffusions or is carried by integral proteins which allow the metabolites and ions to move across the membrane.[4, 60, 66, 80]

Many cytoplasmic proteins are recruited to the inner membranes to initiate signal transduction pathways.[4, 60, 67] These cytoplasmic proteins are peripheral proteins, also known as amphitropic proteins.[67] The functions of these amphitropic proteins can be regulated by lipid bilayers through specific reversible interactions as mentioned above. Therefore, plasma membranes also play key roles in regulation of intracellular signaling pathways. Most amphitropic proteins maintain their soluble inactive forms in cytoplasm. Membrane interactions of these proteins induce conformational changes which provide the access to substrates binding.[80, 83-84] RasGRP and SOS, the major subjects of this research, are among those amphitropic proteins which are regulated via specific interactions with membrane.

Kinetics of SOS catalytic functions with and without membrane

Structure of catalytic domain in SOS

When the regulatory domains (F, DH, PH, and PR) are omitted, the remaining segment of SOS containing REM-Cdc25 domains is termed SOS^{cat}, yet can solely function for the nucleotide exchange activity.[32] A study showed that when Ras was tethered on the lipid membrane, the activity of SOS^{cat} was increased up to 500-fold.[53] The study explained that the colocalization of SOS to the membrane-bound Ras increased the probability of encounters between SOS and Ras, thus increasing the ability of nucleotide exchange in SOS. However, the mechanistic action of the membrane-binding effect on the SOS catalysis activation is still unclear.

The classical activation of Ras by SOS is initiated by recruitment of SOS from cytoplasm to plasma membrane in response to growth factor receptors.[32] Recent studies create a receptor-independent Ras activation model by using Ras tethered to

lipid membrane to recruit SOS to the membrane.[53, 85] The lipid vesicles or supported lipid bilayers are used to mimic the physical property of natural cell membrane. In their study, when Ras is either in solution or tethered to lipid membranes, Ras binds to the allosteric site to induce conformational changes at the SOS active site that allows substrate Ras to bind.[53] In the case that Ras was tethered to the membrane, the study claimed that the binding of Ras to the allosteric site of SOS recruits and localizes SOS^{cat} to the membrane which promotes the stable interaction of SOS to the membrane. The study also showed that, although the allosteric Ras is able to activate SOS^{cat} in solution, the substrate Ras which shows multidimensional movements in solution has less chance to target the active site of SOS.

Due to the unstable interaction of Ras and SOS in cytoplasm, it can be proposed that SOS is catalytically unformed enzyme without membrane. When SOS is recruited to the membrane through the binding of allosteric Ras, SOS becomes a catalytically competent enzyme because membrane functions as supporter that enables SOS to efficiently catalyze the nucleotide exchange of Ras. On the basis of the analysis, a "membrane supplement hypothesis" can be proposed that membrane functions as a supporter that stably holds substrate Ras within the catalytic site of SOS.

Allosteric autoactivation of SOS

Enzymatic activity can be activated or inhibited through the non-covalent interaction of the enzyme with small molecules (effectors/ligands) other than the substrate.[4] This type of control is called allosteric regulation (*allo* means “other”).[4, 86] This term indicates that the ligands bind to the enzyme at a site other than the active site. For convenience, kinetics of allosteric enzymes which do not follow the Michalis-

Menten equation can be mainly classified in two types: ligand concentration dependent- and time dependent-allosteric kinetics.[87] Ligand concentration-dependent allosteric kinetics exhibit only when the allosteric ligand concentration is in steady state. When enzyme activity is a function of ligand concentration at a fixed time, the dependence of the enzyme activity on allosteric ligand concentration can be hyperbolic.[4] On the other hand, time-dependent allosteric kinetics are applied when the ligand concentration increases or decreases with time. A logistic function (sigmoid-like or S shaped) can be used to describe the kinetic features of time-dependent allosteric kinetics. When enzymatic action follows a logistic function of time, the enzymatic action slowly starts with a lag phase, then undergoes a rapid increase, and followed by a deceleration due to the quantity limitation of substrates or enzymes.[87] The autoactivation function is an extension of the logistic function of time with a term of the *reaction initiator* (Figure 1.6). The term *Reaction initiator* is expressed as a ratio of the inactive and active enzymes.[88] Autoactivation process is proceeded by a positive feedback loop which describes that products of an enzymatic reaction feedforward as an allosteric effector to generate more of active enzymes.[89]

A recent study illustrated that the activation of SOS, which occurred though an amplified positive feedback loop, showed an allosteric autoactivation process (Figure 1.7).[87] Mechanistically, SOS is activated by the positive feedback loop in such a way that a fraction of active SOS produces active Ras-GTP. These active Ras-GTP then circle back to the allosteric sites of inactive SOS. In turn, these inactive SOS proteins induce conformational changes to produce more active SOS proteins. As mentioned above, a fraction of the reaction initiator is required to trigger autoactivation.

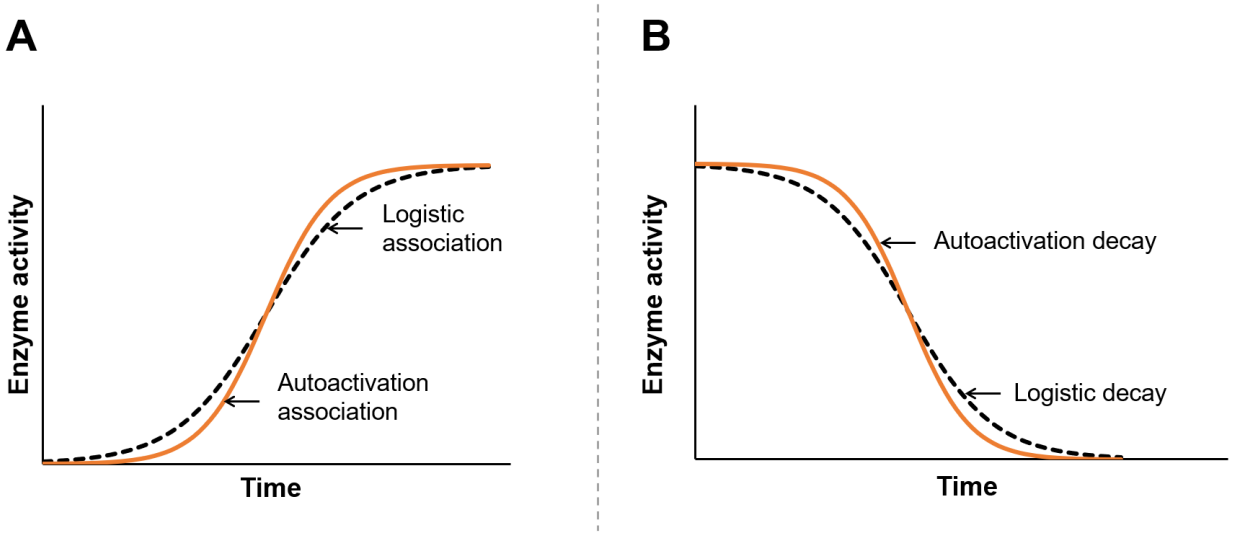

Figure 1.6. Kinetics of logistic and autoactivation processes.

(A) Logistic and autoactivation association curvatures. To create the plot of logistic association, the integrated law of $\gamma = 1/(1 + e^{-kt})$ is used, where γ is a fraction active enzyme, *k* is a first-order rate constant, and t denotes time. To create the plot of autoactivation association curve, the integrated rate law $\gamma = 1/(1 + ([A]_i/[A]_a)\cdot e^{-kt})$ is used, where $[A]_i$ and $[A]_a$ express the inactive and active enzyme fractions respectively. **(B)** Logistic and autoactivation decay curvatures. To create the plot logistic decay, respectively, the integrated law of $\gamma = e^{-kt}$ and $\gamma = 1 - 1/(1 + e^{-kt})$ is used. To create the plot of autoactivation decay curve, the integrated rate law $\gamma = 1 - 1/(1 + [A]_i/[A]_a)\cdot e^{-kt})$ is used, where $[A]_i$ and $[A]_a$ express the inactive and active enzyme fractions respectively. Note that when the ratio $[A]_i/[A]_a = 1$, the logistic and the autoactivation association are the same, and the logistic and the autoactivation decay are also identical.

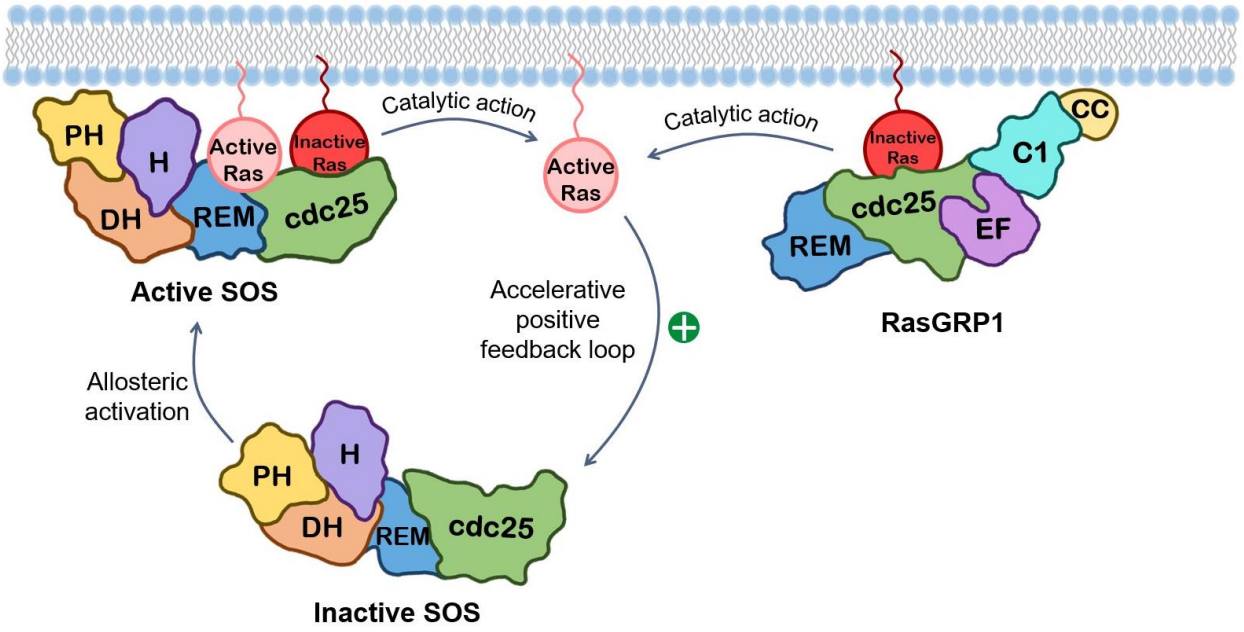

Figure 1.7. Allosteric activation of SOS primed by Ras-GTP produced by RasGRP. DAG-regulated membrane recruitment of RasGRP initiates nucleotide exchange of RasGRP. Activated RasGRP produces active Ras (Ras-GTP) that allosterically activates SOS. The activated SOS generates more of active Ras, which in turn feedforwards to produce more of allosterically activated SOS.

Where does the source of active Ras-GTP to produce a fraction of active SOS come from? In the previous study, when SOS and RasGRP were co-expressed in T-cell, activation of RasGRP appeared ahead of activation of SOS.[32] The activation of SOS successfully proceeded by the activation of RasGRP is termed bimodal activation pattern.[87] RasGRP then produced a fraction of active Ras-GTP that primes full allosteric activation of SOS.[32] Combining this SOS bimodality with RasGRP and the unique kinetic features of SOS autoactivation, RasGRP is postulated to function to produce a fraction of an active Ras-GTP, the reaction initiator that triggers SOS autoactivation.[87]

Relationship between membrane supplement and SOS autoactivation

What is not so clear now is that how the membrane supplement hypothesis is linked to the SOS autoactivation. I hypothesize that the membrane binding of SOS results in activation of SOS that facilitates autoactivation of SOS. This is because the membrane targeting of SOS through the allosteric site produces more active SOS which in turn processes more initiator that leads to autoactivation. In contrast to membrane-associated SOS, SOS in cytoplasm becomes less active. Accordingly, no autoactivation occurs due to lesser initiator is produced. This research will focus on the examination of the link between the membrane supplement hypothesis and SOS autoactivation, which will in turn aid to better understand the SOS catalytic functions in cells autoactivation. I will also examine the function of membrane on the activation of the other members in RasGEF family. From now on, RasGEF which possesses a surface catalytic site that weakens the binding of substrate Ras is considered as "a catalytically unformed RasGEF", and membrane associated RasGEF which stabilizes the binding of substrate Ras is termed "a catalytically competent RasGEF". I hypothesize that an artificial

supporter instead of the plasma membrane also is capable to enhance the binding of SOS to Ras. Thus, I propose to engineer a model of RasGEF connected to a foreign protein that functions as a supporter to mimic catalytically competent RasGEF. In the next chapter, the membrane supplement hypothesis will be examined by comparing the key kinetic features of the catalytically unformed and catalytically competent RasGEF models. This comparison will clarify the function of membrane in the activation of Ras by RasGEF family.

References

1. McCudden, C.; Hains, M.; Kimple, R.; Siderovski, D.; Willard, F., G-protein signaling: back to the future. *Cellular and molecular life sciences* **2005,** *62* (5), 551-577.

2. Ostermeier, C.; Brunger, A. T., Structural basis of Rab effector specificity: crystal structure of the small G protein Rab3A complexed with the effector domain of rabphilin-3A. *Cell* **1999,** *96* (3), 363-374.

3. Sprang, S. R., G protein mechanisms: insights from structural analysis. *Annual review of biochemistry* **1997,** *66* (1), 639-678.

4. Garrett, R.; Grisham, C., Biochemistry, Brooks/Cole, Cengage Learning. **2013**.

5. Takai, Y.; Sasaki, T.; Matozaki, T., Small GTP-binding proteins. *Physiological reviews* **2001,** *81* (1), 153-208.

6. Stanley, R. J.; Thomas, G. M., Activation of G proteins by guanine nucleotide exchange factors relies on GTPase activity. *PloS one* **2016,** *11* (3), e0151861.

7. Dunlap, K.; Holz, G. G.; Rane, S. G., G proteins as regulators of ion channel function. *Trends in neurosciences* **1987,** *10* (6), 241-244.

8. Stryer, L.; Bourne, H. R., G proteins: a family of signal transducers. *Annual review of cell biology* **1986,** *2* (1), 391-419.

9. Michaelson, D.; Ahearn, I.; Bergo, M.; Young, S.; Philips, M., Membrane trafficking of heterotrimeric G proteins via the endoplasmic reticulum and Golgi. *Molecular biology of the cell* **2002,** *13* (9), 3294-3302.

10. Yeagle, P. L., *The membranes of cells*. Academic Press: 2016.

11. Murugan, A. K.; Grieco, M.; Tsuchida, N. In *RAS mutations in human cancers: Roles in precision medicine*, Seminars in cancer biology, Elsevier: 2019; pp 23-35.

12. Hancock, J. F., Ras proteins: different signals from different locations. *Nature reviews Molecular cell biology* **2003,** *4* (5), 373-385.

13. Vögler, O.; Barceló, J. M.; Ribas, C.; Escribá, P. V., Membrane interactions of G proteins and other related proteins. *Biochimica et Biophysica Acta (BBA)-Biomembranes* **2008,** *1778* (7-8), 1640-1652.

14. Ahearn, I. M.; Haigis, K.; Bar-Sagi, D.; Philips, M. R., Regulating the regulator: post-translational modification of RAS. *Nature reviews Molecular cell biology* **2012,** *13* (1), 39-51.

15. Nakhaei-Rad, S.; Haghighi, F.; Nouri, P.; Rezaei Adariani, S.; Lissy, J.; Kazemein Jasemi, N. S.; Dvorsky, R.; Ahmadian, M. R., Structural fingerprints, interactions, and signaling networks of RAS family proteins beyond RAS isoforms. *Critical reviews in biochemistry and molecular biology* **2018,** *53* (2), 130-156.

16. Vetter, I. R., The structure of the G domain of the Ras superfamily. In *Ras Superfamily Small G Proteins: Biology and Mechanisms 1*, Springer: 2014; pp 25-50.

17. Heo, J.; Gao, G.; Campbell, S. L., pH-Dependent Perturbation of Ras− Guanine Nucleotide Interactions and Ras Guanine Nucleotide Exchange. *Biochemistry* **2004,** *43* (31), 10102-10111.

18. Wittinghofer, A.; Pal, E. F., The structure of Ras protein: a model for a universal molecular switch. *Trends in biochemical sciences* **1991,** *16*, 382-387.

19. Wennerberg, K.; Rossman, K. L.; Der, C. J., The Ras superfamily at a glance. *Journal of cell science* **2005,** *118* (5), 843-846.

20. Cox, A. D.; Der, C. J., Ras family signaling: therapeutic targeting. *Cancer biology & therapy* **2002,** *1* (6), 599-606.

21. Jaumot, M.; Yan, J.; Clyde-Smith, J.; Sluimer, J.; Hancock, J. F., The linker domain of the Ha-Ras hypervariable region regulates interactions with exchange factors, Raf-1 and phosphoinositide 3-kinase. *Journal of Biological Chemistry* **2002,** *277* (1), 272-278.

22. Fehrenbacher, N.; Bar-Sagi, D.; Philips, M., Ras/MAPK signaling from endomembranes. *Molecular oncology* **2009,** *3* (4), 297-307.

23. Jackson, J. H.; Cochrane, C. G.; Bourne, J. R.; Solski, P. A.; Buss, J. E.; Der, C. J., Farnesol modification of Kirsten-ras exon 4B protein is essential for transformation. *Proceedings of the National Academy of Sciences* **1990,** *87* (8), 3042-3046.

24. Magee, T.; Newman, C., The role of lipid anchors for small G proteins in membrane trafficking. *Trends in cell biology* **1992,** *2* (11), 318-323.

25. Bar-Sagi, D., A Ras by any other name. *Molecular and cellular biology* **2001,** *21* (5), 1441-1443.

26. Gelb, M. H.; Brunsveld, L.; Hrycyna, C. A.; Michaelis, S.; Tamanoi, F.; Van Voorhis, W. C.; Waldmann, H., Therapeutic intervention based on protein prenylation and associated modifications. *Nature chemical biology* **2006,** *2* (10), 518-528.

27. Xiang, S.; Bai, W.; Bepler, G.; Zhang, X., Activation of Ras by Post-Translational Modifications. In *Conquering RAS*, Elsevier: 2017; pp 97-118.

28. Gregory, M. C.; McLean, M. A.; Sligar, S. G., Interaction of KRas4b with anionic membranes: A special role for PIP2. *Biochemical and biophysical research communications* **2017,** *487* (2), 351-355.

29. Goldenberg, N. M.; Steinberg, B. E., Surface charge: a key determinant of protein localization and function. *Cancer research* **2010,** *70* (4), 1277-1280.

30. Moghadamchargari, Z.; Shirzadeh, M.; Liu, C.; Schrecke, S.; Packianathan, C.; Russell, D. H.; Zhao, M.; Laganowsky, A., Molecular assemblies of the catalytic domain of SOS with KRas and oncogenic mutants. *Proceedings of the National Academy of Sciences* **2021,** *118* (12).

31. Hobbs, G. A.; Bonini, M. G.; Gunawardena, H. P.; Chen, X.; Campbell, S. L., Glutathiolated Ras: characterization and implications for Ras activation. *Free Radical Biology and Medicine* **2013,** *57*, 221-229.

32. Roose, J.; Jun, J.; Rubio, I.; Roose, J., Regulation of Ras exchange factors and cellular localization of Ras activation by lipid messengers in T cells. **2013**.

33. Cherfils, J.; Zeghouf, M., Regulation of small gtpases by gefs, gaps, and gdis. *Physiological reviews* **2013,** *93* (1), 269-309.

34. Hennig, A.; Markwart, R.; Esparza-Franco, M. A.; Ladds, G.; Rubio, I., Ras activation revisited: role of GEF and GAP systems. *Biological chemistry* **2015,** *396* (8), 831-848.

35. Trahey, M.; Milley, R. J.; Cole, G. E.; Innis, M.; Paterson, H.; Marshall, C.; Hall, A.; McCormick, F., Biochemical and biological properties of the human N-ras p21 protein. *Molecular and cellular biology* **1987,** *7* (1), 541-544.

36. Soares, T.; Miller, J.; Straatsma, T., Revisiting the structural flexibility of the complex p21ras-GTP: The catalytic conformation of the molecular switch II. *Proteins: Structure, Function, and Bioinformatics* **2001,** *45* (4), 297-312.

37. Ahmadian, M. R.; Kiel, C.; Stege, P.; Scheffzek, K., Structural fingerprints of the Ras-GTPase activating proteins neurofibromin and p120GAP. *Journal of molecular biology* **2003,** *329* (4), 699-710.

38. Rojas, J. M.; Santos, E., Ras-gefs and Ras gaps. In *RAS Family GTPases*, Springer: 2006; pp 15-43.

39. Katz, M. E.; McCormick, F., Signal transduction from multiple Ras effectors. *Current opinion in genetics & development* **1997,** *7* (1), 75-79.

40. Carnero, A.; Paramio, J. M., The PTEN/PI3K/AKT pathway in vivo, cancer mouse models. *Frontiers in oncology* **2014,** *4*, 252.

41. Hoxhaj, G.; Manning, B. D., The PI3K–AKT network at the interface of oncogenic signalling and cancer metabolism. *Nature Reviews Cancer* **2020,** *20* (2), 74-88.

42. de Castro Carpeño, J.; Belda-Iniesta, C., KRAS mutant NSCLC, a new opportunity for the synthetic lethality therapeutic approach. *Translational Lung Cancer Research* **2013,** *2* (2), 142-151.

43. Rajalingam, K.; Schreck, R.; Rapp, U. R.; Albert, Š., Ras oncogenes and their downstream targets. *Biochimica et Biophysica Acta (BBA)-Molecular Cell Research* **2007,** *1773* (8), 1177-1195.

44. Datta, S. R.; Dudek, H.; Tao, X.; Masters, S.; Fu, H.; Gotoh, Y.; Greenberg, M. E., Akt phosphorylation of BAD couples survival signals to the cell-intrinsic death machinery. *Cell* **1997,** *91* (2), 231-241.

45. Neel, N. F.; Martin, T. D.; Stratford, J. K.; Zand, T. P.; Reiner, D. J.; Der, C. J., The RalGEF-Ral effector signaling network: the road less traveled for anti-Ras drug discovery. *Genes & cancer* **2011,** *2* (3), 275-287.

46. Moghadam, A. R.; Patrad, E.; Tafsiri, E.; Peng, W.; Fangman, B.; Pluard, T. J.; Accurso, A.; Salacz, M.; Shah, K.; Ricke, B., Ral signaling pathway in health and cancer. *Cancer Medicine* **2017,** *6* (12), 2998-3013.

47. Donninger, H.; Schmidt, M. L.; Mezzanotte, J.; Barnoud, T.; Clark, G. J. In *Ras signaling through RASSF proteins*, Seminars in cell & developmental biology, Elsevier: 2016; pp 86-95.

48. Bonfini, L.; Karlovich, C. A.; Dasgupta, C.; Banerjee, U., The Son of sevenless gene product: a putative activator of Ras. *Science* **1992,** *255* (5044), 603-606.

49. Pierre, S.; Coumoul, X., Understanding SOS (son of sevenless). *Biochemical pharmacology* **2011,** *82* (9), 1049-1056.

50. Buday, L.; Downward, J., Many faces of Ras activation. *Biochimica et Biophysica Acta (BBA)-Reviews on Cancer* **2008,** *1786* (2), 178-187.

51. Gureasko, J.; Kuchment, O.; Makino, D. L.; Sondermann, H.; Bar-Sagi, D.; Kuriyan, J., Role of the histone domain in the autoinhibition and activation of the Ras activator Son of Sevenless. *Proceedings of the National Academy of Sciences* **2010,** *107* (8), 3430-3435.

52. Roose, J.; Iwig, J.; Vercoulen, Y.; Das, R.; Barros, T.; Limnander, A.; Che, Y.; Pelton, J.; Wemmer, D.; Roose, J., Structural analysis of autoinhibition in the Ras-specific exchange factor RasGRP1. **2013**.

53. Gureasko, J.; Galush, W. J.; Boykevisch, S.; Sondermann, H.; Bar-Sagi, D.; Groves, J. T.; Kuriyan, J., Membrane-dependent signal integration by the Ras activator Son of sevenless. *Nature Structural and Molecular Biology* **2008,** *15* (5), 452.

54. Madigan, M. T.; Clark, D. P.; Stahl, D.; Martinko, J. M., *Brock biology of microorganisms 13th edition*. Benjamin Cummings: 2010.

55. Ksionda, O.; Limnander, A.; Roose, J. P., RasGRP Ras guanine nucleotide exchange factors in cancer. *Frontiers in biology* **2013,** *8* (5), 508-532.

56. Tazmini, G.; Beaulieu, N.; Woo, A.; Zahedi, B.; Goulding, R. E.; Kay, R. J., Membrane localization of RasGRP1 is controlled by an EF-hand, and by the GEF domain. *Biochimica et Biophysica Acta (BBA)-Molecular Cell Research* **2009,** *1793* (3), 447-461.

57. Das, J.; Rahman, G. M., C1 domains: structure and ligand-binding properties. *Chemical reviews* **2014,** *114* (24), 12108-12131.

58. Li, S.; Tian, X.; Hartley, D. M.; Feig, L. A., Distinct roles for Ras-guanine nucleotide-releasing factor 1 (Ras-GRF1) and Ras-GRF2 in the induction of long-term potentiation and long-term depression. *Journal of Neuroscience* **2006,** *26* (6), 1721-1729.

59. Sacco, E.; Metalli, D.; Spinelli, M.; Manzoni, R.; Samalikova, M.; Grandori, R.; Morrione, A.; Traversa, S.; Alberghina, L.; Vanoni, M., Novel RasGRF1-derived Tat-fused peptides inhibiting Ras-dependent proliferation and migration in mouse and human cancer cells. *Biotechnology advances* **2012,** *30* (1), 233-243.

60. Devlin, T. M., *Biochemistry: With Clinical Correlations*. Wiley: 2010.

61. Maxfield, F. R., Plasma membrane microdomains. *Current opinion in cell biology* **2002,** *14* (4), 483-487.

62. Cooper, G. M., Structure of the plasma membrane. *The cell: A molecular approach* **2000,** *2*.

63. Lomize, A. L.; Pogozheva, I. D.; Lomize, M. A.; Mosberg, H. I., The role of hydrophobic interactions in positioning of peripheral proteins in membranes. *BMC Structural Biology* **2007,** *7* (1), 1-30.

64. Khan, H. M.; He, T.; Fuglebakk, E.; Grauffel, C.; Yang, B.; Roberts, M. F.; Gershenson, A.; Reuter, N., A role for weak electrostatic interactions in peripheral membrane protein binding. *Biophysical journal* **2016,** *110* (6), 1367-1378.

65. Vigh, L.; Escribá, P. V.; Sonnleitner, A.; Sonnleitner, M.; Piotto, S.; Maresca, B.; Horváth, I.; Harwood, J. L., The significance of lipid composition for membrane activity: new concepts and ways of assessing function. *Progress in lipid research* **2005,** *44* (5), 303-344.

66. Yèagle, P. L., Lipid regulation of cell membrane structure and function. *The FASEB journal* **1989,** *3* (7), 1833-1842.

67. Cho, W.; Stahelin, R. V., Membrane-protein interactions in cell signaling and membrane trafficking. *Annu. Rev. Biophys. Biomol. Struct.* **2005,** *34*, 119-151.

68. Li, S.; Jang, H.; Zhang, J.; Nussinov, R., Raf-1 cysteine-rich domain increases the affinity of K-Ras/Raf at the membrane, promoting MAPK signaling. *Structure* **2018,** *26* (3), 513-525. e2.

69. Oancea, E.; Meyer, T., Protein kinase C as a molecular machine for decoding calcium and diacylglycerol signals. *Cell* **1998,** *95* (3), 307-318.

70. Lichtenbergova, L.; Yoon, E. T.; Cho, W., Membrane penetration of cytosolic phospholipase A2 is necessary for its interfacial catalysis and arachidonate specificity. *Biochemistry* **1998,** *37* (40), 14128-14136.

71. Bunney, T. D.; Katan, M., Phospholipase C epsilon: linking second messengers and small GTPases. *Trends in cell biology* **2006,** *16* (12), 640-648.

72. Downward, J., Mechanisms and consequences of activation of protein kinase B/Akt. *Current opinion in cell biology* **1998,** *10* (2), 262-267.

73. Anderson, K. E.; Coadwell, J.; Stephens, L. R.; Hawkins, P. T., Translocation of PDK-1 to the plasma membrane is important in allowing PDK-1 to activate protein kinase B. *Current Biology* **1998,** *8* (12), 684-691.

74. Senin, I. I.; Fischer, T.; Komolov, K. E.; Zinchenko, D. V.; Philippov, P. P.; Koch, K.-W., Ca2+-myristoyl switch in the neuronal calcium sensor recoverin requires different functions of Ca2+-binding sites. *Journal of Biological Chemistry* **2002,** *277* (52), 50365-50372.

75. Ladokhin, A. S.; White, S. H., Folding of amphipathic α-helices on membranes: energetics of helix formation by melittin. *Journal of molecular biology* **1999,** *285* (4), 1363-1369.

76. Giménez-Andrés, M.; Čopič, A.; Antonny, B., The many faces of amphipathic helices. *Biomolecules* **2018,** *8* (3), 45.

77. Pacheco-Rodriguez, G.; Patton, W. A.; Adamik, R.; Yoo, H.-S.; Lee, F.-J. S.; Zhang, G.-F.; Moss, J.; Vaughan, M., Structural elements of ADP-ribosylation factor 1 required for functional interaction with cytohesin-1. *Journal of Biological Chemistry* **1999,** *274* (18), 12438-12444.

78. Lee, J.; Taneva, S. G.; Holland, B. W.; Tieleman, D. P.; Cornell, R. B., Structural basis for autoinhibition of CTP: phosphocholine cytidylyltransferase (CCT), the regulatory enzyme in phosphatidylcholine synthesis, by its membrane-binding amphipathic helix. *Journal of Biological Chemistry* **2014,** *289* (3), 1742-1755.

79. Borgon, R. A.; Vonrhein, C.; Bricogne, G.; Bois, P. R.; Izard, T., Crystal structure of human vinculin. *Structure* **2004,** *12* (7), 1189-1197.

80. Muller, M. P.; Jiang, T.; Sun, C.; Lihan, M.; Pant, S.; Mahinthichaichan, P.; Trifan, A.; Tajkhorshid, E., Characterization of lipid–protein interactions and lipid-mediated modulation of membrane protein function through molecular simulation. *Chemical reviews* **2019,** *119* (9), 6086-6161.

81. Magarkar, A.; Parkkila, P.; Viitala, T.; Lajunen, T.; Mobarak, E.; Licari, G.; Cramariuc, O.; Vauthey, E.; Róg, T.; Bunker, A., Membrane bound COMT isoform is an interfacial enzyme: general mechanism and new drug design paradigm. *Chemical Communications* **2018,** *54* (28), 3440-3443.

82. Gaspar, D.; Lúcio, M.; Rocha, S.; Lima, J. C.; Reis, S., Changes in PLA2 activity after interacting with anti-inflammatory drugs and model membranes: evidence for the involvement of tryptophan residues. *Chemistry and physics of lipids* **2011,** *164* (4), 292-299.

83. Hayashi, N.; Matsubara, M.; Titani, K.; Taniguchi, H., Involvement of basic amphiphilic α-helical domain in the reversible membrane interaction of amphitropic proteins: Structural studies by mass spectrometry, circular dichroism, and nuclear magnetic resonance. In *Techniques in Protein Chemistry*, Elsevier: 1997; Vol. 8, pp 555-564.

84. Wells, R. C.; Hill, R. B., The cytosolic domain of Fis1 binds and reversibly clusters lipid vesicles. *PLoS One* **2011,** *6* (6), e21384.

85. Iversen, L.; Tu, H.-L.; Lin, W.-C.; Christensen, S. M.; Abel, S. M.; Iwig, J.; Wu, H.-J.; Gureasko, J.; Rhodes, C.; Petit, R. S., Ras activation by SOS: Allosteric regulation by altered fluctuation dynamics. *Science* **2014,** *345* (6192), 50-54.

86. Ferré, S.; Ciruela, F.; Casadó, V.; Pardo, L., Oligomerization of G protein-coupled receptors: Still doubted? *Progress in molecular biology and translational science* **2020,** *169*, 297-321.

87. Hoang, H. M.; Umutesi, H. G.; Heo, J., Allosteric autoactivation of SOS and its kinetic mechanism. *Small GTPases* **2019**, 1-16.

88. Heo, J.; Halbleib, C. M.; Ludden, P. W., Redox-dependent activation of CO dehydrogenase from Rhodospirillum rubrum. *Proceedings of the National Academy of Sciences* **2001,** *98* (14), 7690-7693.

89. Gadgil, C. J.; Kulkarni, B., Autocatalysis in biological systems. *AIChE journal* **2009,** *55* (3), 556-562.

CHAPTER 2

PROTEIN-BASED MEMBRANE MIMIC OF RASGEFS REVEALS THE NOVEL FUNCTION OF CELL MEMBRANE IN THE CATALYSIS OF RASGEFS

Abstract

Ras plays critical roles in the regulation of various cell signaling events. Ras is primarily activated by Ras Guanine Exchange factors (RasGEFs) including Son of Sevenless (SOS), Ras Guanine Nucleotide Releasing Factor (RasGRF), and Ras Guanine Nucleotide Releasing Protein (RasGRP). The structures of RasGEFs can be divided into catalytic and regulatory domains. Crystal structure analyses of these RasGEFs suggest that catalytic sites of RasGEFs are shallow. Thus, unless otherwise their bulky substrate Ras is upheld by membrane, RasGEFs are unable to hold their substrate Ras within their catalytic sites and thus are unformed for the catalysis. Therefore, a membrane supplement hypothesis is proposed, where RasGEFs are catalytically unformed in cytoplasm, and RasGEFs docking on membrane become catalytically competent. The results of previous studies which showed enhancement of the SOS catalysis at membrane support this hypothesis. To examine this membrane supplement hypothesis, an engineered RasGRP is designed by fusing the catalytic domain of RasGRP1 (RasGRP1^{cat}), one of RasGRP isomers, with a foreign protein proliferating cell nuclear antigen (PCNA) to produce an engineered PCNA-RasGRP1^{cat} protein adduct. PCNA serves as a mechanical fixture that mimics the function of membrane for the RasGEF catalysis. Kinetic comparison of the catalytically unformed and engineered RasGRPs suggests that the fused PCNA is capable to enhance Ras binding interaction with and correctly impose Ras on the active site of the engineered PCNA-RasGRP1^{cat}. These results support the membrane supplement hypothesis that membrane functions as a supporter for the sustaining and strengthening of the binding interactions of RasGEFs with the substrate Ras to promote the nucleotide exchange of Ras.

Amphitropic proteins are soluble proteins whose catalytic actions are regulated by reversible interactions with membrane. However, the general kinetic mechanism of the role of the membrane in the catalytic action of amphitropic proteins has not been established. The crystal structure analyses of selected amphitropic proteins indicate that they also are unformed. Studies show that the catalysis of these unformed amphitropic proteins also is enhanced upon their membrane binding. Therefore, the membrane supplement hypothesis proposed within this study can be applicable for the membrane-dependent catalytic function of certain amphitropic proteins.

Introduction

Ras is a small GTPase that binds a nucleotide (either GTP or GDP).[1-3] The Ras-dependent signaling pathways control cell growth, proliferation, differentiation, and apoptosis.[1-6] Ras function is regulated by the cycling between its inactive GDP- and active GTP-bound forms.[6-10] Ras binds GDP or GTP with high affinity; however, its intrinsic nucleotide exchange rate is very slow.[11-13] Ras guanine exchange factors (RasGEFs) are capable to enhance the intrinsically slow Ras nucleotide exchange rate.[6, 14-16] RasGEFs function by the perturbation of the multiple interactions of Ras with Mg^{2+} and the bound GDP or GTP, resulting in facilitation of the release of the bound GDP or GTP, which in turn allows the binding of a fresh GDP or GTP to produce a nucleotide displaced Ras (displacement of GDP with GTP or *vice versa*).[15, 17] In cells, GTP is ~10 fold more abundant than GDP.[18] Therefore, the action of RasGEFs in cells mostly produces an active GTP-bound form of Ras.[15, 17]

RasGEF family includes three members: Son of Sevenless (SOS), Ras Guanine Nucleotide Releasing Factor (RasGRF), and Ras Guanine Nucleotide Releasing Protein (RasGRP).[19] They all contain a catalytic core which consists of Ras exchange motif and Cdc25 homology domain (REM-Cdc25).[20] REM-Cdc25 also is termed catalytic domain. However, the mechanism of the RasGRP and RasGRF catalysis differs from that of the SOS catalysis (Figure 2.1).[20-22] The catalytic domain of SOS (SOS^{cat}) possesses two substrate Ras binding sites: the catalytic site where the substrate Ras is bound to and catalyzes the Ras nucleotide exchange, and the allosteric site which is occupied by the nucleotide-loaded Ras.[16, 23] The binding of nucleotide-loaded Ras to the allosteric site mediates the conformational change at the catalytic site that enhances the catalytic

function of SOS.[24] On the other hand, the catalytic domain of RasGRP ($RasGRP^{cat}$) and of RasGRF ($RasGRF^{cat}$) have only one substrate Ras binding site, which serves as a catalytic site of RasGRP and RasGRF. [27-28]

Although all RasGEFs commonly contain the REM-Cdc25 core for their catalytic function, they are yet distinguished by their regulatory domains.[16, 23, 25] The regulatory domains in SOS include Histone-like fold (H), Dbl homology (DH) domain, Pleckstrin homology (PH) domain, and proline-rich (PR) domain.[26-31] In contrast, the regulatory domains of RasGRP1 at the C-terminal include EF hands domain, diacylglycerol-binding (C1) domain, and a coiled-coil (CC) domain which is unique in RasGRP1 and absent in other RasGRP proteins.[20, 25, 32-33] Unlike with SOS and RasGRP, regulatory domains of RasGRF consist of CC domain, ilimaquinone (IQ) domain, DH domain, and two PH domains.[16, 20]

The crystal structures of RasGEFs (Figure 2.1) suggest that the bowl-shaped catalytic domains of RasGEFs are too shallow to uphold the bulky Ras substrate. It can be postulated that RasGEFs are catalytically unformed unless otherwise they function with membrane, which secures the substrate binding within their active sites. Accordingly, a novel membrane supplement hypothesis is proposed, in which RasGEFs in cytoplasm are catalytically unformed due to the failure of upholding the substrate Ras within their catalytic sites. When RasGEFs are recruited to membrane, RasGEFs become catalytically competent due to the membrane-mediated stabilization of substrate Ras within their catalytic sites that enhances the catalytic function of RasGEFs.

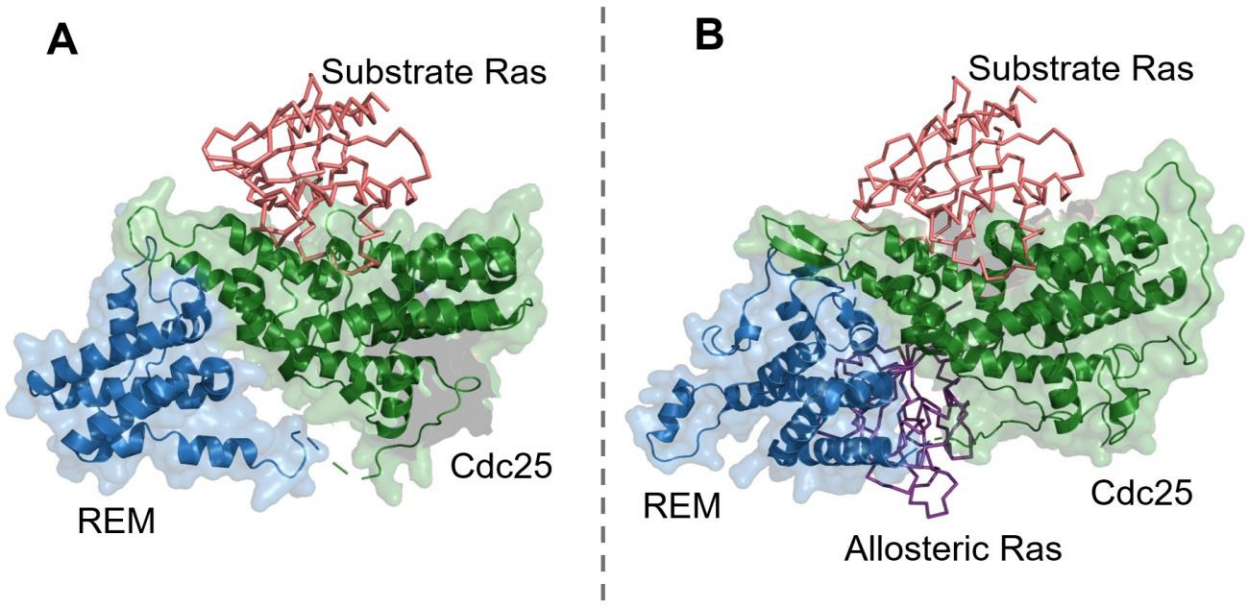

Figure 2.1. Comparison of the mechanism of the action of RasGRP^{cat} and SOS^{cat} catalysis.

(A) Model of RasGRP^{cat} catalysis. Catalytic domain of RasGRP (RasGRP^{cat}) has only one binding site for Ras. The RasGRP catalysis that activates Ras occurs when the substrate Ras directly interacts with the active site on the Cdc25 domain of RasGRP. **(B)** Model of SOS catalysis. The catalytic domain of SOS (SOS^{cat}) contains the active site where the substrate Ras is bound and processes nucleotide exchange activity, and the allosteric site which is occupied by the nucleotide-loaded Ras. The SOS catalysis that activates Ras occurs only when the binding of nucleotide-loaded Ras to the allosteric site causes the conformational change at the active site, following by the interaction of substrate Ras with the active site where the nucleotide exchange activity of SOS is stimulated. Model of RasGRF catalysis is omitted because it is not used in this study.

Studies show that, unless otherwise SOS interacts with membrane, the regulatory domains of SOS autoinhibit SOS catalytic function by blocking the Ras access to the SOS allosteric site.[26, 28, 30, 34-37] A recent study shows that the SOS membrane-binding interaction that eliminates the effect of SOS autoinhibition exhibits a dramatic increase in the catalytic activity of SOS.[28] This result suggests that membrane appears to release the autoinhibition of regulatory domains of SOS but also contributes to the enhancement of SOS catalysis. The latter case is of interest, as it supports the membrane supplement hypothesis.

To examine the membrane supplement hypothesis, I designed an engineered form of RasGEF which consists of two protein moieties: (1) a catalytically unformed RasGEF (that only partially functions without membrane or a protein mechanical fixture) and (2) a support or mechanical fixture protein (that substitutes membrane) (Figure A-3). For convenience, the REM-Cdc25 domain of RasGRP1 (RasGRP1^{cat}) is selected as a model construct of the catalytically unformed RasGRP. This selection is because unlike SOS, RasGRP has only one substrate Ras binding site. This selection, therefore, eliminates the kinetic complication of SOS associated with the SOS allostery. Proliferating cell nuclear antigen (PCNA) was chosen as a supporter or a mechanical fixture of the engineered protein. This is because PCNA lacks the Ras guanine nucleotide exchange function yet possesses a dome configuration that can mechanically support the substrate Ras within its cavity. To fuse RasGRP1^{cat} with PCNA to produce an engineered form of RasGRP, D375C RasGRP1^{cat} and G176C PCNA mutants were produced. The cysteines introduced of these mutants were then connected by a disulfide bond that yields an engineered RasGRP (D375C RasGRP1^{cat}-

G176C PCNA adduct). The comparison of the key kinetic features of the engineered RasGRP with those of the catalytically unformed RasGRP suggests that PCNA functions as a supporter that enhances the catalytic function of RasGRP. This is explained by the membrane supplement hypothesis that membrane functions as a mechanical fixture that enhances the binding interactions of the catalytic site of RasGEFs with substrate Ras, resulting in promotion of the catalysis of RasGEFs including SOS, RasGRP, and RasGRF.

A recent study shows that, unlike other RasGEFs, SOS is uniquely autoactivated though an accelerative positive feedback loop action.[38] The study also proposed that an accelerative positive feedback loop action drives SOS to be autoactivated *per se*. The study further shows that SOS autoactivation is enhanced when SOS is anchored on membrane.[38] However, the mechanism of the action of the membrane-mediated enhancement of the SOS autoactivation is yet to be investigated. The results of this study with respect to the membrane supplement hypothesis also provide insight into the role of membrane in the enhancement of SOS autoactivation.

Materials and Methods

Expression and purification of Ras. Full-length of Harvey Ras (residue 1-189) was cloned into the maltose binding fusion protein vector (pMAL-c2e), expressed, and purified from the BL21 strain of *E. coli*. Isolated colonies were inoculated into 30 mL Lysogeny broth (LB) containing 100 μg/mL ampicillin and incubated at 37 °C at 250 rpm overnight until the optical density at 600 nm (OD_{600}) reached 0.5. The overnight culture was then grown into 400 mL of LB at 37 °C at 250 rpm. As soon as OD_{600} reached 0.6, the culture was induced by adding isopropyl-β-D-thiogalactopyranoside (IPTG) to a final

concentration of 1 mM. The induced cells were incubated overnight at 18 °C and harvested by centrifugation at 8000 rpm at 4 °C for 10 minutes, then frozen at −80 °C. The cell pellets were resuspended in 20 mL of a pre-chilled lysis buffer (20 mM Tris-HCl, 200 mL NaCl, and 1 mM EDTA, pH 7.4), and sonicated in short pulses of 10 seconds on ice for 2 minutes. The supernatant was harvested by centrifugation at 8000 rpm at 4 °C for 20 minutes. Amylose resin (NEB) was loaded onto a 2.5 × 10 cm column and pre-equilibrated with lysis buffer. After all supernatant was loaded onto the amylose resin column, the column was washed with a wash buffer (20 mL Tris, 500 mM NaCl, and 1 mM EDTA, pH 7.4). The fusion protein was eluted from the column with 5 mL of 10 mM maltose solution. Protein-containing fractions were pooled and concentrated by using an Amicon Centricon tube (10 kDa cut-off).

Expression and purification of RasGRP1^{cat}. The full-length sequences of RasGRP1 and the cloning vector pET his6 MBP TEV LIC were the gifts from Dominic Esposito (Addgene, plasmid # 70527) and Scott Gradia (Addgene, plasmid # 29708), respectively. This project did not focus on cell signaling; therefore, all the regulatory domains of RasGRP1 were omitted in this study. RasGRP1^{cat} domain (residue 50-468) was amplified by PCR using specific primers (Forward primer: 5’ – GGTTCCaatattATGGTGTCTCTGGGACATTTAGCC – 3’; Reverse primer: 5’ – GGAAggatccTTAGCTAATGGTTTTTGGATCAGGTTT – 3’); *Ssp*I and *Bam*HI sites are indicated by lower case letters. RasGRP1^{cat} construct was cloned into pET his6 MBP TEV LIC cloning vector. The pET his6 MBP TEV LIC – RasGRP1^{cat} plasmid was then transformed into One Shot Mach 1 TM T1 Chemically Single Competent Cells (Invitrogen). Single colonies were picked randomly to screen for the presence of inserts.

The cloning vector containing RasGRP1^{cat} gene was then transformed into BL21 (DE3) competent cells (NEB). Expression of the MBP-RasGRP1^{cat} fusion protein was induced by adding IPTG to a final concentration of 1mM and incubating overnight at 18 °C. The induced cells were harvested by centrifugation at 8000 rpm at 4 °C for 10 minutes, then frozen at −80 °C. The cell pellets were resuspended in a 20 mL pre-chilled lysis buffer (20 mM sodium phosphate, 300 mM NaCl, and 10 mM imidazole, pH 7.4) supplemented with 250 U/mL nuclease and 1 mg/mL lysozyme. After the cell pellets were sonicated, the lysate was clarified by centrifugation at 8000 rpm at 4 °C for 20 minutes. The supernatant was loaded onto a HisPur™ Ni-NTA resin (Thermo Scientific) column pre-equilibrated with 20 mL of lysis buffer. The column was washed with a wash buffer (20 mL sodium phosphate, 300 mM NaCl, and 20 mM imidazole, pH 7.4). The protein was eluted from the column with 10 mL of an elution buffer (20 mL sodium phosphate, 300 mM NaCl, and 500 mM imidazole, pH 7.4). The eluates were pooled and further purified by size-exclusion chromatography in a Tris buffer (20 mM Tris-HCl, and 50 mM NaCl, pH 7.4) using Sephadex G-50 (GE Life Sciences) column. Protein-containing fractions were pooled and concentrated by using an Amicon Centricon tube (10 kDa cut-off).

Expression and purification of PCNA. The sequences of PCNA and the cloning vector pET his6 TEV LIC were the gifts from Daniel Gerlich (Addgene, plasmid # 26461) and Scott Gradia (Addgene, plasmid # 29653), respectively. The sequence of PCNA (residue 1-255) was amplified by PCR using specific primers (Forward primer: 5’ – GGTTCCaatattATGTTCGAGGCGCGCCTGGTC – 3’; Reverse primer: 5’ – GGCCggatccTTAGATCTTGGGAGCCAAGTAGTA – 3’); *Ssp*I and *Bam*HI sites are indicated by lower case letters. PCNA construct was cloned into pET his6 TEV LIC

cloning vector. The pET his6 TEV LIC – PCNA plasmid was then transformed into NEB Turbo competent E. *coli* (NEB). Single colonies were picked randomly to screen for the presence of inserts. The cloning vector containing PCNA insert was then transformed into BL21 strain of *E. coli*. PCNA protein was expressed and purified as for the MBP-RasGRP1^{cat} protein.

Design of a disulfide bridge between the catalytically unformed RasGRP and PCNA to produce the catalytically competent engineered RasGRP. The program PyMOL was used to predict sites for introduction of disulfide bond in the catalytically competent engineered RasGRP. The parameters (bond angles and bond length) used in determining the acceptability of a particular disulfide bond are described in Figure A-4.[39]

Site-directed mutagenesis. Mutations were introduced to either the pET his6 MBP TEV LIC – RasGRP1^{cat} plasmid or the pET his6 TEV LIC – PCNA plasmid using the Phusion™ Site-Directed Mutagenesis Kit (Thermo Scientific). Asp375 of RasGRP1^{cat} was mutated to cysteine using specific primers (Forward primer: 5' – CCTGACTATCTGGAGTGCGGGAAAGTGAACGTC – 3'; Reverse primer: 5' – CATGGCTTCATACAGGGAGATGAGGTCCTT – 3'). Gly176 of PCNA was mutated to cysteine using specific primers (Forward primer: 5' – CAAGTGGAGAACTTTGCAATGGAAACA – 3'; Reverse primer: 5' – CAGAAAATTTCACTCCGTCTTTTGCAC – 3'). D375C RasGRP1^{cat} and G176C PCNA mutated plasmids were transformed into NEB Turbo competent *E*. *coli* (NEB) and subsequently into BL21 strain of *E. coli*. D375C RasGRP1^{cat} and G176C PCNA proteins were expressed and purified as for the MBP-RasGRP1^{cat} protein.

Formation of disulfide bond. Since D375C RasGRP1^{cat} and G176C PCNA proteins were originally stored in (20 mM Tris-HCl and 50 mM NaCl, pH 7.4), these proteins were first equilibrated with higher pH by using a gel filtration column pre-equilibrated with buffer A (100 mM Tris-HCl, 200 mM NaCl, and 1 mM EDTA, pH 8.7). The eluents were pooled and concentrated using an Amicon Centricon (10 kDa cut-off). 5,5'-dithiobis(2-nitrobenzoic acid) (DTNB) was used as a reaction mediator for the disulfide bonding formation between D375C RasGRP1^{cat} and G176C PCNA (Figure 2.2). A 40-fold molar access of DTNB (2 mg/mL) in 0.2 M potassium phosphate buffer (pH 7) was added to G176C PCNA (pH 8.7). After 2 hours of the incubation at room temperature, the mixture was desalted on a Sephadex G-25 (GE Life Sciences) column equilibrated in a buffer A. The fractions containing protein (G176C PCNA -TNB) were pooled and concentrated using an Amicon Centricon (10 kDa cut-off). D375C RasGRP1^{cat} (pH 8.7) was added to G176C PCNA -TNB following the 1:1 mixing molar ratio. This mixture was incubated for 24 hours at room temperature and then loaded onto a Sephadex G-75 (GE Life Sciences) column equilibrated in a Tris buffer. The protein peak was pooled and concentrated using an Amicon Centricon (10 kDa cut-off).

Loading mant-GDP on Ras. A reaction mixture was prepared by mixing 100 μM Ras, 2-folds molar excess of 2'-(or-3')-O-(N-Methylanthraniloyl) Guanosine 5'-Diphosphate (mant-GDP), 2 mM EDTA (pH 7.4), and 200 mM ammonium sulfate. The reaction was incubated at room temperature without shaking for 90 minutes and protected from light. During the incubation, Sephadex G-50 column was pre-equilibrated with a nucleotide exchange buffer (20 mM Tris-HCl, 50 mM NaCl, and 10 mM $MgCl_2$, pH 7.4). The entire reaction fraction was then loaded onto the G-50 column to remove unbound mant-GDP.

Step 1:

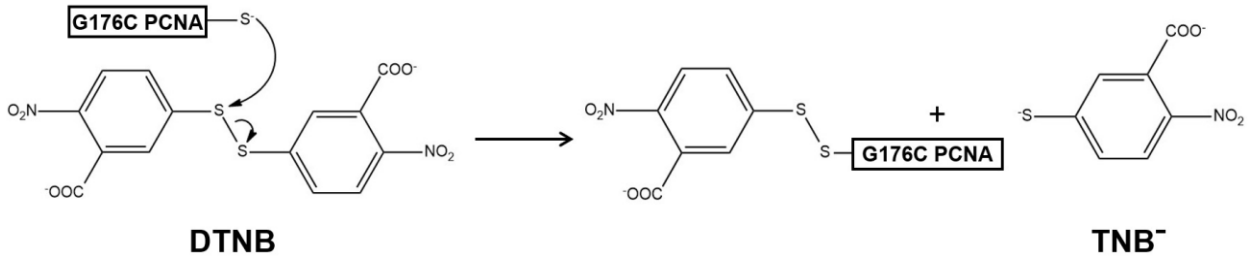

Step 2:

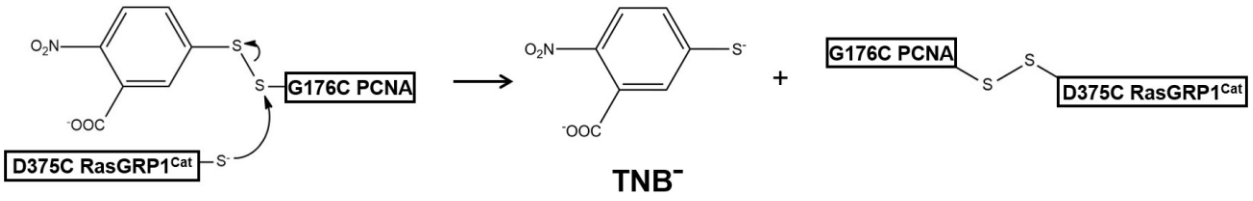

Figure 2.2. Mechanism of a disulfide-bridge formation between two cysteine residues by using DTNB.

In the first step, G176C PCNA was deprotonated to produce a cysteine thiolate sidechain by raising the pH from 7.4 to 8.7. The cysteine thiolate of G176C PCNA nucleophilic attacked on one of the two sulfur atoms of DTNB to form a disulfide bond between 2-nitro-5-thiobenzoic acid (TNB) and G176C PCNA and generate the colored product TNB. In the next reaction step, D375C RasGRP1^{cat} was deprotonated to produce a cysteine thiolate sidechain by raising the pH from 7.4 to 8.7, which in turn reacted with the G176C PCNA-TNB adduct from step 1 to produce a disulfide bonded G176C PCNA-D375C RasGRP1^{cat} (engineered RasGRP) and TNB.

After the eluents were pooled and concentrated using an Amicon Centricon (10 kDa cut-off), the mant-GDP loaded Ras product was placed in 1.5 mL centrifuge tubes wrapped around by aluminum foil to protect from light.

Nucleotide exchange assays. Various concentrations of labeled mant-GDP-bound Ras (0.2-20.0 μM) were added in nucleotide exchange assay buffer containing 1.0 μM RasGEF (catalytically unformed RasGRP or engineered RasGRP) and an excess amount of unlabeled GDP (1.0 mM). For each concentration of mant-GDP-bound Ras, changes in fluorescence intensities corresponding to the exchange of bound mant-GDP with unlabeled GDP by RasGEF were monitored over time at excitation wavelength (λ_{ex}) of 355 nm and emission wavelength (λ_{em}) of 448 nm using a fluorescence spectrometer (PerkinElmer LS 55).

Determination of the equilibrium dissociation constant. Ras was incubated with a 40-folds molar excess of rhodamine B (RB) at room temperature for 30 minutes (Figure C-2). The mixture was loaded onto the Sephadex G-25 column pre-equilibrated with the Tris buffer to remove the unbound RB. The eluents were pooled and concentrated using an Amicon Centricon (10 kDa cut-off). Various concentrations of Ras (0.6-10.0 μM) were added in the Tris buffer containing 1.0 μM RasGEF (catalytically unformed RasGRP or catalytically competent engineered RasGRP). For each concentration of Ras, change in the rhodamine fluorescence can be monitored at λ_{ex} of 554 nm and λ_{em} of 580 nm using a fluorescence spectrometer (PerkinElmer LS 55). The binding of RasGEF to Ras resulted in an increase in the intensity of the rhodamine fluorescence.

Results

Preparation of proteins. The purity of all protein samples in this study was more than 95% pure as determined by the SDS-PAGE analysis (Figure A-5). The concentrations of protein were measured using the Pierce™ BCA Protein Assay Kit (Thermo Fisher Scientific). Efforts to express and purify H-Ras and RasGRP1^{cat} proteins without soluble tags were unsuccessful. After the N-terminal maltose-binding protein (MBP) tag was removed, the proteins became insoluble. Therefore, MBP tag remained attached to the proteins to enhance the solubility.

Probing potential protein that function as mechanical fixture. The protein that mimicked plasma membrane was chosen from Protein Data Bank (PDB). Because there are more than 180,000 protein structures deposited in the PDB, some criteria were applied to narrow down for the searching of potential proteins: The chosen protein must be a monomeric form of protein that has the size in the range of 200-400 residues to sufficiently ensconce the catalytic site of RasGRP1^{cat}. The monomeric protein also preferably possesses a dome configuration to maintain the substrate Ras within the catalytic site of RasGRP1^{cat}. PCNA was chosen as a support protein because it fits the categories, and it also lacks nucleotide exchange activity.

Preparation of a disulfide bridge between the catalytically unformed RasGRP1^{cat} and PCNA. I first analyzed whether there was any free cysteine residue present at the protein surface that could form an unanticipating disulfide bridge between these two proteins. In the crystal structure of RasGRP1^{cat}, there is one free cysteine residue that exposes to the protein surface (Cys80). Similarly, PCNA also has one free cysteine residue that exposes to the protein surface (Cys81). The optimal range to form a

disulfide bridge between two cysteine residues is 1.6-2.4 Å.[39] However, the closest distance between the two residues Cys80 of RasGRP1^{cat} and Cys81 of PCNA can be 11.5 Å which is incompatible for the formation of disulfide bond. (Figure A-6). Accordingly, Cys80 residue in RasGRP1^{cat} and Cys81 residue in PCNA were excluded for the analysis of a potential disulfide bond formation between RasGRP1^{cat} and PCNA by using PyMOL.

By using the program PyMOL, I have analyzed 121 potential pairs of the potential mutants of loop 1A and 1B of PCNA and loop 2 of RasGRP1^{cat} (Figure 2.3 and Table A-1). The best mutant pair that satisfies the bond length and bond angle to have a disulfide bridge between RasGRP1^{cat} and PCNA was determined to be D375C of RasGRP1^{cat} and G176C of PCNA (Figure 2.4). Therefore, D375C of RasGRP1^{cat} and G176C of PCNA were produced by using PCR-based methods for site-directed mutagenesis (see Materials and Methods).

DTNB was used to crosslink D375C RasGRP1^{cat} with G176C PCNA that produces an engineered RasGRP (Figure 2.4). A SDS-PAGE analysis was then performed to examine whether the disulfide bond is formed between Cys375 of RasGRP1^{cat} and Cys176 of PCNA. As shown in lane 4 of Figure 2.5, the 117 kDa band of the catalytically competent engineered RasGRP was observed when the enzyme was kept in a buffer that lacks reducing agents. When the engineered enzyme was treated with a reducing agent such as *β*-mercaptoethanol, the enzyme was broken into a heavy chain (88 kDa) and a light chain (29 kDa) that represent, respectively, D375C RasGRP1^{cat} and G176C PCNA. These results together suggest that the two cysteine residues were successfully cross-linked with one another through a disulfide bond

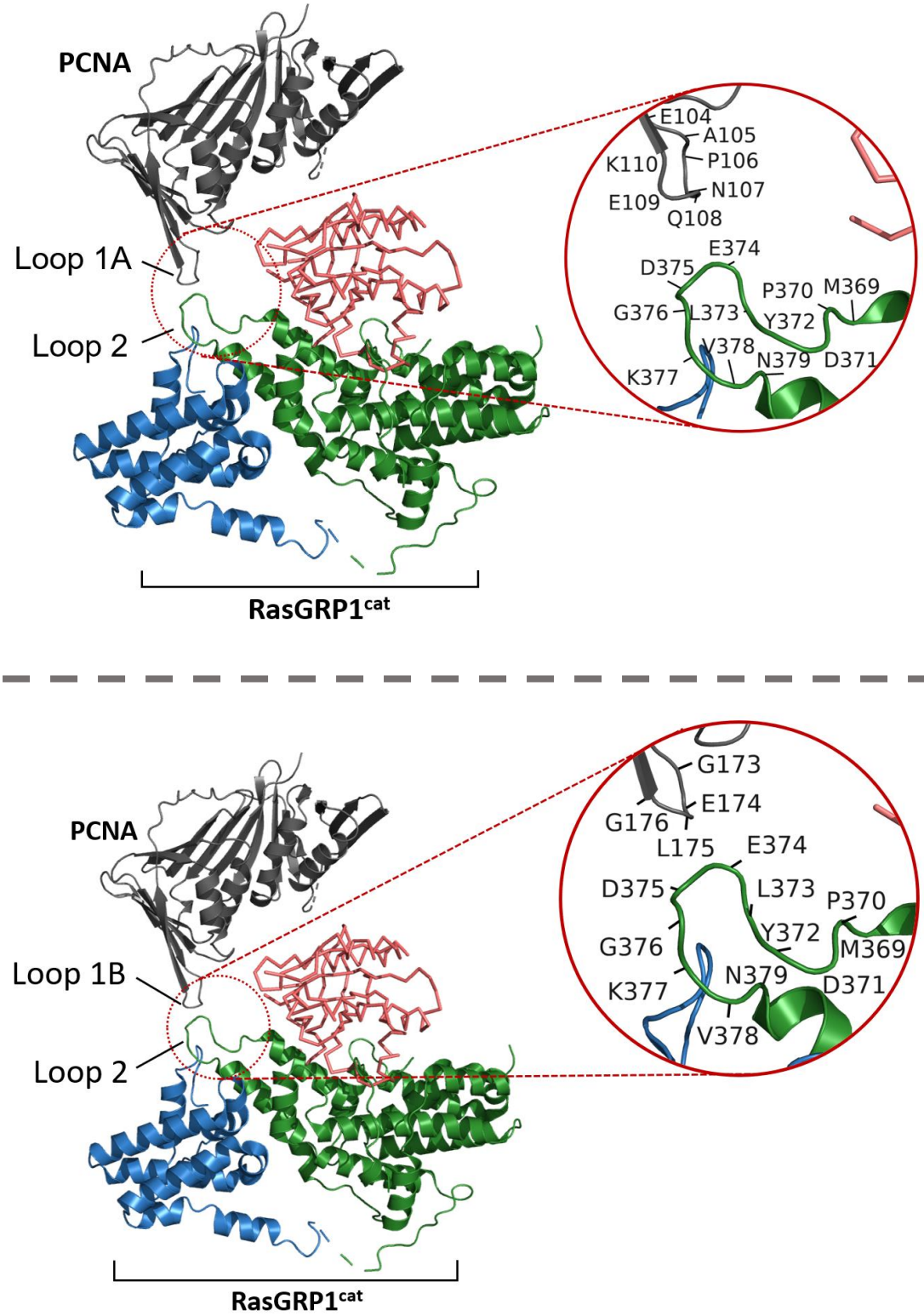

Figure 2.3. Potential residues for the mutation in Loop 1 of PCNA and Loop 2 of RasGRP1^{cat}.

Figure 2.3. Potential residues for mutation in Loop 1 of PCNA and Loop 2 of RasGRP1^{cat}.

Residues shown on Loop 1A (top) and 1B (bottom) of PCNA and Loop 2 of RasGRP1^{cat} are potential candidates for the mutation to cysteine. This mutation allows PCNA to link to RasGRP1^{cat} through a disulfide bridge to produce an engineered RasGRP (RasGRP1^{cat}-PCNA). These images were created using PyMOL. PCNA (PDB 6FCM) is shown in *gray*. REM and Cdc25 domains of RasGRP1^{cat} (PDB 4L9M) are, respectively, shown in *blue* and *green*. Ras (PDB 6AXG) is shown in *deep salmon*.

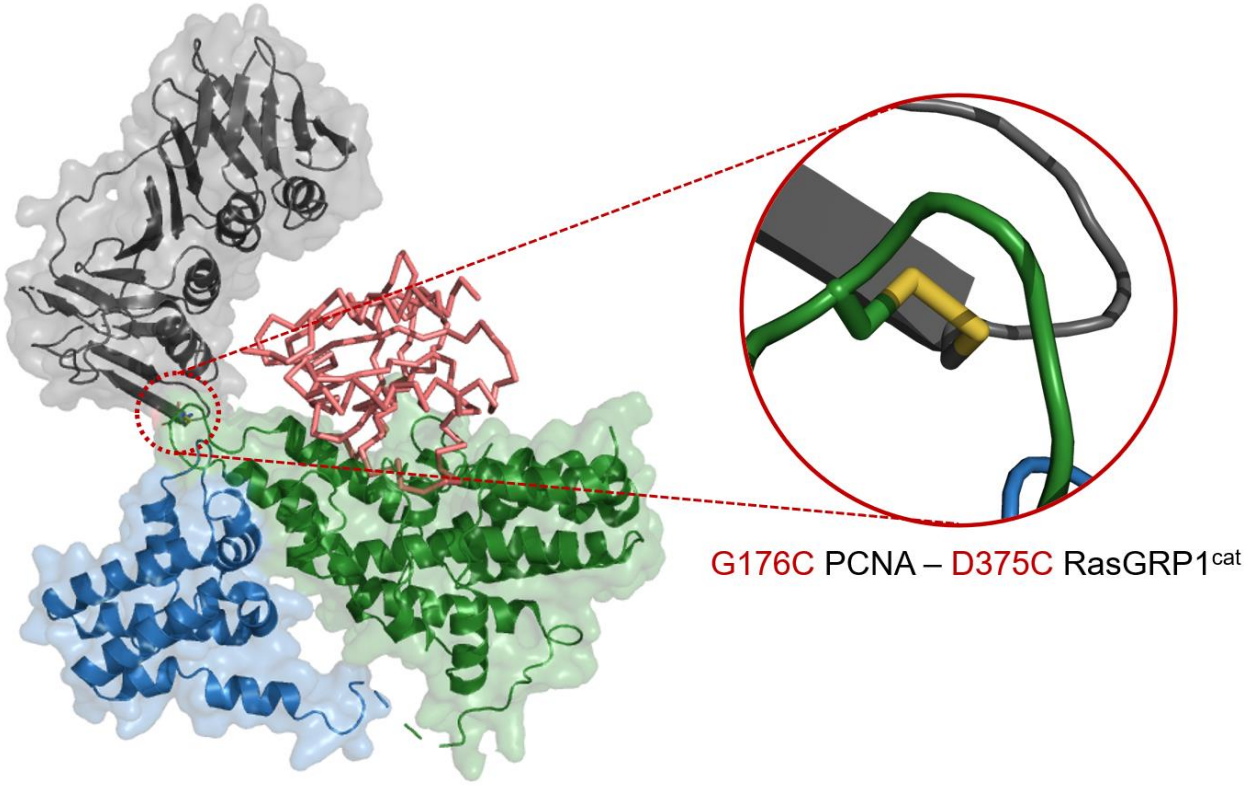

Figure 2.4. Configuration of the catalytically competent engineered RasGRP.

The best model protein configuration selected for the construction of the catalytically competent engineered RasGRP is shown as above. After checking 121 potential pairs of mutation from loop 1 of PCNA and loop 2 of RasGRP1^{cat} (see Table B-1), the pair selected that qualifies for the bond angle of disulfide bridge and forms suitable pocket size for Ras binding is D375C of RasGRP1^{cat} and G176C of PCNA. This image was created using PyMOL. PCNA (PDB 6FCM) is shown in *gray*. REM and Cdc25 domains of RasGRP1^{cat} (PDB 4L9M) are, respectively, shown in *blue* and *green*. A disulfide bond which connects PCNA and RasGRP1^{cat} is shown in yellow.

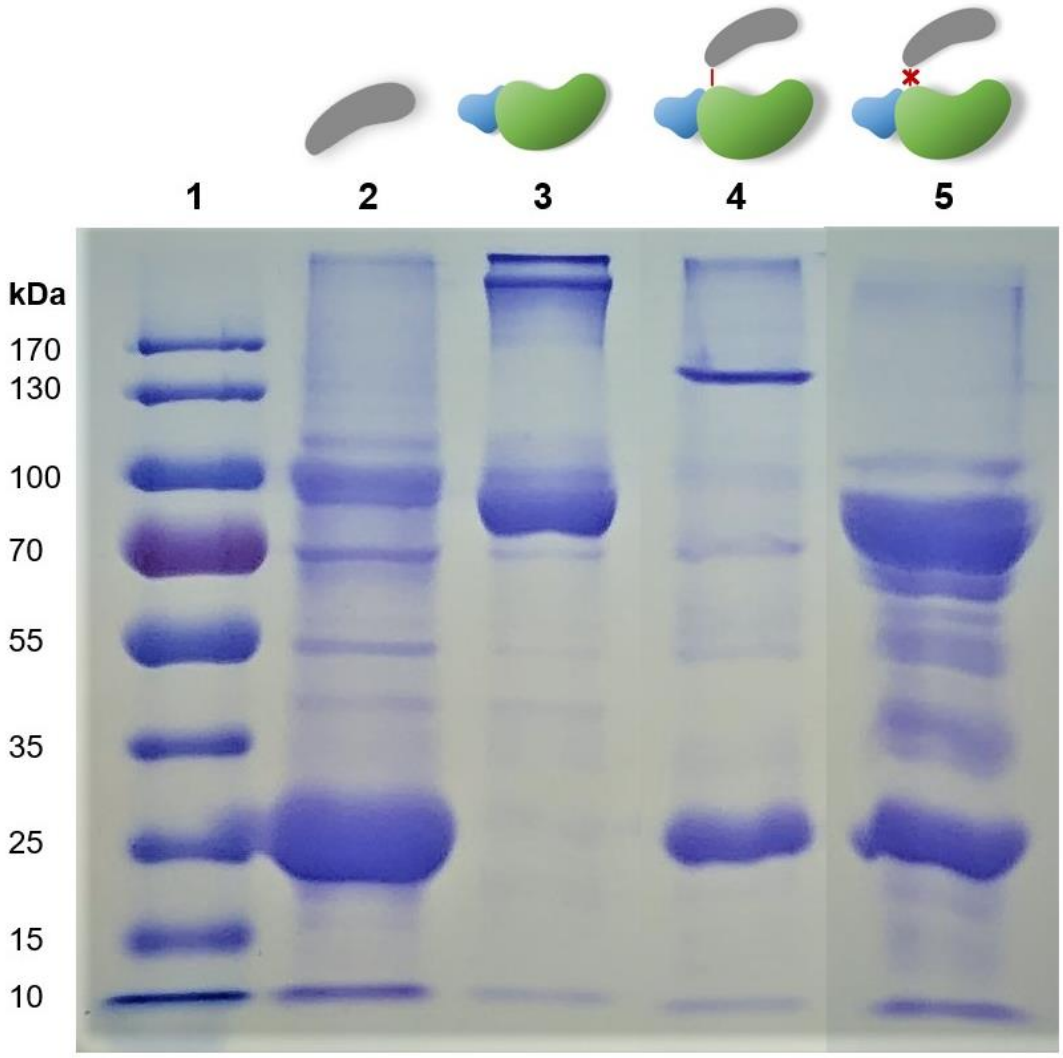

Figure 2.5. Analysis of the catalytically competent engineered RasGRP by using SDS-PAGE (8%).

Lane 1: Molecular weight standard. Lane 2: non-reduced (NR) G176C PCNA protein, 29 kDa. Lane 3: NR D75C RasGRP1^{cat} protein, 88 kDa. Lane 4: NR catalytically competent engineered RasGRP enzyme, 117 kDa. Lane 5: Reduced (R) catalytically competent engineered RasGRP enzyme. Samples in lane 2-4 were treated with sample buffer without *β*-mercaptoethanol. Sample in lane 5 was treated with sample buffer containing *β*-mercaptoethanol.

to form an engineered RasGRP.

Kinetic model of the RasGEF catalytic action. Scheme 1 summarizes the classic RasGEF-mediated Ras nucleotide exchange with classic kinetic parameters.[38]

$$\text{RasGEF} + \text{Ras•GDP} \underset{k_{-1}}{\overset{k_1}{\rightleftharpoons}} \text{RasGEF•Ras} \xrightarrow{k_{cat}} \text{RasGEF} + \text{Ras•GDP} \qquad \textbf{Scheme 1}$$

The parameter k_1 denotes the first-order rate constant of the substrate Ras•GDP association to RasGEF to produce the RasGEF•Ras binary complex. The parameter k_{-1} reflects the first-order rate constant of the dissociation of the RasGEF•Ras binary complex to produce RasGEF and Ras•GDP, and the parameter k_{cat} denotes the catalytic turnover rate constant for the production of RasGEF and Ras•GDP from the RasGEF•Ras binary complex. Michaelis-Menten constant (K_m) represents the ratio of all rate constants (($k_{-1}+k_{cat}$)/k_1), and Dissociation constant (K_D) expresses the ratio of rate constants without k_{cat} (k_{-1}/k_1). The values of the kinetic parameters, k_1, k_{-1}, and k_{cat}, reflect the rates of each of the given steps of the RasGEF catalytic actions (Scheme 1). Thus, a comparative analysis of these kinetic parameters of the engineered RasGRP with those of catalytically unformed RasGRP (RasGRP1^{cat}) will allow to examine whether membrane functions to enhance the substrate Ras binding and/or catalysis of RasGEF. The maximal reaction velocity (V_{max}) values of RasGEF for nucleotide exchange of Ras also were converted to k_{cat} by dividing V_{max} with total enzyme concentration [E_T] ($k_{cat} = V_{max}/[E_T]$). The parameter k_{cat} reflects the rate-limiting turnover number for the overall enzymatic process.

To determine the value of k_1 and k_{-1} of RasGEF for nucleotide exchange of Ras, K_m and K_D of RasGEF for nucleotide exchange of Ras were determined. K_m and K_D were then deconvoluted into k_1 and k_{-1} of RasGEF for nucleotide exchange of Ras by using equations (5) and (6) (Appendix C).[40] It is noteworthy that the values of K_m in combination with k_{cat} and K_D *per se* inherently implicate, respectively, the catalytic efficiency of enzyme and the enzyme substrate-binding feature. Thus, a comparison of the values of K_m in combination with k_{cat} and K_D of the engineered RasGRP with those of the catalytically unformed RasGRP was conducted within this study.

Comparative classic kinetic analyses of catalytic actions of catalytically unformed and engineered RasGRPs. The typical kinetic analysis of the RasGEF-mediated nucleotide exchange of Ras is to use the fluorescence mant-tagged GDP (mant-GDP). The mant-GDP was preloaded onto Ras to yield Ras•mant-GDP. RasGEF was added to the assay solution containing Ras•mant-GDP and an excess amount of unlabeled GDP. RasGEF mediates the nucleotide exchange of the Ras•mant-GDP with fresh unlabeled GDP in solution. The mant-GDP was displaced with the unlabeled GDP to produce Ras•GDP and free mant-GDP. The mant fluorescence intensity decreased during the RasGEF-mediated nucleotide exchange of Ras process because the mant fluorescence intensity of the free mant-GDP is lower than that of the Ras•mant-GDP.

Prior to the detailed analyses of kinetic parameters of engineered RasGRP for the nucleotide exchange of Ras, a preliminary analysis was performed to examine whether the mutation of Asp375 to cysteine to produce D375C RasGRP1^{cat} alters the nucleotide exchange rate of the catalytically unformed RasGRP1^{cat}. As shown in Figure 2.6, the initial rate values of wt RasGRP1^{cat} (5.0×10^{-2} s^{-1}) and D375C RasGRP1^{cat} (6.3

× 10^{-2} s^{-1}) were close to one another. The result suggested that the mutant D375C of RasGRP1^{cat} did not affect the catalytic function of RasGRP1^{cat}. Figure 2.6 also showed that the initial rate value of G176C PCNA (1.6 × 10^{-2} s^{-1}) is minimal. This result confirmed that the protein supporter G176C PCNA did not facilitate the nucleotide exchange of Ras. The initial rate values of D375C RasGRP1^{cat} in the presence and absence of G176C PCNA were, respectively, determined to be 5.8 × 10^{-2} s^{-1} and 6.3 × 10^{-2} s^{-1}(Figure 2.6). The similarity of the values indicated that G176C PCNA did not alter the catalytic function of D375C RasGRP1^{cat}, thereby suggesting that G176C PCNA only functions as a supporter or mechanical fixture that upholds the substrate Ras within the catalytic site of RasGRP1^{cat}.

Comparison of the catalytic efficiency of the catalytically unformed RasGRP with that of the catalytically competent engineered RasGRP. A comparison of the K_m and k_{cat} values of the catalytically unformed and competent engineered RasGRPs for Ras is shown in Table 2.1. The K_m values of the catalytically unformed and catalytically competent engineered RasGRPs are not significantly different (Table 2.1). The k_{cat} value of catalytically competent engineered RasGRP is ~2-fold larger than that of catalytically unformed RasGRP (Figure 2.7). The difference and similarity in the values of k_{cat} and K_m values, respectively, indicate that the difference in the catalytic efficiency (k_{cat}/K_m) of the catalytically unformed and catalytically competent engineered RasGRPs for Ras is primarily rooted in the k_{cat} step of the kinetic process of RasGRP. The catalytic efficiency was increased when the mechanical fixture (i.e., the PCNA supporter) was introduced to the catalytically unformed RasGRP enzyme. The results detailed

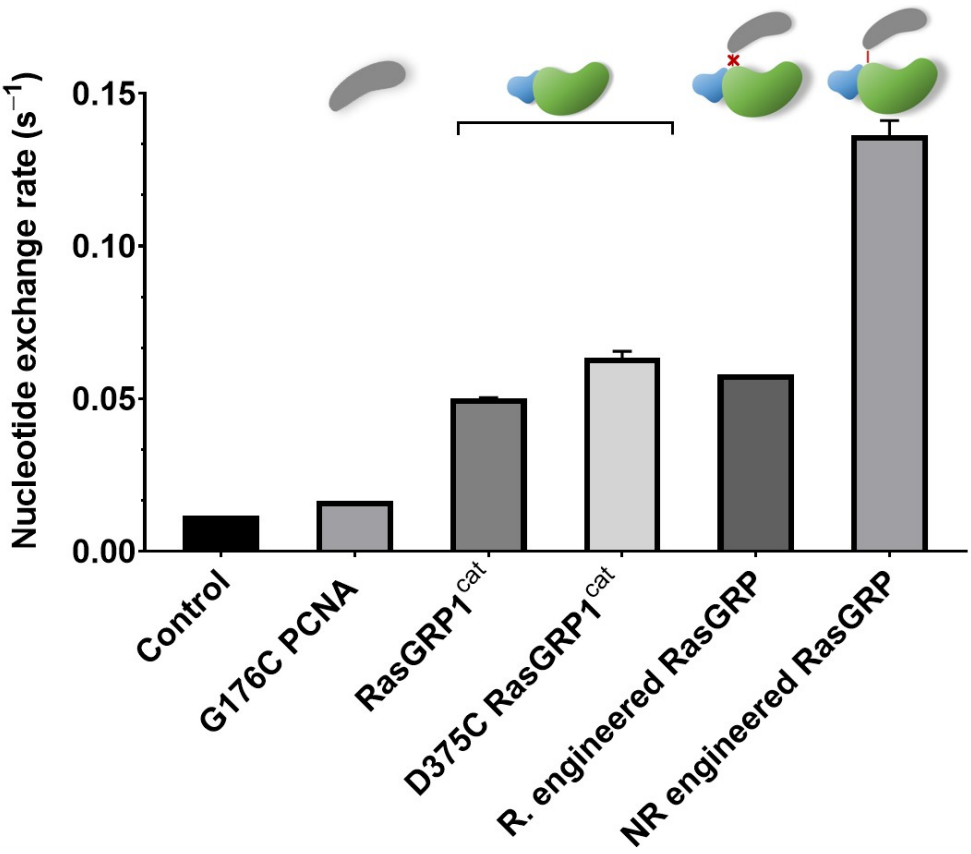

Figure 2.6. Comparison of the nucleotide exchange rates of Ras by various forms of RasGEF.

Mant-GDP-Ras (1.0 μM) was placed in the nucleotide exchange assay buffer containing 1.0 mM unlabeled GDP. In each experiment, a minimal amount of enzyme (1.0 μM) was added to facilitate the exchange of mant-GDP with unlabeled GDP. The control experiment also was performed in the absence of enzyme under the identical experimental conditions. The fluorescence intensity was monitored over time. The nucleotide exchange rate of Ras (the slope representing the change in fluorescence intensity over time) was determined. The plot was created using GraphPad Prism.

the membrane supplement hypothesis that membrane functions as a supporter that enhances the catalysis of RasGEF by properly aligning Ras with the docking site of RasGEF.

Comparison of the substrate Ras binding affinity to the catalytically unformed RasGRP with that of the catalytically competent engineered RasGRP. Titration of the catalytically unformed and catalytically competent engineered RasGRPs with the RB-Ras complex gives dissociation constants K_D of the catalytically unformed and catalytically competent engineered RasGRPs for nucleotide exchange of Ras (Figure 2.8). The results suggest that the catalytically competent engineered RasGRP has a tighter binding affinity with Ras compared to that of the catalytically unformed RasGRP. The K_D values along with kinetic constants K_m and k_{cat} can be used to determine the detailed rate constants k_1 and k_{-1} (see above *Kinetic model of RasGEF* section).[40] As shown in Table 2.1, k_1 value of the catalytically competent engineered RasGRP for Ras is ~2-fold larger than that of the catalytically unformed RasGRP. However, k_{-1} value of the catalytically competent engineered and catalytically unformed RasGRPs are similar to one another. The results suggest that the supporter PCNA in the catalytically competent engineered RasGRP functions to enhance the Ras association to but not dissociation from the catalytic site of RasGRP. The results also further specify the membrane supplement hypothesis as that membrane sustains the binding of Ras within the catalytic pocket to enhance the Ras association to the catalytic site of RasGEF.

	Catalytically unformed RasGRP (RasGRP1^{cat})	Catalytically competent engineered RasGRP (RasGRP1^{cat}–PCNA)
K_m (μM)	5.3 ± 0.5	4.5 ± 0.6
k_{cat} (min^{-1})	$1.1 \times 10^{-1} \pm 0.0$	$3.2 \times 10^{-1} \pm 0.1 \times 10^{-1}$
k_{cat}/K_m ($\mu M^{-1}min^{-1}$)	$2.1 \times 10^{-2} \pm 0.2 \times 10^{-2}$	$7.1 \times 10^{-2} \pm 0.9 \times 10^{-2}$
K_D (μM)	$3.3 \times 10^{-1} \pm 2.8 \times 10^{-1}$	$1.2 \times 10^{-1} \pm 1.5 \times 10^{-1}$
k_1 ($\mu M^{-1}min^{-1}$)	$3.9 \times 10^{-2} \pm 0.5 \times 10^{-2}$	$7.3 \times 10^{-2} \pm 1.0 \times 10^{-2}$
k_{-1} (min^{-1})	$1.3 \times 10^{-2} \pm 1.1 \times 10^{-2}$	$8.7 \times 10^{-3} \pm 1.2 \times 10^{-2}$

Table 2.1. Comparison of kinetic parameters of the catalytically unformed and catalytically competent engineered RasGRPs for the nucleotide exchange of Ras. The kinetic values K_m, k_{cat}, k_{cat}/K_m, K_D, k_1, and k_{-1} of RasGRP1^{cat} and the catalytically competent engineered RasGRP are listed in the table above. Detailed calculations of these values are shown in Appendix C. In the case of the catalytically unformed RasGRP, a catalytic amount of RasGRP1^{cat} (1.8 μM) was used for the nucleotide exchange assay of Ras. In the case of the catalytically competent engineered RasGRP, a catalytic amount of catalytically competent engineered RasGRP (1.0 μM) was used for the nucleotide exchange assay of Ras.

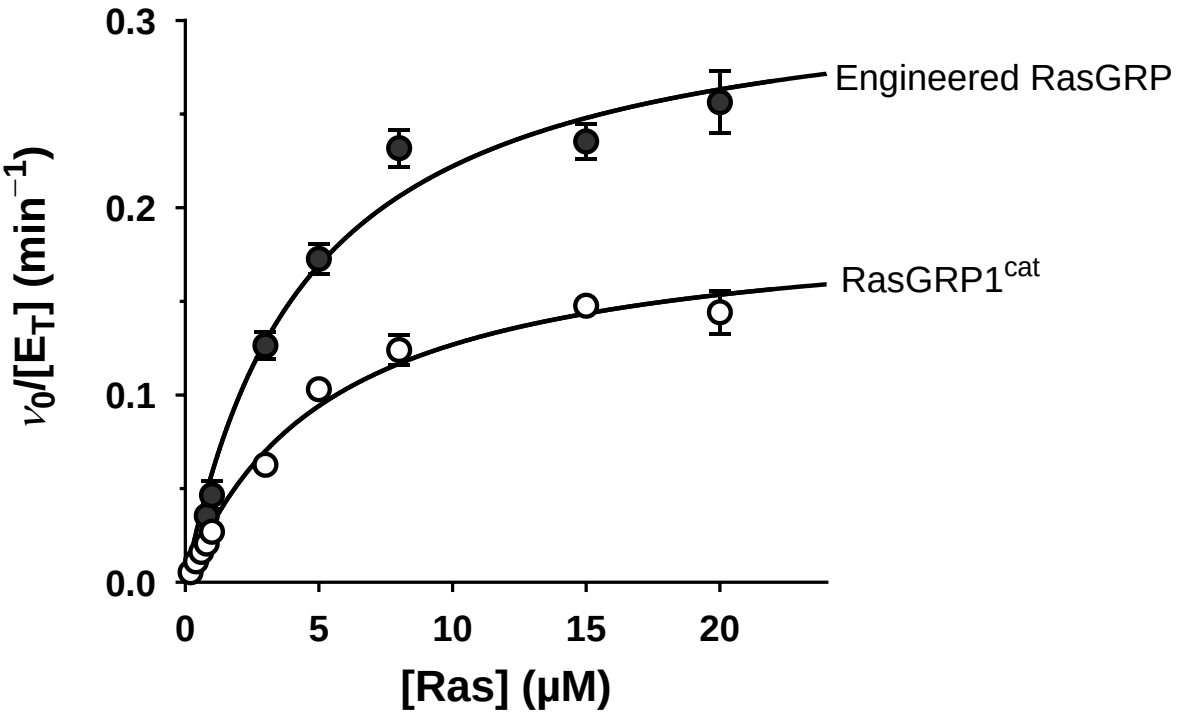

Figure 2.7. Determination of catalytic parameters of the catalytically unformed and catalytically competent engineered RasGRPs for the nucleotide exchange of Ras.

Mant-GDP-Ras (0.2-20.0 μM) was added to the nucleotide exchange buffer containing constant amount of catalytically unformed RasGRP (RasGRP1^{cat}) (1.8 μM) or the catalytically competent engineered RasGRP (1.0 μM). For each concentration of mant-GDP-Ras, change in the fluorescence intensity was monitored over time. The RasGRP activity was determined by obtaining the initial rates (v_0, the slope representing the change in fluorescence intensity over time). The V_{max} value of RasGRP was divided by total concentration of enzyme ([E_T]) ($V_{max}/[E_T]$) that yields the k_{cat} value. The plot of $v_0/[E_T]$ of RasGRP1^{cat} for the nucleotide exchange of Ras versus the concentration of mant-GDP-Ras was fit to a simple hyperbola (r^2 = 0.9828) to yield a K_m and k_{cat} values

Figure 2.7. Determination of catalytic parameters of the catalytically unformed and catalytically competent engineered RasGRPs for the nucleotide exchange of Ras. (cont.)

of 5.3 $\pm$ 0.5 μM and 1.1 × 10^{-1} min^{-1}, respectively. The plot of $\nu_0/[E_T]$ of the catalytically competent engineered RasGRP versus concentration of mant-GDP-Ras was fit to a simple hyperbola (r^2 = 0.9775) to have a K_m and k_{cat} values of 4.5 $\pm$ 0.6 μM and 3.2 × 10^{-1} $\pm$ 0.1 × $10^{-1}$$min^{-1}$, respectively.

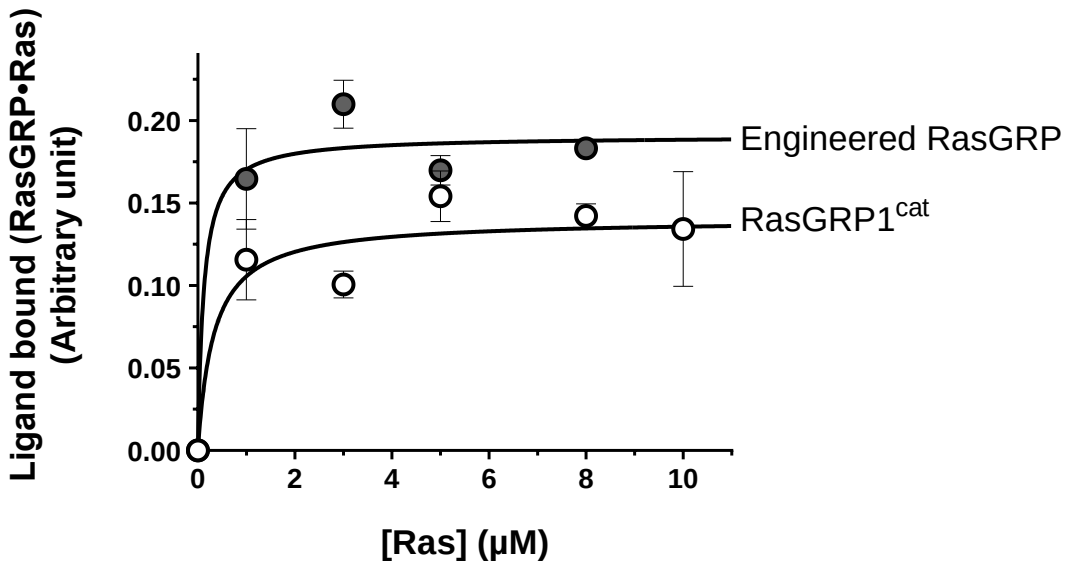

Figure 2.8. Determination of dissociation constants of the catalytically unformed and competent engineered RasGRPs for the nucleotide exchange of Ras.

In each case, RasGRP (1.0 μM) was titrated with various amounts of Ras (0.6-10.0 μM) and the corresponding changes in the fluorescence intensity were monitored. Fluorescence intensity of RB was monitored at λ_{ex} of 554 nm and λ_{em} of 580 nm. Changes in RB fluorescence intensity at 554 nm were converted to the ligand bound (RasGRP-Ras). Detailed calculations are shown in Appendix C. The plot of the ligand bound form of the catalytically unformed RasGRP (RasGRP1^{cat}) with Ras against concentration of Ras was fit to a simple hyperbola (r^2 = 0.8591) to yield a K_D value of $3.3 \times 10^{-1} \pm 2.8 \times 10^{-1}$ μM. The plot of the ligand bound form of the catalytically competent engineered RasGRP against concentration of Ras was fit to a simple hyperbola (r^2 = 0.9224) to yield a K_D value of $1.2 \times 10^{-1} \pm 1.5 \times 10^{-1}$ μM.

Discussion and Conclusion

In this study, the membrane supplement hypothesis is proposed. The hypothesis also was examined by using a model of engineered RasGRP. RasGRP1^{cat} is used as a form of the catalytically unformed RasGRP, and the catalytically competent RasGRP is obtained by producing an engineered form of RasGRP. The configuration of the engineered enzyme is unique as a foreign protein PCNA is linked to RasGRP1^{cat}. SOS^{cat} anchors the membrane through the binding of membrane-tethered Ras to its allosteric site. However, RasGRP1^{cat} does not have a site for membrane anchoring. Therefore, this project uses the foreign protein PCNA to mimic membrane as it proposed to serve as a supporter for the substrate Ras within the RasGRP1^{cat} catalytic site that aids the function of the RasGRP1^{cat} catalysis. The comparative kinetic analyses of the catalytically unformed RasGRP (RasGRP1^{cat}) together with the engineered RasGRP indicate that the K_m value of the engineered RasGRP is similar to that of the catalytically unformed RasGRP. However, the k_1 and k_{cat} values of the engineered RasGRP are ~2-fold larger than those of the catalytically unformed RasGRP. These results detailed the membrane supplement hypothesis as that the artificial supporter functions to enhance the substrate Ras binding to and its catalysis in the active site of RasGRP. The increase in the k_{cat} value of the engineered RasGRP is intriguing as it suggests that the supporter also aids the substrate Ras to correctly align and poise at the active site of the engineered RasGRP. The analyses result detailed membrane supplement hypothesis as membrane functions as a supporter for RasGEFs including SOS by securing, aligning, and posing the binding of the substrate Ras at the active site of RasGEFs. Therefore, when applied to SOS, the membrane binding of SOS activates

SOS, which in turn produces more of active Ras, thereby facilitating SOS autoactivation.

There are many signaling enzymes that are recruited to the membrane upon stimulation to carry out their biological processes. These enzymes are described as amphitropic proteins which maintain a compact structure in the cytosol and are fully activated when localized to cell membrane.[41-44] This research aims to answer the following questions: Why is the membrane translocation necessary to those amphitropic enzymes? And how does membrane-protein interaction affect enzyme catalysis? To address the role of the membrane in the kinetic action of amphitropic enzymes, I compare two potential outcomes of amphitropic enzyme after the membrane binding event. The first case relates to enzymes whose active site is brought distally from the membrane surface (Figure A-8). Membrane interaction induces a conformational change that helps expose the buried catalytic domain of these enzymes to the aqueous phase. Membrane in this case only functions to release autoinhibition effect of regulatory domains that in turn unmasks the active site of enzyme to enable substrate binding. Examples illustrating this case are protein kinase C (PKC), protein kinase B (PKB, or AKT), and 3-phosphoinositide-dependent protein kinase-1 (PDK1) (Figure A-9).[41, 45-46] In the second case, after amphitropic enzyme is recruited to membrane, catalytic site of enzyme is brought proximally toward the membrane surface (Figure A-8). In this case, membrane binding also displaces the autoinhibitory domains, which in turn results in fully activation of the enzyme. However, when considering the case of SOS, in the absence of regulatory domains, the membrane-bound SOS^{cat} still shows the enhancement in the catalytic function.[28] Therefore, in the second case, membrane

functions for not only the release of the autoinhibition of SOS by regulatory domains but also allowing the access of substrate to the catalytic site of SOS. The crystal structures of several enzymes which fall into the second case reveal that those enzymes usually display this common feature: the catalytic site possesses a very shallow binding pocket which challenges the bulky substrate to be accommodated inside the catalytic domain. This implies that the action of membrane that brings the catalytic site of enzyme into proximity with the membrane surface is not redundant. This study focuses on the unique role of membrane in the function of enzymes that fall into the second case. The purpose of this study also is to examine whether membrane contributes to orienting the substrate as well as improving its stability inside the catalytic cavity of enzyme, thus enhancing the enzyme catalytic activity.

The proposed kinetic roles of membrane localization in enzyme catalytic action are not limited to the RasGEF family proteins. There are many signaling enzymes which require the presence of membrane to enhance their catalysis. First example is phospholipase A_2 (PLA_2) enzymes which catalyze the hydrolysis of the ester bond at the *sn*-2 position of phospholipid substrates to liberate free fatty acids that are essential for inflammation and immune responses.[47-49] Most PLA_2s are water-soluble proteins which translocate to the membrane interface to access the phospholipid substrate and catalyze the hydrolysis.[48] PLA_2 exhibits high specificity for its phospholipid substrate; therefore, the binding of the enzyme to the membrane is distinct from the binding of a phospholipid substrate molecule to the catalytic site.[50] PLA_2 superfamily is classified into 6 types: cytosolic PLA_2 ($cPLA_2$), secreted PLA_2 ($sPLA_2$), calcium-independent PLA_2 ($iPLA_2$), platelet-activating factor acetylhydrolase (PAF-AH), lysosomal PLA_2 ($LPLA_2$),

and adipose-PLA_2 ($AdPLA_2$).[48] The association of PLA_2 with membrane can be driven by either electrostatic or non-electrostatic forces, and the membrane binding plays important role in its catalysis.[51] For example, aromatic residues at the interfacial binding surface of $sPLA_2$ are important for the interaction of enzyme with zwitterionic membrane.[51-52] It was shown that the aromatic residues Trp19, Trp64, and Phe61 play critical roles in the interfacial binding surface of cobra venom $sPLA_2$.[51] Mutations of these residues to Ala resulted in 30- to 50-fold decrease in the binding affinity of $sPLA_2$ to phospholipid substrate, and ~40-fold decrease in the relative catalytic efficiency of $sPLA_2$.[51] $cPLA_2$, another member in PLA_2 superfamily, binds to membrane upon the regulation of intramolecular calcium which binds to the calcium binding site at the C2 domain of $cPLA_2$.[48] A study demonstrated that the catalytic activity of $cPLA_2$ when $cPLA_2$ is recruited to membrane is 20-fold higher than that when the binding of $cPLA_2$ to membrane is restricted.[49] It is noteworthy that phospholipid substrate molecules are too bulky to be fully accommodated by the small active-site cavity of PLA_2s (figure A-10). Membrane might function as a supporter that brings the phospholipid substrates closer to the active site of PLA_2, and the interfacial binding might help stabilize the bulky substrate at the active site that in turn enhances the catalysis of PLA_2.

Another example is catechol-O-methyltransferase (COMT), an enzyme that plays critical role in the inactivation and metabolism of catecholamines (dopamine, epinephrine, and norepinephrine), catechol estrogens and catechol containing xenobiotics.[53] COMT is linked to Parkinson's disease which is characterized by dopaminergic neuronal loss that affects movement behavior.[53-54] COMT exists in two major forms, the membrane-bound COMT (MB-COMT) and the soluble COMT (S-

COMT).[53, 55-57] Human S-COMT and MB-COMT have similar catalytic mechanism following a sequential order in which COMT binds its cofactor S-adenosyl methionine (ADOMET) first, then Mg^{2+} ion, and catechol substrate at last.[53, 58] COMT transfers the methyl group from ADOMET to one of the phenylic hydroxyl groups of catechol substrate.[58] The only difference in the catalytic activity between S-COMT and MB-COMT is that the catechol substrate has higher affinity with MB-COMT than that with S-COMT.[56, 58-59] Kinetic analyses of COMT in hypothetical human brain showed that the K_m value of S-COMT for dopamine is ~14-fold higher than that of MB-COMT for dopamine.[58-59] These studies also proved that under physiological concentration of dopamine in the brain, MB-COMT methylates dopamine ~2-fold more rapidly than S-COMT.[58-59] A structural study of COMT observed that the interaction of MB-COMT with ADOMET induced a conformational change which drove the catalytic domain of MB-COMT toward the membrane surface (Figure A-11).[53] Based on these kinetic and structural evidences, I speculate that membrane functions as a supporter which holds the catechol substrate in the active site of COMT through orienting the catalytic domain of COMPT close to the membrane surface that in turn stabilizes the substrate binding and enhances the catalysis of MB-COMT.

The last example to point out is Recoverin, a member of the EF-hand superfamily. Recoverin is a neuronal calcium sensor protein which is recruited to membrane to be fully activated.[60-62] Recoverin is expressed in retinal photoreceptor cells and originally purified from retinal rod outer segments (ROS) of vertebrates.[62-63] Recoverin consists of four EF-hands, but only two of them (EF-hand 2 and 3) bind Ca^{2+} to initiate the inactivation of rhodopsin kinase (RK).[63-64] The N-terminal myristoyl group

of recoverin is regulated upon the change of intracellular Ca^{2+}.[63] In the light, when the concentration of Ca^{2+} is low, the membrane-bound RK (substrate of recoverin) terminates the activity of photoexcited rhodopsin by phosphorylating it.[65] In the meantime, recoverin in the cytoplasm sequesters the myristoyl group inside its hydrophobic cleft.[63-64] This compact structure maintains recoverin at the cytoplasm due to the loss of binding affinity with membrane.[63] In the dark, at high concentration of Ca^{2+}, recoverin is recruited to membrane to stabilizes the methylated form of RK to prevent the phosphorylation of RK on rhodopsin.[63, 65] Specifically, Ca^{2+} first interacts with EF-hand 3 of recoverin that in turn triggers a rearrangement of EF-hand 2; then the binding of Ca^{2+} to EF-hand 2 of recoverin leads to the exposure of the buried myristoyl group to aqueous environment that in turn enables the insertion of myristoyl group of recoverin into the ROS disk membrane to inactivate RK.[62, 64, 66] The myristoyl group is shown to be primarily responsible for the anchoring of recoverin to membrane.[63] Explicitly, myristoylated recoverin was shown to be ~12-fold more active than the nonmyristoylated recoverin.[67] It was also proven that the inactivation of RK by recoverin decreased ~7-fold in the absence of membrane.[65] I notice that RK (66 kDa) is too bulky compared with the small size of recoverin (23 kDa) (Figure A-12). Therefore, in this case, membrane might play a role as supporter which enhance the binding of recoverin to RK, thus inactivating the phosphorylation of RK on the light-sensitive rhodopsin.

It is notable that there was no clear rationalization for the role of membrane in the enhanced kinetic features of amphitropic enzymes upon their binding to membrane. The membrane supplement hypothesis firstly provides an explanation for the effect of membrane on the catalysis of amphitropic enzymes with a classic kinetic view. On the

basic of the kinetic analysis within this research, it can be explicated that many amphitropic enzymes are catalytically unformed. This is because amphitropic enzymes possess a shallow cavity at their active sites. The shallow cavity of their active sites is a challenge to secure their bulky substrates. The challenge is nonetheless overcome by the binding of amphitropic enzymes to membrane, in which supports to place and precisely orient the bulky substrate within their catalytic sites, thereby enhancing their catalytic actions. It is possible that, in the kinetic perspectives, the common feature of the shallow catalytic sites of amphitropic enzymes that can be accommodated by membrane is evolved as an "on/off switch" for the regulations of these enzyme functions: their binding to membrane is the kinetically "on" state, whereas their dissociation from membrane is the kinetically "off" state.

I would anticipate that the results shown within this study that support the membrane supplement hypothesis will provide insight into the general kinetic mechanism of the action of amphitropic enzymes associated with their membrane-binding interactions. Finally, it must be emphasized that some factors such as alternating membrane compositions or targeting potential key protein residues near the binding interface between amphitropic enzymes and membrane might be involved in the control of the binding strength of substrate to the catalytic domain of membrane-bound enzyme.

References

1. Heo, J.; Gao, G.; Campbell, S. L., pH-Dependent Perturbation of Ras− Guanine Nucleotide Interactions and Ras Guanine Nucleotide Exchange. *Biochemistry* **2004,** *43* (31), 10102-10111.

2. Campbell, S. L.; Khosravi-Far, R.; Rossman, K. L.; Clark, G. J.; Der, C. J., Increasing complexity of Ras signaling. *Oncogene* **1998,** *17* (11), 1395-1413.

3. Wittinghofer, A.; Pal, E. F., The structure of Ras protein: a model for a universal molecular switch. *Trends in biochemical sciences* **1991,** *16*, 382-387.

4. Adjei, A. A., Blocking oncogenic Ras signaling for cancer therapy. *Journal of the National Cancer Institute* **2001,** *93* (14), 1062-1074.

5. Zenonos, K.; Kyprianou, K., RAS signaling pathways, mutations and their role in colorectal cancer. *World journal of gastrointestinal oncology* **2013,** *5* (5), 97.

6. Fehrenbacher, N.; Bar-Sagi, D.; Philips, M., Ras/MAPK signaling from endomembranes. *Molecular oncology* **2009,** *3* (4), 297-307.

7. Devlin, T. M., *Textbook of biochemistry*. John Wiley & Sons: 2011.

8. Vojtek, A. B.; Der, C. J., Increasing complexity of the Ras signaling pathway. *Journal of Biological Chemistry* **1998,** *273* (32), 19925-19928.

9. Reuter, C. W.; Morgan, M. A.; Bergmann, L., Targeting the Ras signaling pathway: a rational, mechanism-based treatment for hematologic malignancies? *Blood, The Journal of the American Society of Hematology* **2000,** *96* (5), 1655-1669.

10. Ward, A. F.; Braun, B. S.; Shannon, K. M., Targeting oncogenic Ras signaling in hematologic malignancies. *Blood, The Journal of the American Society of Hematology* **2012,** *120* (17), 3397-3406.

11. Wennerberg, K.; Rossman, K. L.; Der, C. J., The Ras superfamily at a glance. *Journal of cell science* **2005,** *118* (5), 843-846.

12. Spiegel, J.; Cromm, P. M.; Zimmermann, G.; Grossmann, T. N.; Waldmann, H., Small-molecule modulation of Ras signaling. *Nature chemical biology* **2014,** *10* (8), 613-622.

13. Self, A.; Hall, A., Measurement of intrinsic nucleotide exchange and GTP hydrolysis rates. *Methods in enzymology* **1995,** *256*, 67-76.

14. Bivona, T. G.; Philips, M. R., Ras pathway signaling on endomembranes. *Current opinion in cell biology* **2003,** *15* (2), 136-142.

15. Bos, J. L.; Rehmann, H.; Wittinghofer, A., GEFs and GAPs: critical elements in the control of small G proteins. *Cell* **2007,** *129* (5), 865-877.

16. Rojas, J. M.; Santos, E., Ras-gefs and Ras gaps. In *RAS Family GTPases*, Springer: 2006; pp 15-43.

17. Stanley, R. J.; Thomas, G. M., Activation of G proteins by guanine nucleotide exchange factors relies on GTPase activity. *PloS one* **2016,** *11* (3), e0151861.

18. Trahey, M.; Milley, R. J.; Cole, G. E.; Innis, M.; Paterson, H.; Marshall, C.; Hall, A.; McCormick, F., Biochemical and biological properties of the human N-ras p21 protein. *Molecular and cellular biology* **1987,** *7* (1), 541-544.

19. Nakhaei-Rad, S.; Haghighi, F.; Nouri, P.; Rezaei Adariani, S.; Lissy, J.; Kazemein Jasemi, N. S.; Dvorsky, R.; Ahmadian, M. R., Structural fingerprints, interactions, and signaling networks of RAS family proteins beyond RAS isoforms. *Critical reviews in biochemistry and molecular biology* **2018,** *53* (2), 130-156.

20. Roose, J.; Jun, J.; Rubio, I.; Roose, J., Regulation of Ras exchange factors and cellular localization of Ras activation by lipid messengers in T cells. **2013**.

21. Hennig, A.; Markwart, R.; Esparza-Franco, M. A.; Ladds, G.; Rubio, I., Ras activation revisited: role of GEF and GAP systems. *Biological chemistry* **2015,** *396* (8), 831-848.

22. Roose, J. P.; Mollenauer, M.; Ho, M.; Kurosaki, T.; Weiss, A., Unusual interplay of two types of Ras activators, RasGRP and SOS, establishes sensitive and robust Ras activation in lymphocytes. *Molecular and cellular biology* **2007,** *27* (7), 2732-2745.

23. Buday, L.; Downward, J., Many faces of Ras activation. *Biochimica et Biophysica Acta (BBA)-Reviews on Cancer* **2008,** *1786* (2), 178-187.

24. Quilliam, L. A., New insights into the mechanisms of SOS activation. *Science's STKE* **2007,** *2007* (414), pe67-pe67.

25. Roose, J.; Iwig, J.; Vercoulen, Y.; Das, R.; Barros, T.; Limnander, A.; Che, Y.; Pelton, J.; Wemmer, D.; Roose, J., Structural analysis of autoinhibition in the Ras-specific exchange factor RasGRP1. **2013**.

26. Sondermann, H.; Soisson, S. M.; Boykevisch, S.; Yang, S.-S.; Bar-Sagi, D.; Kuriyan, J., Structural analysis of autoinhibition in the Ras activator Son of sevenless. *Cell* **2004,** *119* (3), 393-405.

27. Sondermann, H.; Soisson, S. M.; Bar-Sagi, D.; Kuriyan, J., Tandem histone folds in the structure of the N-terminal segment of the ras activator Son of Sevenless. *Structure* **2003,** *11* (12), 1583-1593.

28. Gureasko, J.; Galush, W. J.; Boykevisch, S.; Sondermann, H.; Bar-Sagi, D.; Groves, J. T.; Kuriyan, J., Membrane-dependent signal integration by the Ras activator Son of sevenless. *Nature Structural and Molecular Biology* **2008,** *15* (5), 452.

29. Rojas, J. M.; Oliva, J. L.; Santos, E., Mammalian son of sevenless Guanine nucleotide exchange factors: old concepts and new perspectives. *Genes & cancer* **2011,** *2* (3), 298-305.

30. Yadav, K. K.; Bar-Sagi, D., Allosteric gating of Son of sevenless activity by the histone domain. *Proceedings of the National Academy of Sciences* **2010,** *107* (8), 3436-3440.

31. Takai, Y.; Sasaki, T.; Matozaki, T., Small GTP-binding proteins. *Physiological reviews* **2001,** *81* (1), 153-208.

32. Ksionda, O.; Limnander, A.; Roose, J. P., RasGRP Ras guanine nucleotide exchange factors in cancer. *Frontiers in biology* **2013,** *8* (5), 508-532.

33. Fuller, D. M.; Zhu, M.; Song, X.; Ou-Yang, C.-w.; Sullivan, S. A.; Stone, J. C.; Zhang, W., Regulation of RasGRP1 function in T cell development and activation by its unique tail domain. *PloS one* **2012,** *7* (6), e38796.

34. Smith, M. J.; Neel, B. G.; Ikura, M., NMR-based functional profiling of RASopathies and oncogenic RAS mutations. *Proceedings of the National Academy of Sciences* **2013,** *110* (12), 4574-4579.

35. Lee, Y. K.; Low-Nam, S. T.; Chung, J. K.; Hansen, S. D.; Lam, H. Y. M.; Alvarez, S.; Groves, J. T., Mechanism of SOS PR-domain autoinhibition revealed by single-molecule assays on native protein from lysate. *Nature communications* **2017,** *8* (1), 1-11.

36. Gureasko, J.; Kuchment, O.; Makino, D. L.; Sondermann, H.; Bar-Sagi, D.; Kuriyan, J., Role of the histone domain in the autoinhibition and activation of the Ras activator Son of Sevenless. *Proceedings of the National Academy of Sciences* **2010,** *107* (8), 3430-3435.

37. Christensen, S. M.; Tu, H.-L.; Jun, J. E.; Alvarez, S.; Triplet, M. G.; Iwig, J. S.; Yadav, K. K.; Bar-Sagi, D.; Roose, J. P.; Groves, J. T., One-way membrane trafficking of SOS in receptor-triggered Ras activation. *Nature structural & molecular biology* **2016,** *23* (9), 838-846.

38. Hoang, H. M.; Umutesi, H. G.; Heo, J., Allosteric autoactivation of SOS and its kinetic mechanism. *Small GTPases* **2019**, 1-16.

39. Sowdhamini, R.; Srinivasan, N.; Shoichet, B.; Santi, D. V.; Ramakrishnan, C.; Balaram, P., Stereochemical modeling of disulfide bridges. Criteria for introduction into proteins by site-directed mutagenesis. *Protein Engineering, Design and Selection* **1989,** *3* (2), 95-103.

40. Heo, J.; Thapar, R.; Campbell, S. L., Recognition and activation of Rho GTPases by Vav1 and Vav2 guanine nucleotide exchange factors. *Biochemistry* **2005,** *44* (17), 6573-6585.

41. Downward, J., Mechanisms and consequences of activation of protein kinase B/Akt. *Current opinion in cell biology* **1998,** *10* (2), 262-267.

42. Burn, P., Talking point Amphitropic proteins: a new class of membrane proteins. *Trends in biochemical sciences* **1988,** *13* (3), 79-83.

43. Epand, R. M., Lipid polymorphism and protein–lipid interactions. *Biochimica et Biophysica Acta (BBA)-Reviews on Biomembranes* **1998,** *1376* (3), 353-368.

44. Halskau, O.; Muga, A.; Martínez, A., Linking new paradigms in protein chemistry to reversible membrane-protein interactions. *Current Protein and Peptide Science* **2009,** *10* (4), 339-359.

45. Oancea, E.; Meyer, T., Protein kinase C as a molecular machine for decoding calcium and diacylglycerol signals. *Cell* **1998,** *95* (3), 307-318.

46. Anderson, K. E.; Coadwell, J.; Stephens, L. R.; Hawkins, P. T., Translocation of PDK-1 to the plasma membrane is important in allowing PDK-1 to activate protein kinase B. *Current Biology* **1998,** *8* (12), 684-691.

47. Kim, J.; Lee, K. W.; Lee, H. J., Polyphenols suppress and modulate inflammation: possible roles in health and disease. In *Polyphenols in human health and disease*, Elsevier: 2014; pp 393-408.

48. Mouchlis, V. D.; Bucher, D.; McCammon, J. A.; Dennis, E. A., Membranes serve as allosteric activators of phospholipase A2, enabling it to extract, bind, and hydrolyze phospholipid substrates. *Proceedings of the National Academy of Sciences* **2015,** *112* (6), E516-E525.

49. Lichtenbergova, L.; Yoon, E. T.; Cho, W., Membrane penetration of cytosolic phospholipase A2 is necessary for its interfacial catalysis and arachidonate specificity. *Biochemistry* **1998,** *37* (40), 14128-14136.

50. Ghomashchi, F.; Yu, B. Z.; Berg, O.; Jain, M. K.; Gelb, M. H., Interfacial catalysis by phospholipase A2: substrate specificity in vesicles. *Biochemistry* **1991,** *30* (29), 7318-7329.

51. Sumandea, M.; Das, S.; Sumandea, C.; Cho, W., Roles of aromatic residues in high interfacial activity of Naja naja atra phospholipase A2. *Biochemistry* **1999,** *38* (49), 16290-16297.

52. Gaspar, D.; Lúcio, M.; Rocha, S.; Lima, J. C.; Reis, S., Changes in PLA2 activity after interacting with anti-inflammatory drugs and model membranes: evidence for the involvement of tryptophan residues. *Chemistry and physics of lipids* **2011,** *164* (4), 292-299.

53. Magarkar, A.; Parkkila, P.; Viitala, T.; Lajunen, T.; Mobarak, E.; Licari, G.; Cramariuc, O.; Vauthey, E.; Róg, T.; Bunker, A., Membrane bound COMT isoform is an interfacial enzyme: general mechanism and new drug design paradigm. *Chemical Communications* **2018,** *54* (28), 3440-3443.

54. Müller, T., Catechol-O-methyltransferase inhibitors in Parkinson's disease. *Drugs* **2015,** *75* (2), 157-174.

55. LUNDSTR, K.; Salminen, M.; Jalanko, A.; SAVOLAINEN, R.; Ulmanen, I., Cloning and Characterization of Human Placental Catechol--Methyltransferase cDNA. *DNA and cell biology* **1991,** *10* (3), 181-189.

56. Chen, J.; Song, J.; Yuan, P.; Tian, Q.; Ji, Y.; Ren-Patterson, R.; Liu, G.; Sei, Y.; Weinberger, D. R., Orientation and cellular distribution of membrane-bound catechol-O-methyltransferase in cortical neurons: implications for drug development. *Journal of biological chemistry* **2011,** *286* (40), 34752-34760.

57. Myöhänen, T. T.; Schendzielorz, N.; Männistö, P. T., Distribution of catechol-O-methyltransferase (COMT) proteins and enzymatic activities in wild-type and soluble COMT deficient mice. *Journal of neurochemistry* **2010,** *113* (6), 1632-1643.

58. Vidgren, J.; Ovaska, M., Structural aspects in the inhibitor design of catechol O-methyltransferase. In *Structure-based drug design*, Routledge: 2018; pp 343-363.

59. Reenilä, I.; Männistö, P., Catecholamine metabolism in the brain by membrane-bound and soluble catechol-o-methyltransferase (COMT) estimated by enzyme kinetic values. *Medical hypotheses* **2001,** *57* (5), 628-632.

60. Senin, I. I.; Fischer, T.; Komolov, K. E.; Zinchenko, D. V.; Philippov, P. P.; Koch, K.-W., Ca2+-myristoyl switch in the neuronal calcium sensor recoverin requires different functions of Ca2+-binding sites. *Journal of Biological Chemistry* **2002,** *277* (52), 50365-50372.

61. Potvin-Fournier, K.; Valois-Paillard, G.; Lefèvre, T.; Cantin, L.; Salesse, C.; Auger, M., Membrane fluidity is a driving force for recoverin myristoyl immobilization in zwitterionic lipids. *Biochemical and biophysical research communications* **2017,** *490* (4), 1268-1273.

62. BURGOYNE, R. D.; WEISS, J. L., The neuronal calcium sensor family of Ca2+-binding proteins. *Biochemical Journal* **2001,** *353* (1), 1-12.

63. Desmeules, P.; Grandbois, M.; Bondarenko, V. A.; Yamazaki, A.; Salesse, C., Measurement of Membrane Binding between Recoverin, a Calcium-Myristoyl Switch Protein, and Lipid Bilayers byAFM-Based Force Spectroscopy. *Biophysical journal* **2002,** *82* (6), 3343-3350.

64. Senin, I. I.; Vaganova, S. A.; Weiergräber, O. H.; Ergorov, N. S.; Philippov, P. P.; Koch, K.-W., Functional restoration of the Ca2+-myristoyl switch in a recoverin mutant. *Journal of molecular biology* **2003,** *330* (2), 409-418.

65. Kutuzov, M. A.; Andreeva, A. V.; Bennett, N., Regulation of the methylation status of G protein-coupled receptor kinase 1 (rhodopsin kinase). *Cellular signalling* **2012,** *24* (12), 2259-2267.

66. Calvez, P.; Demers, E.; Boisselier, E.; Salesse, C., Analysis of the contribution of saturated and polyunsaturated phospholipid monolayers to the binding of proteins. *Langmuir* **2011,** *27* (4), 1373-1379.

67. Erickson, M. A.; Lagnado, L.; Zozulya, S.; Neubert, T. A.; Stryer, L.; Baylor, D. A., The effect of recombinant recoverin on the photoresponse of truncated rod photoreceptors. *Proceedings of the National Academy of Sciences* **1998,** *95* (11), 6474-6479.

APPENDIX A: FIGURES

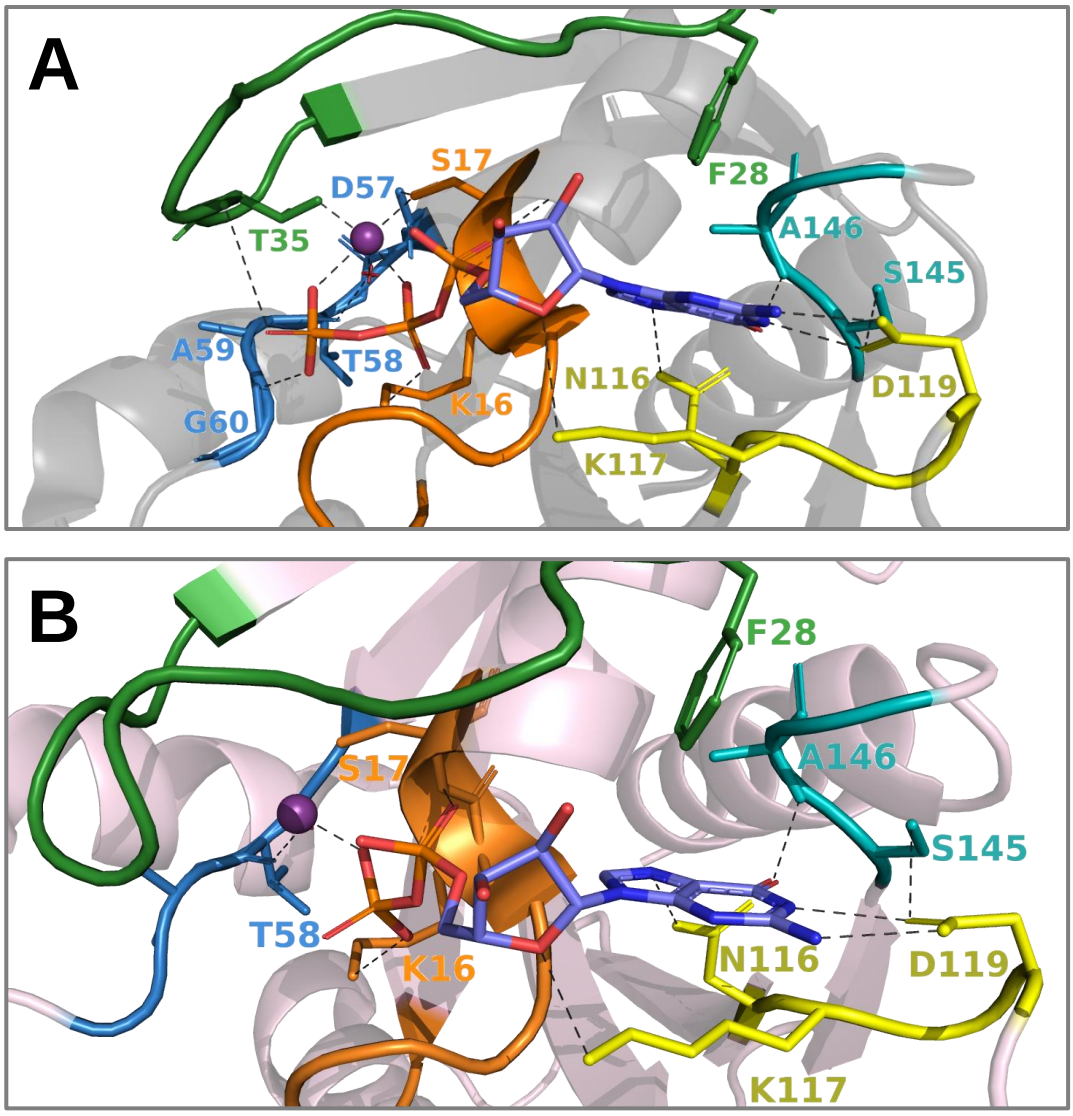

Figure A-1. Conformational change in the Ras switch regions upon its binding of GTP and GDP.

(A) Key Ras residues participating in the Ras GTP-binding interaction (PDB 2CE2). Ras protein is shown in light gray. Magnesium ion (Mg^{2+}) is shown in purple. P-loop (shown in *orange*) wraps around and interacts with the β- and γ-phosphates of the guanine nucleotide. In addition, the hydroxyl group of the serine coordinates with the magnesium ion. Switch I (shown in *green*) contains a conserved threonine residue involving in

Figure A-1. Conformational change in the Ras switch regions upon its binding of GTP and GDP. (Cont.)

Mg^{2+} coordination and sensing the presence of γ-phosphate of the guanine nucleotide. Besides, the purine base of guanine nucleotide is stabilized by the phenylalanine residue on switch I region. Switch II region (shown in *blue*) involves in the binding of Mg^{2+} and the γ-phosphate of the guanine nucleotide. G4 region (shown in *yellow*) interacts with the guanine base. The asparagine and aspartate of G4 form hydrogen bonds with nitrogen and oxygen atoms of the purine. The amino group of lysine also forms part of binding pocket of the guanine base by interacting with the oxygen of the ribose ring. In G5 region (shown in *cyan*), the main chain NH of alanine binds to the oxygen of the purine, and the serine side chain aids to stabilize the aspartate of the adjacent loop G4. **(B)** Key Ras residues involve in the Ras GDP binding interaction (PDB 2CL7). Ras protein is shown in *light pink*. Other color codes are the same as in **(A)**. When the γ-phosphate of the guanine nucleotide is cleaved off, the switch I and switch II regions become mobile since the interactions of the γ-phosphate with the side chain hydroxyl group of threonine in switch I and the main chain nitrogen of glycine in switch II are lost. These images were created using PyMOL.

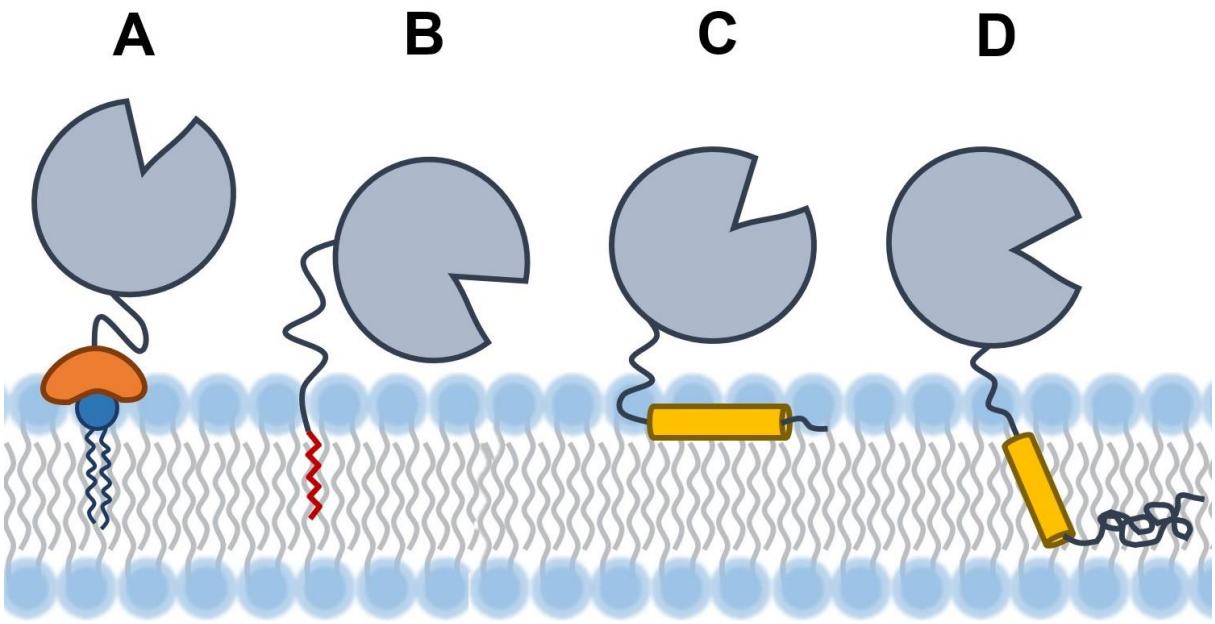

Figure A-2. Models of reversible interactions of membrane proteins.

Several ways that proteins reversibly interact with membrane are shown.[1-2] Membrane binding interaction might displace the regulatory domains form the active site of these proteins. **(A)** Protein is recruited to membrane *via* membrane-targeting domains (shown in *orange*) which bind specific phospholipid head group. **(B)** Protein interacts with membrane through the covalent lipid anchor (shown in *red*) which is inserted into the lipid bilayer. **(C)** Protein binds to membrane via the amphipathic α-helix (shown in *yellow*) which lies parallel to membrane surface. The polar face of the α-helix contacts with aqueous enviroment, whereas the hydrophobic face of the α-helix interacts with hyrophobic region in between the bilayers. **(D)** Protein interacts with membrane by deeply inserting hydrophobic α-helix or hydrophobic loop into the membrane.

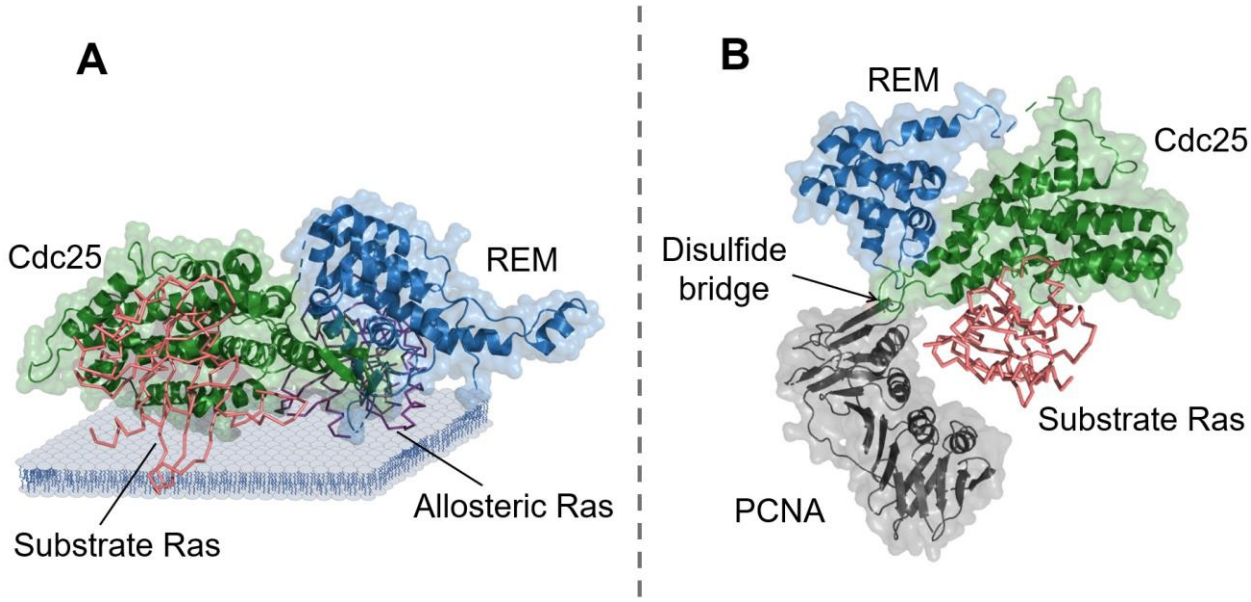

Figure A-3. Ras SOS-binding interaction in the presence of plasma membrane or a protein supporter.

(A) SOS^{cat} activation model associated with membrane (PDB 1XD2). Ras initially docks on membrane. The membrane-anchored Ras then recruits SOS^{cat} (REM-Cdc25 domains) to the membrane by binding to the allosteric site of SOS^{cat}. This colocalization enhances nucleotide exchange of Ras. This is because membrane functions as a supporter or a mechanical fixture that upholds substrate Ras in the active site of SOS^{cat}, so that SOS^{cat} is capable to efficiently catalyze nucleotide exchange of Ras. Without membrane, SOS^{cat} is catalytically unformed. This is because the structure of Cdc25 domain of SOS which possesses a shallow catalytic pocket that cannot sustain the binding interaction of Ras to SOS. In contrast, the membrane-associated SOS^{cat} is catalytically competent because membrane functions to secure the binding of Ras to SOS. REM and Cdc25 domains of SOS^{cat} are, respectively, depicted in *blue* and *green*. Substrate Ras and allosteric Ras are, respectively, shown in *deep salmon* and *purple*.

Figure A-3. Ras SOS-binding interaction in the presence of plasma membrane or a protein supporter. (cont.)

(B) RasGRP1^{cat} activation model with a protein supporter. An engineered RasGRP that connects proliferating cell nuclear antigen (PCNA) with catalytic domain of RasGRP1 (RasGRP1^{cat}) is produced to examine the role of membrane in the nucleotide exchange of Ras. The REM-Cdc25 domains of RasGRP1 (RasGRP1^{cat}) is functionally and sequentially equivalent to the REM-Cdc25 domain of SOS (SOS^{cat}). PCNA (residues 1-255) is chosen as a supporter protein which is equivalent to the membrane in function. PCNA (PDB 6FCM) is shown in *gray*. REM and Cdc25 domains of RasGRP1^{cat} (PDB 4L9M) are, respectively, shown in *blue* and *green*. Substrate Ras (PDB 6AXG) is shown in *deep salmon*. These images were created using PyMOL.

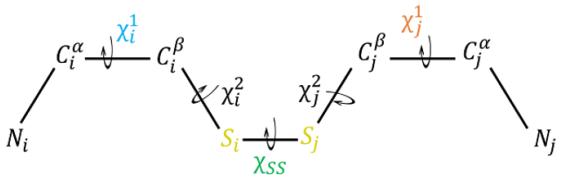

$1.6\ \text{Å} \leq r_{SS} \leq 2.4\ \text{Å}$	and	$60° \leq \lvert\chi_{SS}\rvert \leq 120°$
	AND	
$30° \leq \lvert\chi_i^1\rvert \leq 90°$	or	$150° \leq \lvert\chi_i^1\rvert \leq 180°$
	AND	
$30° \leq \lvert\chi_j^1\rvert \leq 90°$	or	$150° \leq \lvert\chi_j^1\rvert \leq 180°$

Figure A-4. Bond angles and bond lengths of a disulfide bridge between two cysteine residues.

The parameters of the bond angles and bond lengths that are used in determining the acceptability of a particular disulfide bond between two cysteine residues are shown.[3]

i, j: indicate two distinct residues

r_{SS}: S_i–S_j distance

χ_{SS}: dihedral angle C_i^β–S_i–S_j–C_j^β

χ_i^1: dihedral angle $N_i - C_i^\alpha - C_i^\beta - S_i$

χ_j^1: dihedral angle $N_j - C_j^\alpha - C_j^\beta - S_j$

χ_i^2: dihedral angle $C_i^\alpha - C_i^\beta - S_i - S_j$

χ_j^2: dihedral angle $C_j^\alpha - C_j^\beta - S_j - S_i$

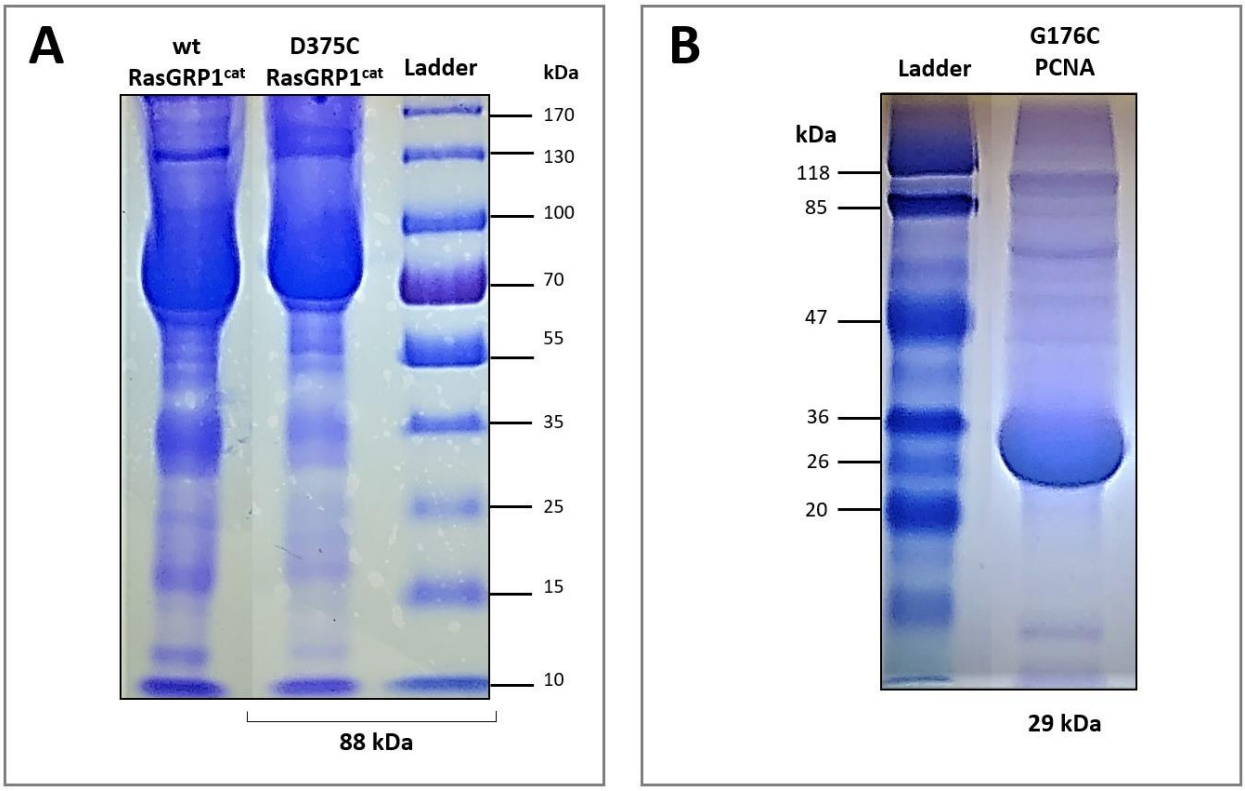

Figure A-5. SDS-PAGE analyses of RasGRP1^{cat} and PCNA.

(A) Qualification of wt RasGRP1^{cat} and D375C RasGRP1^{cat}. Lane 1: Wild type (wt) RasGRP1^{cat}, 88 kDa.; Lane 2: D375C RasGRP1^{cat}, 88 kDa.; and Lane 3: Molecular weight marker. **(B)** Qualification of G176C PCNA. Lane 1: Molecular weight marker; and Lane 2: G176C PCNA, 29 kDa.

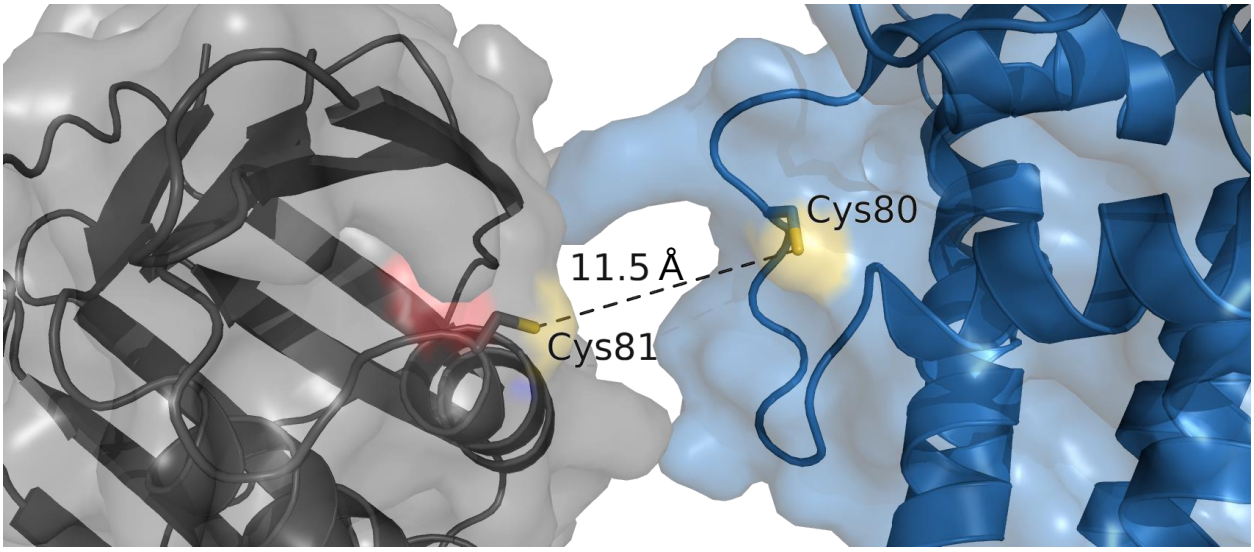

Figure A-6. Identification of free Cysteine residues on the interface between RasGRP1^{cat} and PCNA.

In the crystal structure of RasGRP1^{cat}, one free cysteine residue is exposed to solvent (Cys80). Similarly, PCNA has one free cysteine residue that exposes to the solvent (Cys81). The optimal range to form a disulfide bridge between two cysteine residues is 1.6-2.4 Å (Figure A-4). However, the possible closest distance between the two residues, Cys80 of RasGRP1^{cat} and Cys81 of PCNA, is determined to be ~11.5 Å which is incompatible for the formation of the disulfide bond between them. Therefore, these solvent-exposed free cysteine residues presenting at the interface between these two proteins are unlike to form a disulfide bond. This image is created using PyMOL. The protein structure and surface of PCNA (PDB 6FCM) was shown in *gray*. The protein structure and surface of REM domain of RasGRP1^{cat} (PDB 4L9M) was shown in *blue*. The cysteine residues are shown in *stick*.

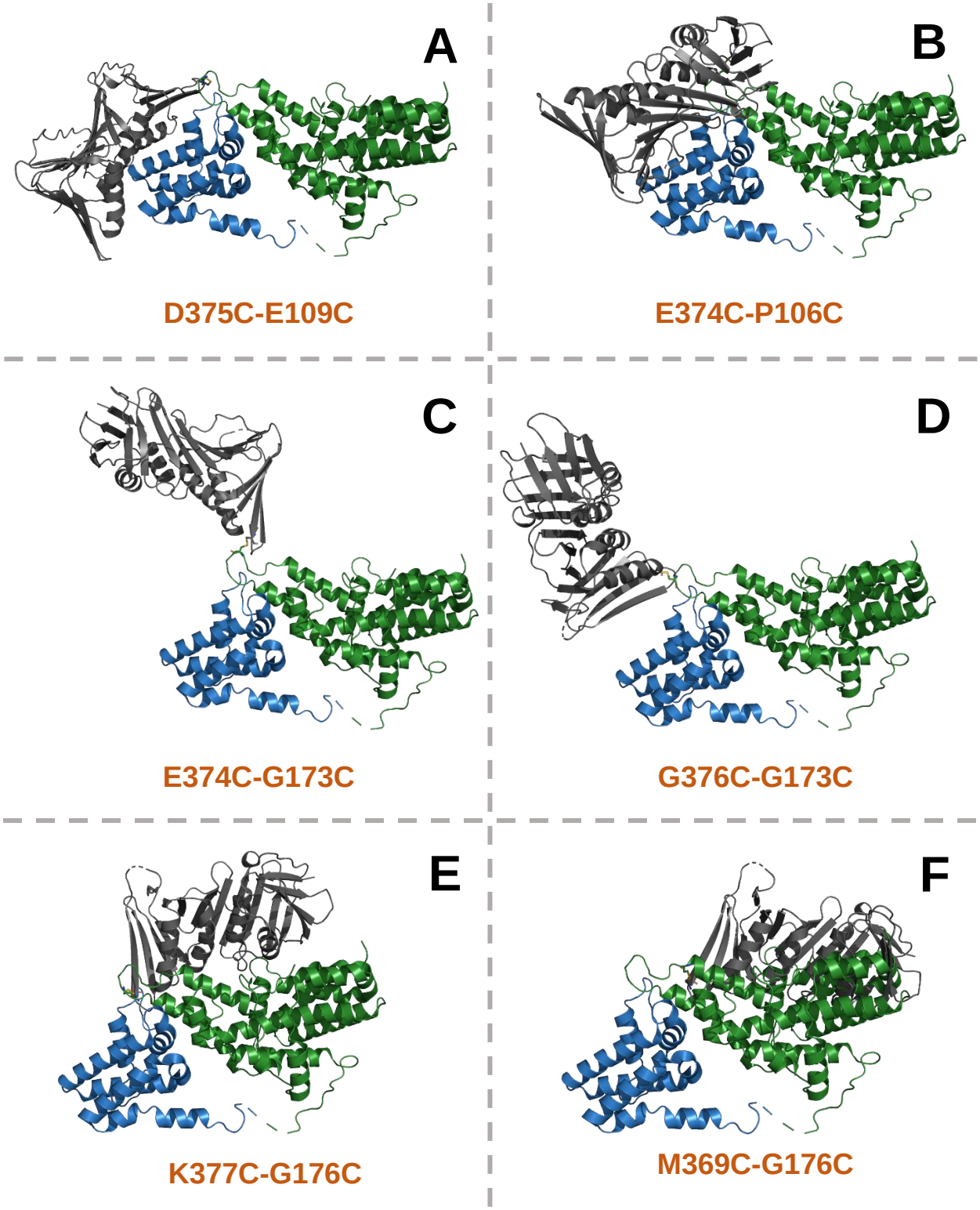

Figure A-7. Examples of representative engineered RasGRPs.

Figure A-7. Examples of representative engineered RasGRPs.

The putaitve engineered RasGRP shown in **(A)**, **(B)**, **(C)**, and **(D)** fail to uphold the substrate Ras within the binding pocket of RasGRP1^{cat} since the PCNA rotates far away from the catalytic site of RasGRP1. The putaitve catalytically engineered RasGRP shown in **(E)** and **(F)** also fail to target the substrate Ras since the binding pocket created in between PCNA and RasGRP1^{cat} are too narrow for the substrate Ras to enter the catalytic site of RasGRP1^{cat}. All images are created using PyMOL. REM and Cdc25 domains of RasGRP1^{cat} (PDB 4L9M) are shown in *blue* and *green*, respectively. PCNA (PDB 6FCM) was shown in *gray*.

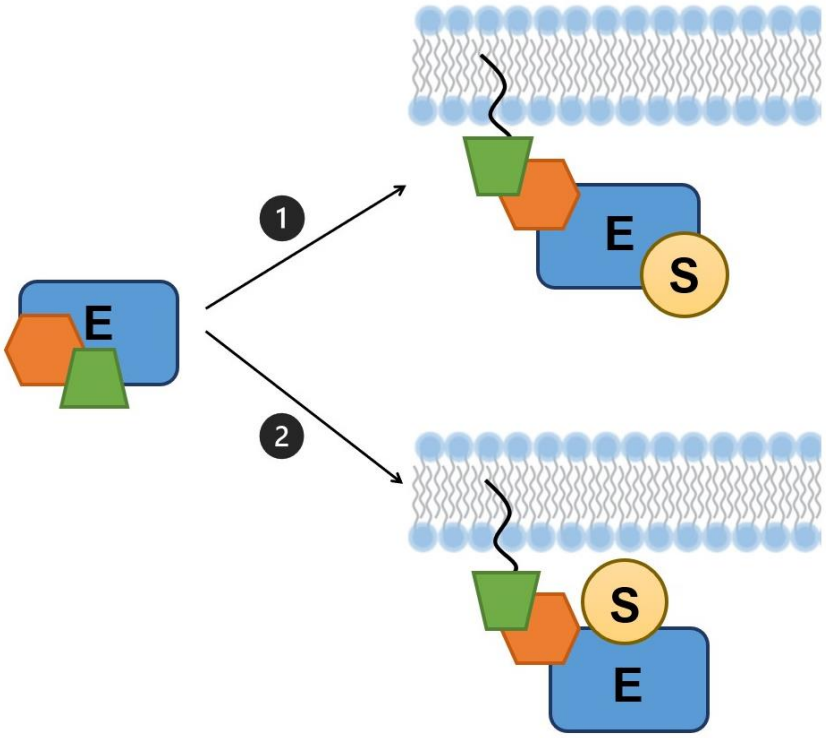

Figure A-8. Potential paths of the activation of amphipathic enzyme with its membrane binding interaction.

Novel model mechanism of the amphipathic enzyme activation with membrane is proposed. Catalytic domain of enzyme (E) was shown in *blue*. Substrate (S) was shown in *yellow*. Regulatory domains were shown in *orange* and *green*. Case 1 (top): enzyme is recruited from cytosol to membrane and undergoes conformational change upon binding to membrane. After the autoinhibition of regulatory domains are released, the active site of enzyme exposes to aqueous environment followed by the binding of substrate. Substrate does not show any interaction with membrane. Case 2 (bottom): Recruitment of amphitropic enzyme to membrane induces a conformational change of enzyme that releases the autoinhibition of regulatory domains. In this case, active site of enzyme is brought close to the membrane surface. Membrane contributes to the stability of substrate by holding the substrate steady inside catalytic pocket of enzyme.

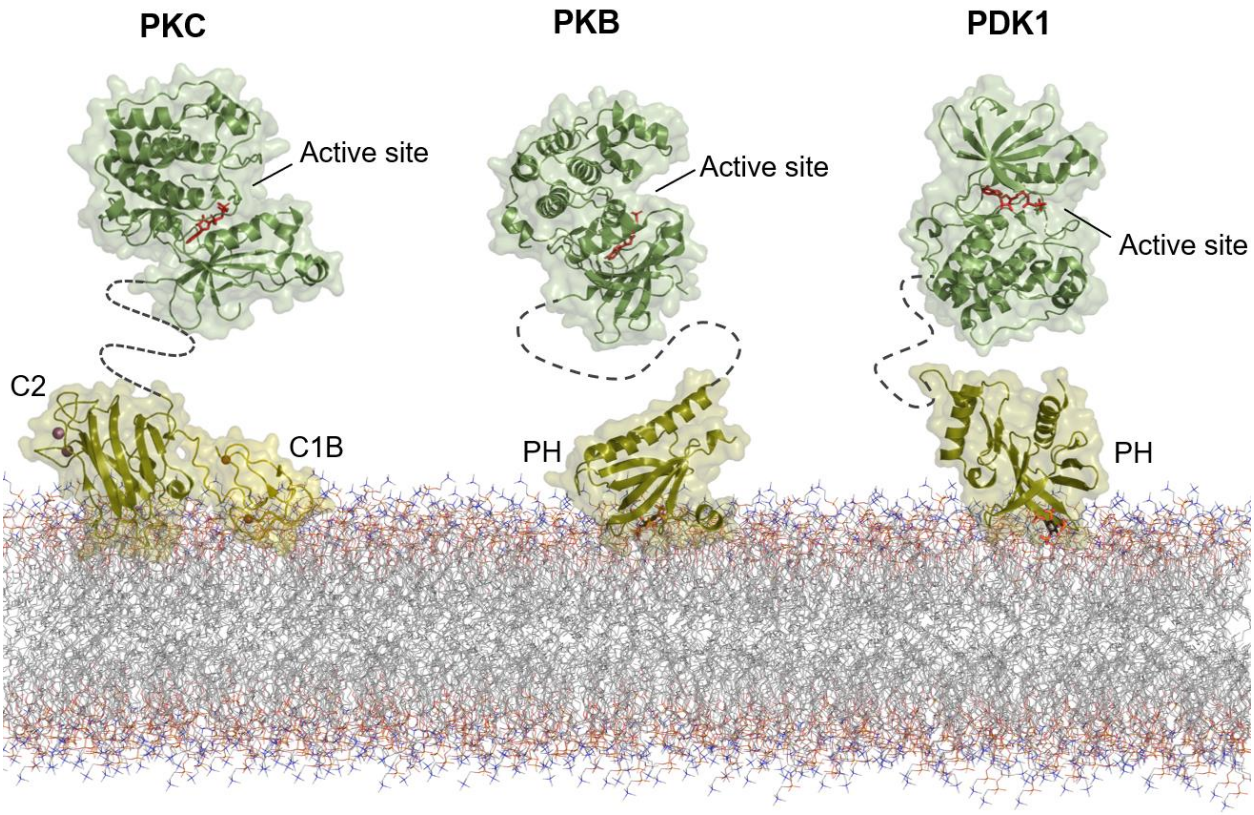

Figure A-9. Activation mechanism of PKC, PKB, and PDK1 by their membrane binding interactions.

Activation mechanism of Protein kinase C (PKC), Protein kinase B (PKB), and 3-phosphoinositide-dependent protein kinase-1 (PDK1) by their binding to membrane are shown.[4-6] PKC (PDB 3PFQ) is recruited to membrane through the electrostatic interaction of C2 domain to membrane followed by hydrophobic interaction of C1B domain. PKB (PDB 1O6L and 1UNQ) and PDK1 (PDB 1H1W and 1W1D) bind to membrane through the interaction of PH domain with PIP_2 on membrane. Their membrane binding interactions displace the autoinhibitory domains that in turn lead to the exposure of their phosphorylation site. The active sites of theses enzymes locate distally toward aqueous environment. Phosphorylation events afterward activate these proteins. In each crystal structure, the kinase domain in which the active site is located

Figure A-9. Activation mechanism of PKC, PKB, and PDK1 by their membrane binding interactions. (cont.)

is highlighted in *green*, and regulatory domain is highlighted in *yellow*. The linker which connects the kinase domain and regulatory domain is shown in *dash line*. This image was created using PyMOL.

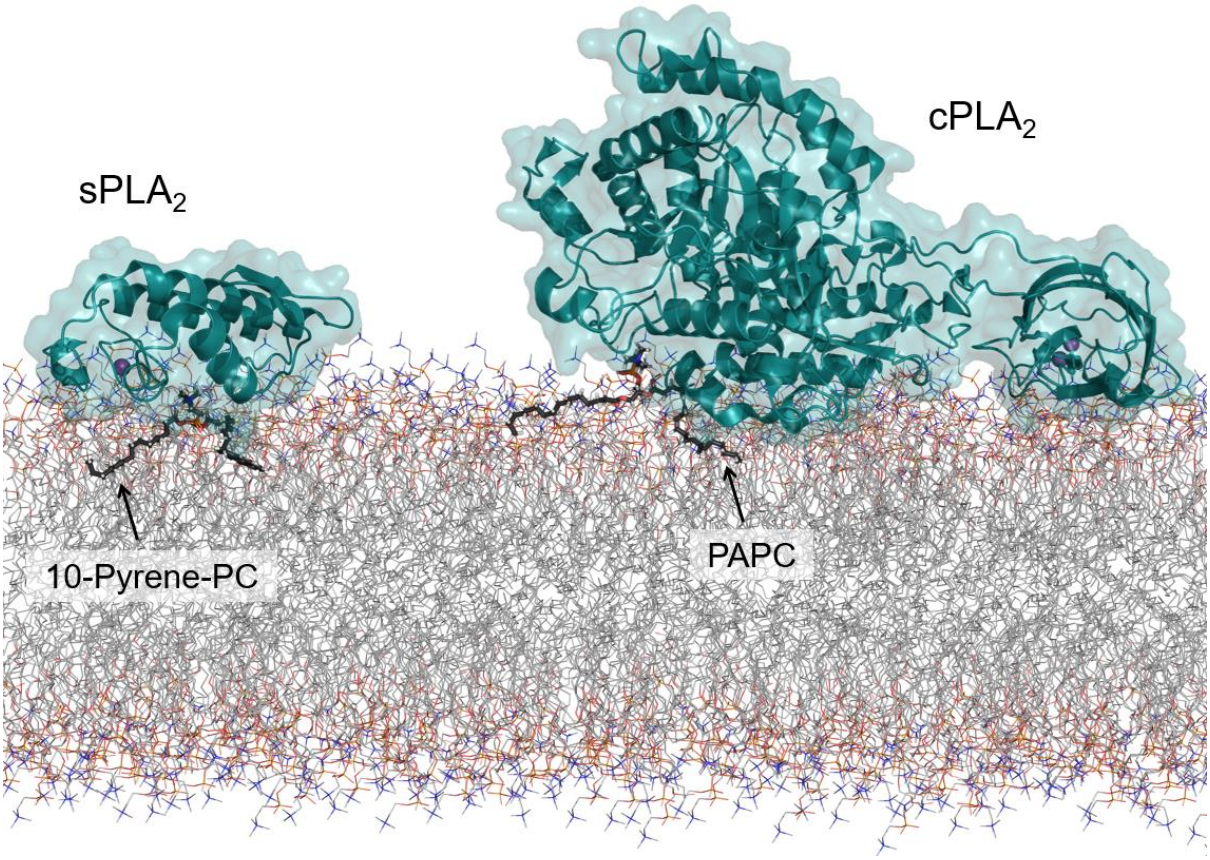

Figure A-10. Activation of $sPLA_2$ and $cPLA_2$ by interaction with phospholipid membrane.

Activation mechanism of secreted phospholipase A_2 ($sPLA_2$) and cytosolic phospholipase A_2 ($cPLA_2$) by their binding to membrane is shown.[7-8] Most extracellular $sPLA_2$s (PDB 1CJY) bind anionic membranes using their cationic residues on the interfacial binding surface. However, aromatic residues such as Trp19, Trp64 and Phe61 at the interface of $sPLA_2$ are involved in the interaction of $sPLA_2$ with zwitterionic membrane. $sPLA_2$ recruited to membrane becomes fully activated. A His-Asp dyad at the catalytic site of $sPLA_2$ hydrolyzes the *sn*-2 position of phospholipid substrate to yield fatty acids and lysophospholipids. In contrast, the binds of calcium to the calcium binding site at the C2 domain of intracellular $cPLA_2$ (PDB 1POB) is responsible for the translocation of $cPLA_2$ to membrane. At membrane, $cPLA_2$ becomes fully activated so

Figure A-10. Activation of $sPLA_2$ and $cPLA_2$ by interaction with phospholipid membrane. (cont.)

that it hydrolyzes the *sn*-2 position of phospholipid substrate using a catalytic dyad of Ser/Asp at the catalytic site. The phospholipid substrate of $sPLA_2$ and cPLA2 are, respectively, 1-Palmitoyl-2-pyrenedecanoyl Phosphatidylcholine (10-Pyrene-PC) and 1-palmitoyl-2-arachidonoyl-sn-phosphatidylcholine (PAPC) (shown in *black stick*). This image was prepared with PyMOL.

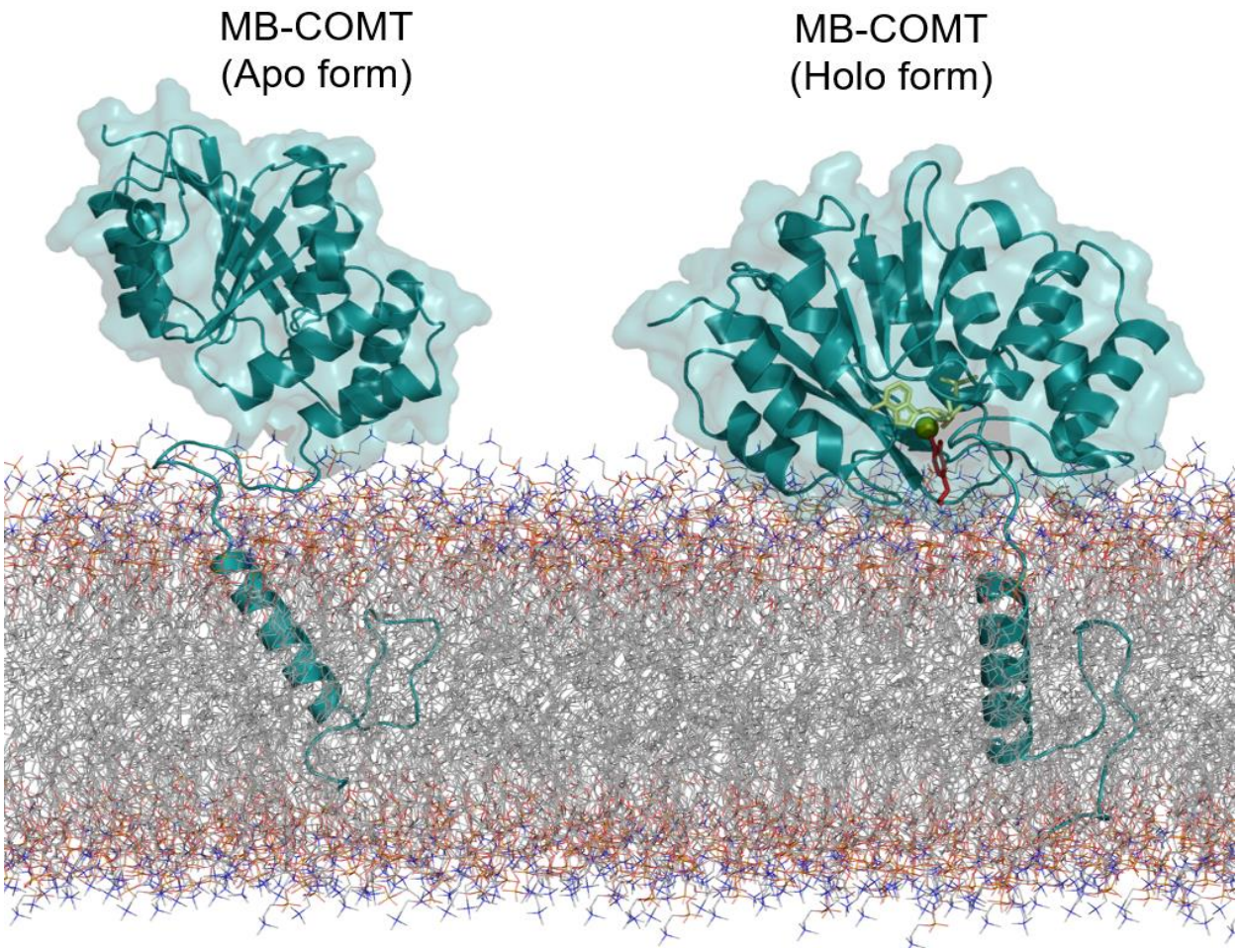

Figure A-11. Activation mechanism of the interaction of catalytic domain of MB-COMT in apo and holo forms with membrane.

Activation of catechol-O-methyltransferase (COMT) by interaction with membrane is shown.[9] Membrane-bound catechol-O-methyltransferase (MB-COMT) (PDB 2CL5) differs from water soluble COMT (S-COMT) in the addition of a 51-residue long segment which anchors to the lipid membrane. The apo form of MB-COMT (left) is unable to bind substrate due to the location of it catalytic site which faces outside of the membrane surface. Binding of the cofactor, S-adenosyl methionine (ADOMET) (shown in *yellow*), induces a conformational change which orients the catalytic site of MB-COMT so that the catalytic site is proximal to the membrane interface. This holo form of

Figure A-11. Activation mechanism of the interaction of catalytic domain of MB-COMT in apo and holo forms with membrane. (cont.)

MB-COMT (right) is now activated and able to bind Mg^{2+} ion (shown in *green sphere*), then interacts with substrate (dopamine shown in r*ed*) at the membrane surface. This image was prepared with PyMOL.

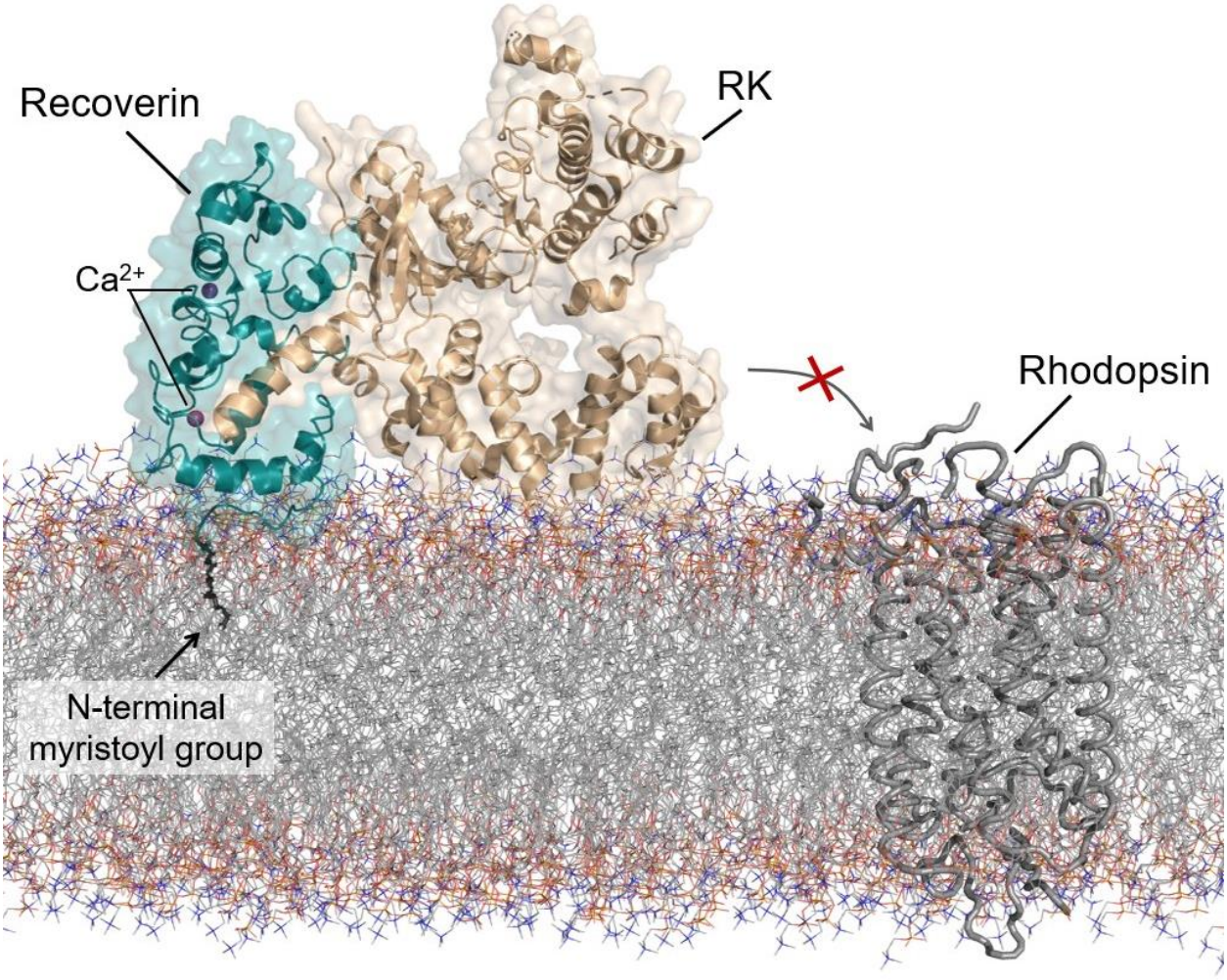

Figure A-12. Activation of Recoverin by its binding to membrane with the increment of Ca^{2+} level.

Novel model mechanism of Recoverin activation upon membrane binding is shown. In the dark, Ca^{2+} binds to recoverin (PDB 1JSA) to trigger a conformational change that exposes the N-terminal myristoyl group to aqueous environment. Recoverin is then able to anchor to membrane through the N-terminal myristoyl group to become active enzyme. At the membrane, the activated recoverin interacts with its substrate, rhodopsin kinase (RK) (PDB 3C51), to prevent RK from activating phosphorylation of rhodopsin (PDB 1F88). This image was prepared with PyMOL.

References

1. Garrett, R.; Grisham, C., Biochemistry, Brooks/Cole, Cengage Learning. **2013**.

2. Devlin, T. M., *Biochemistry: With Clinical Correlations*. Wiley: 2010.

3. Sowdhamini, R.; Srinivasan, N.; Shoichet, B.; Santi, D. V.; Ramakrishnan, C.; Balaram, P., Stereochemical modeling of disulfide bridges. Criteria for introduction into proteins by site-directed mutagenesis. *Protein Engineering, Design and Selection* **1989,** *3* (2), 95-103.

4. Downward, J., Mechanisms and consequences of activation of protein kinase B/Akt. *Current opinion in cell biology* **1998,** *10* (2), 262-267.

5. Oancea, E.; Meyer, T., Protein kinase C as a molecular machine for decoding calcium and diacylglycerol signals. *Cell* **1998,** *95* (3), 307-318.

6. Anderson, K. E.; Coadwell, J.; Stephens, L. R.; Hawkins, P. T., Translocation of PDK-1 to the plasma membrane is important in allowing PDK-1 to activate protein kinase B. *Current Biology* **1998,** *8* (12), 684-691.

7. Lichtenbergova, L.; Yoon, E. T.; Cho, W., Membrane penetration of cytosolic phospholipase A2 is necessary for its interfacial catalysis and arachidonate specificity. *Biochemistry* **1998,** *37* (40), 14128-14136.

8. Sumandea, M.; Das, S.; Sumandea, C.; Cho, W., Roles of aromatic residues in high interfacial activity of Naja naja atra phospholipase A2. *Biochemistry* **1999,** *38* (49), 16290-16297.

9. Magarkar, A.; Parkkila, P.; Viitala, T.; Lajunen, T.; Mobarak, E.; Licari, G.; Cramariuc, O.; Vauthey, E.; Róg, T.; Bunker, A., Membrane bound COMT isoform is an interfacial enzyme: general mechanism and new drug design paradigm. *Chemical Communications* **2018,** *54* (28), 3440-3443.

APPENDIX B: TABLES

		RasGRP1^{cat} - Loop 2										
		M369C (71.5%)	P370C (71.5%)	D371C (56.4%)	Y372C (70.4%)	L373C (80.0%)	E374C (64.3%)	D375C (64.8%)	G376C (55.3%)	K377C (53.2%)	V378C (73.6%)	N379C (73.6%)
PCNA - Loop 1A	E104C (55.2%)											
	A105C (80.0%)											
	P106C (69.7%)											
	N107C (71.7%)											
	Q108C (77.1%)											
	E109C (73.3%)											
	K110C (62.1%)											
PCNA- Loop 1B	G173C (81.3%)											
	E174C (57.2%)											
	L175C (64.5%)											
	G176C (81.3%)											

Table B-1. Analysis of 121 potential pairs of mutation from loop 1 of PCNA and loop 2 of RasGRP1^{cat}.

Table B-1. Analysis of 121 potential pairs of mutation from loop 1 of PCNA and loop 2 of RasGRP1^{cat}.

The *Mutagenesis* function and *Fuse* Command of PyMOL were used to predict which residues on Loop 1A and 1B of PCNA and Loop 2 of RasGRP1^{cat} can be mutated to cysteines. The percentage written under each mutated residue indicates the efficiency of cysteine mutation. For example, *E104C (55.2%)* means there is only 55.2% chance that residue E104 can be mutated to cysteine. For each disulfide bond formed by the mutation pair, PCNA will be rotated to different direction (see examples in Figure A-7). Therefore, the catalytically competent engineered RasGRP model must satisfy two conditions: (1) The χ_{SS} angle of disulfide bond must be in the range 60-120°, and (2) the binding pocket created in between PCNA and RasGRP1^{cat} should be able to hold the substrate Ras within the cavity of RasGRP1^{cat}. Each color code in the table represents different condition of the engineered model of RasGRP1. Cells highlighted in *blue* indicate that these models fail to hold the substrate Ras within the binding pocket of RasGRP1^{cat} since the PCNA rotates far away from the catalytic site of RasGRP1. Cells highlighted in *yellow* indicate that these models fail to bind the substrate Ras since the binding pocket created in between PCNA and RasGRP1^{cat} are too narrow for the substrate Ras to enter the catalytic site of RasGRP1^{cat}. The chosen pair (highlighted in *green*) D375C of RasGRP1^{cat} and G176C of PCNA qualifies for the bond angle of a disulfide bridge and produces a suitable pocket size for the binding of Ras on RasGRP1^{cat}.

APPENDIX C: SUPPLEMENTARY DATA

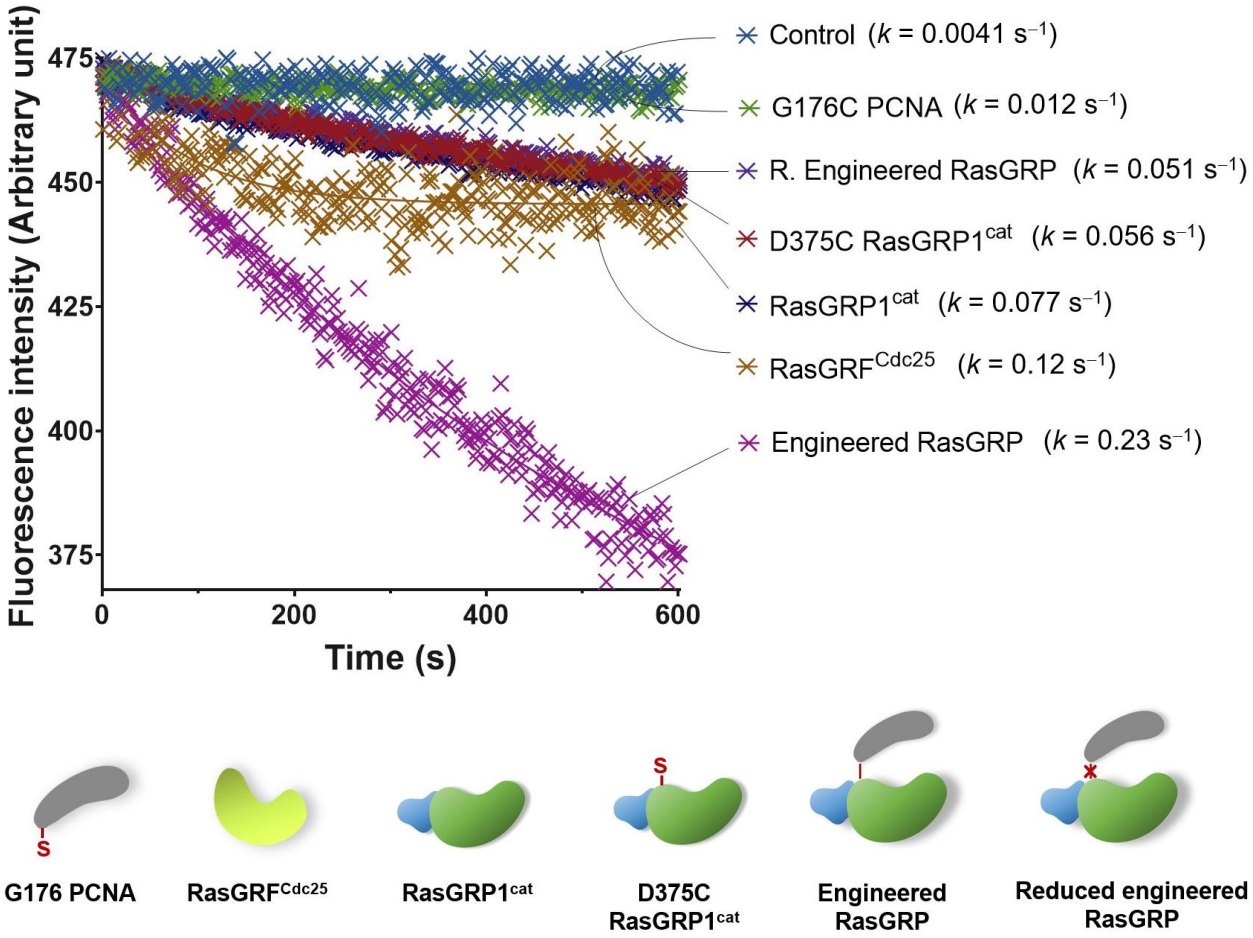

Figure C-1. The rate of GEF-catalyzed nucleotide exchange of Ras.

Mant-GDP-Ras (1.0 μM) was placed in the nucleotide exchange buffer containing excess amount of unlabeled GDP (1.0 mM). In each experiment, a minimal amount of enzyme such as 1.0 μM of G176C PCNA, 1.0 μM of reduced (R) engineered RasGRP, 1.0 μM of catalytic domain of RasGRP1 (RasGRP1^{cat}), 1.0 μM of D375C RasGRP1^{cat}, 1.0 μM of Cdc25 domain of RasGRF (RasGRF^{Cdc25}), or 1.0 μM of engineered RasGRP, was added to facilitate the exchange of mant-GDP with unlabeled GDP. The control experiment data was performed under the identical experimental conditions in the absence of enzyme. Changes in fluorescence intensity were monitored over time at λ_{ex}

of 554 nm and λ_{em} of 580 nm using PerkinElmer LS 55. The initial mant fluorescence changes within the first 150 seconds (*k*) were determined.

The initial rate value of G176C PCNA was not significantly different from the control which represents the intrinsic nucleotide exchange of Ras. This result confirmed that the protein supporter G176C PCNA did not affect the intrinsic the nucleotide exchange of Ras. The similarity of initial rate values of D375C RasGRP1^{cat} and wild type RasGRP1^{cat} proved that the mutant D375C of RasGRP1^{cat} did not affect the catalytic function of RasGRP1^{cat}. The initial rate values of D375C RasGRP1^{cat} in the presence and absence of G176C PCNA were, respectively, 0.056 s^{-1} and 0.051 s^{-1}. The similarity of these values indicated that G176C PCNA did not alter the catalytic function of D375C RasGRP1^{cat}, thereby suggesting that G176C PCNA only functions as a supporter or mechanical fixture that secure the binding of substrate Ras within the catalytic site of RasGRP1^{cat}. The initial rate of RasGRP1^{cat} was also compared with that of RasGRF^{Cdc25} which usually serves as kinetic reference for the catalytic domains of other RasGEF members. The result indicates that catalytic domains of all RasGEFs in general, and RasGRP1^{cat} and RasGRF^{Cdc25} in particular, have relatively weak nucleotide exchange activity in the absence of membrane. The initial rate value of engineered RasGRP^{cat} was significantly higher than that of wild type RasGRP1^{cat}. This comparison showed that RasGRP1^{cat}-catalyzed nucleotide exchange of Ras was enhanced in the presence of the fused PCNA protein that mimicked the plasma membrane.

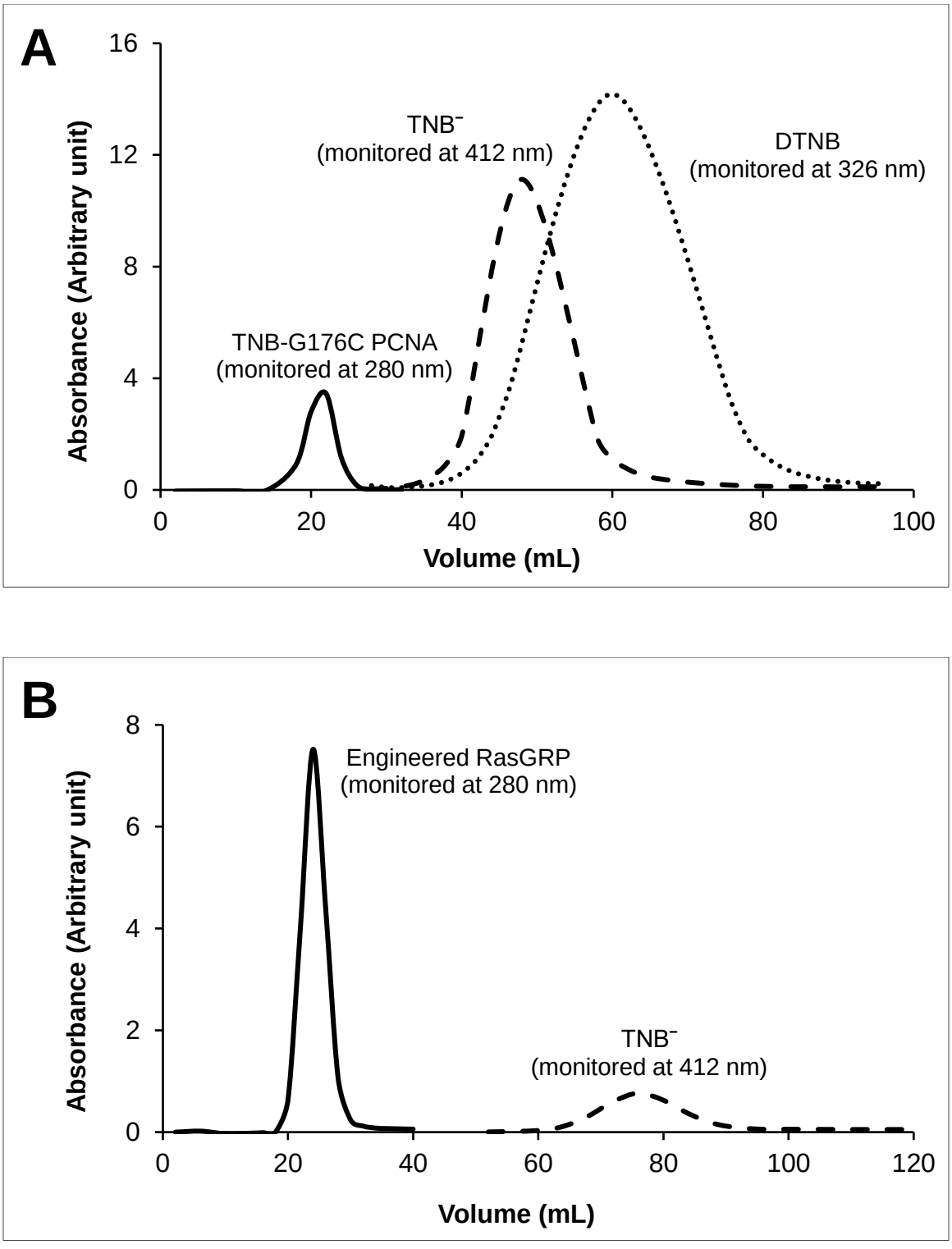

Figure C-2. Elution profile of the preparation of engineered enzyme.

Figure C-2. Elution profile of the preparation of engineered enzyme.

(A) Elution curve of Step 1 (Mechanism on Figure 2.2 above). 5,5'-dithiobis(2-nitrobenzoic acid) (DTNB) reacts with the deprotonated cysteine residue of PCNA G176C to yield a mixed disulfide and 2-nitro-5-thiobenzoic acid (TNB^-). The first peak (in *orange*) depicts the mixed disulfide (PCNA G176C-TNB) whose absorbance is measured at 280 nm. The second peak (in *dark yellow*) represents the TNB^- which is measured at 412 nm. The third peak (in *light yellow*) indicates the remaining DTNB which is detected at 326 nm. The present of the third peak demonstrates that the entire amount of G176C PCNA is completely converted to G176C PCNA -TNB. **(B)** Elution curve of Step 2 (Mechanism on Figure 2.2 above). The intermediate G176C PCNA-TNB in **(A)** is mixed with the deprotonated cysteine residue of $RasGRP1^{cat}$ D375C to yield a mixed disulfide and 2-nitro-5-thiobenzoic acid (TNB^-). The first peak (in *blue*) depicts the mixed disulfide (final product D375C Ras $GRP1^{cat}$- PCNA G176C) which is detected at 280 nm. The second peak (in *dark yellow*) represents the TNB^- which is measured at 412 nm.

Determination of kinetic parameters of RasGRP1^{cat} with Ras

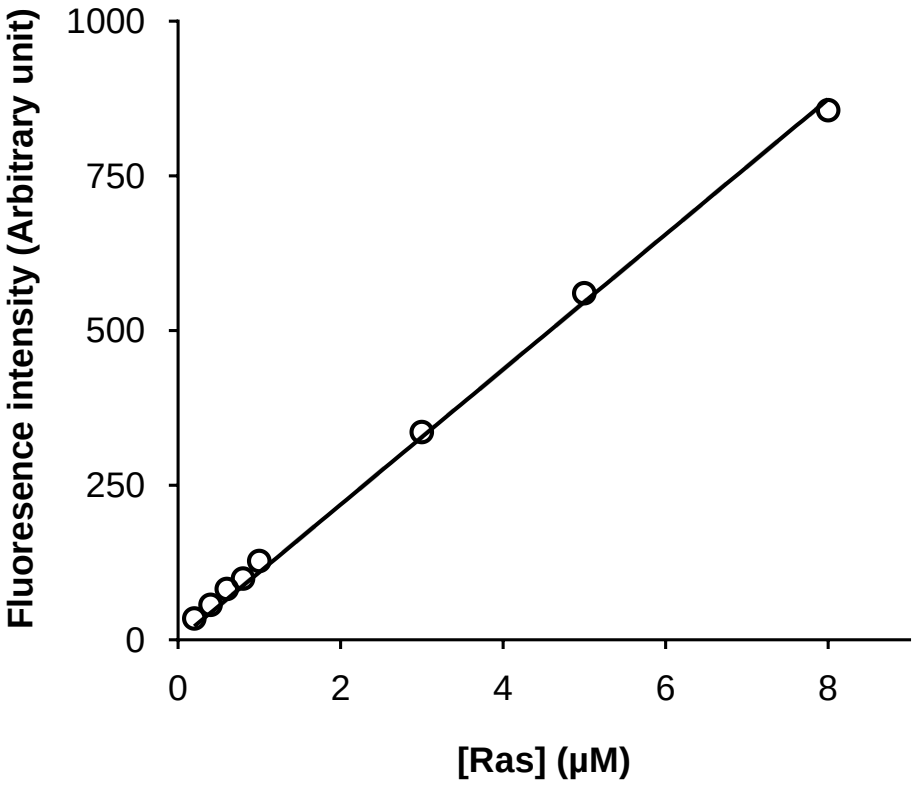

Figure C-3. Blank titration of mant-GDP-Ras in buffer.

Mant fluorescence intensities of various concentrations of Ras (0.2-8.0 μM) in the nucleotide exchange buffer (20 mM Tris-HCl, 50 mM NaCl, and 10 mM $MgCl_2$, pH 7.4) were monitored at λ_{ex} of 554 nm and λ_{em} of 580 nm using PerkinElmer LS 55. The mant fluorescence intensities against Ras concentrations were fit to a linear function (r^2 = 0.9625) to yield a slope of 109.2 μM^{-1}.

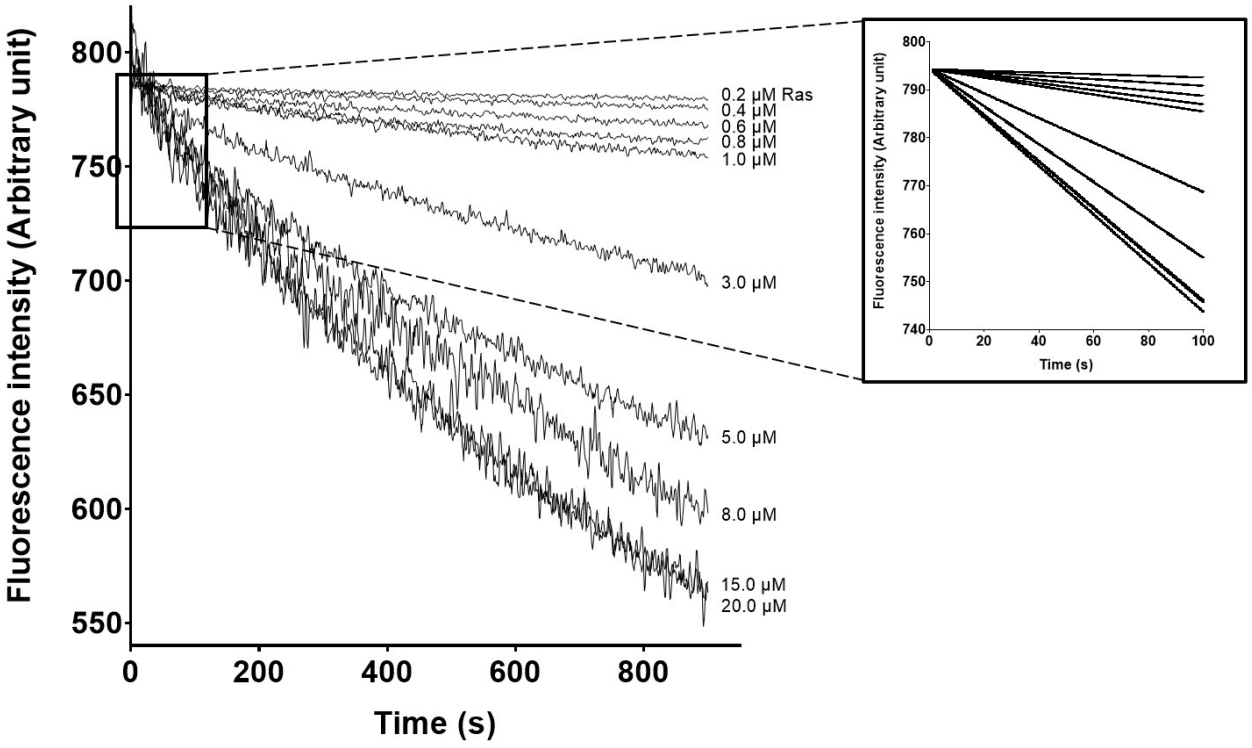

Figure C-4. Change in the mant fluorescence intensity at various concentrations of Ras in the presence of RasGRP1^{cat}.

Mant-GDP-Ras (0.2-20.0 μM) was titrated with 1.0 μM of RasGRP1^{cat} in the nucleotide exchange buffer containing an excess amount of unlabeled GDP (1.0 mM). Inset shows the initial mant fluorescence changes upon the titrations within 100 seconds. The displacement of mant-GDP with unlabeled GDP resulted in the decrease of fluorescence intensity. Changes in fluorescence intensity at each concentration of mant-GDP-Ras added were monitored over time at λ_{ex} of 554 nm and λ_{em} of 580 nm using PerkinElmer LS 55.

Directly proportional relationship between concentration of Ras and the total mant fluorescence intensity change can be expressed as follow:

$$\Delta FL = \alpha \times [Ras]^{ex}, \quad \text{or} \quad [Ras]^{ex} = \Delta FL/\alpha \qquad (1)$$

where ΔFL denotes the total mant fluorescence intensity change; α denotes the slope obtained from Figure C-4; $[Ras]^{ex}$ denotes amount of Ras that undergoes the nucleotide exchange.

Initial rates (ν_0) within the first 100 seconds were calculated by determining the slopes ΔFL/time as shown in Figure C-4 (Inset) and converted to $[Ras]^{ex}$/time as follows:

$$\nu_0 = [Ras]^{ex}/\text{time} = (\Delta FL/\alpha)/\text{time} = \frac{1}{\alpha}(\Delta FL/\text{time}) \quad (2)$$

By dividing initial rate ν_0 with total amount of enzyme used in the assay (denoted as $[E_T]$), the ratio $\nu_0/[E_T]$ was then plotted against concentration of Ras as shown in Figure 2.7. The plot was fitted to a simple hyperbola to obtain Michaelis-Menten constant (K_m), and catalytic turnover rate (k_{cat}) values. The maximum velocity (V_{max}) was calculated using the formula below:

$$k_{cat} = V_{max} / [E_T] \qquad (3)$$

Determination of dissociation constant of RasGRP1^{cat} with Ras

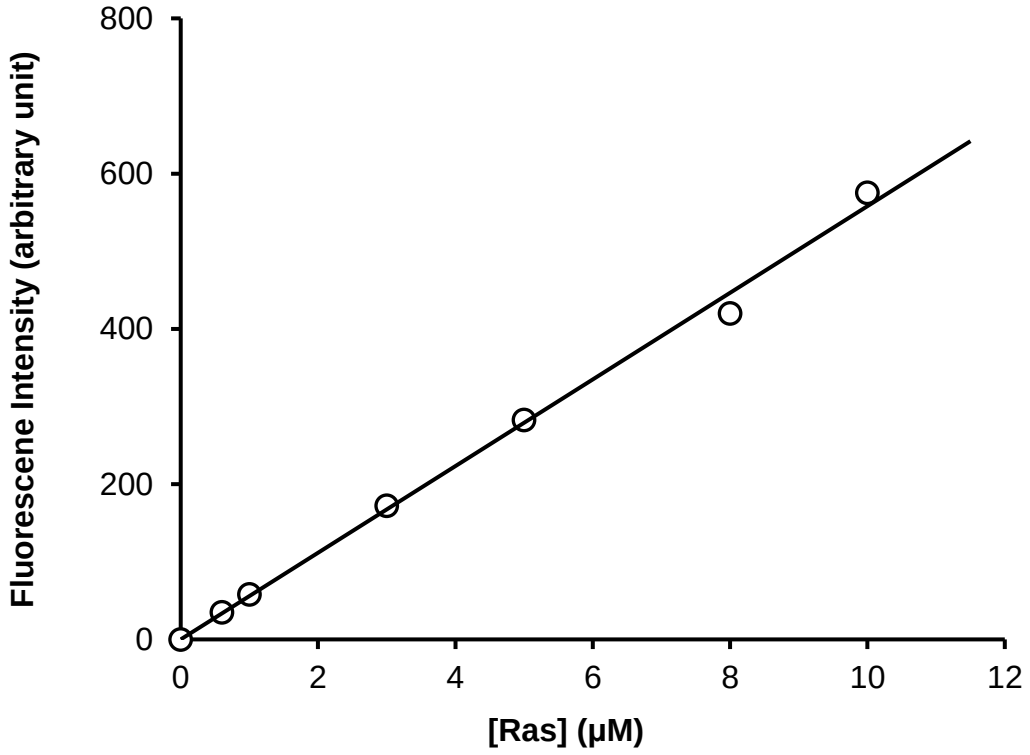

Figure C-5. Blank titration of a buffer with RB-tagged Ras.

A titration of a buffer with various concentrations of Ras (0.6-10 μM) in the Tris buffer (20 mM Tris-HCl and 50 mM NaCl, pH 7.4) was performed to calibrate Rhodamine B (RB) fluorescence intensities with respect to the Ras concentrations. The changes in RB fluorescence intensities against Ras concentrations were fit to a linear function (r^2 = 0.9983) to yield a slope of 55.8 μM^{-1}.

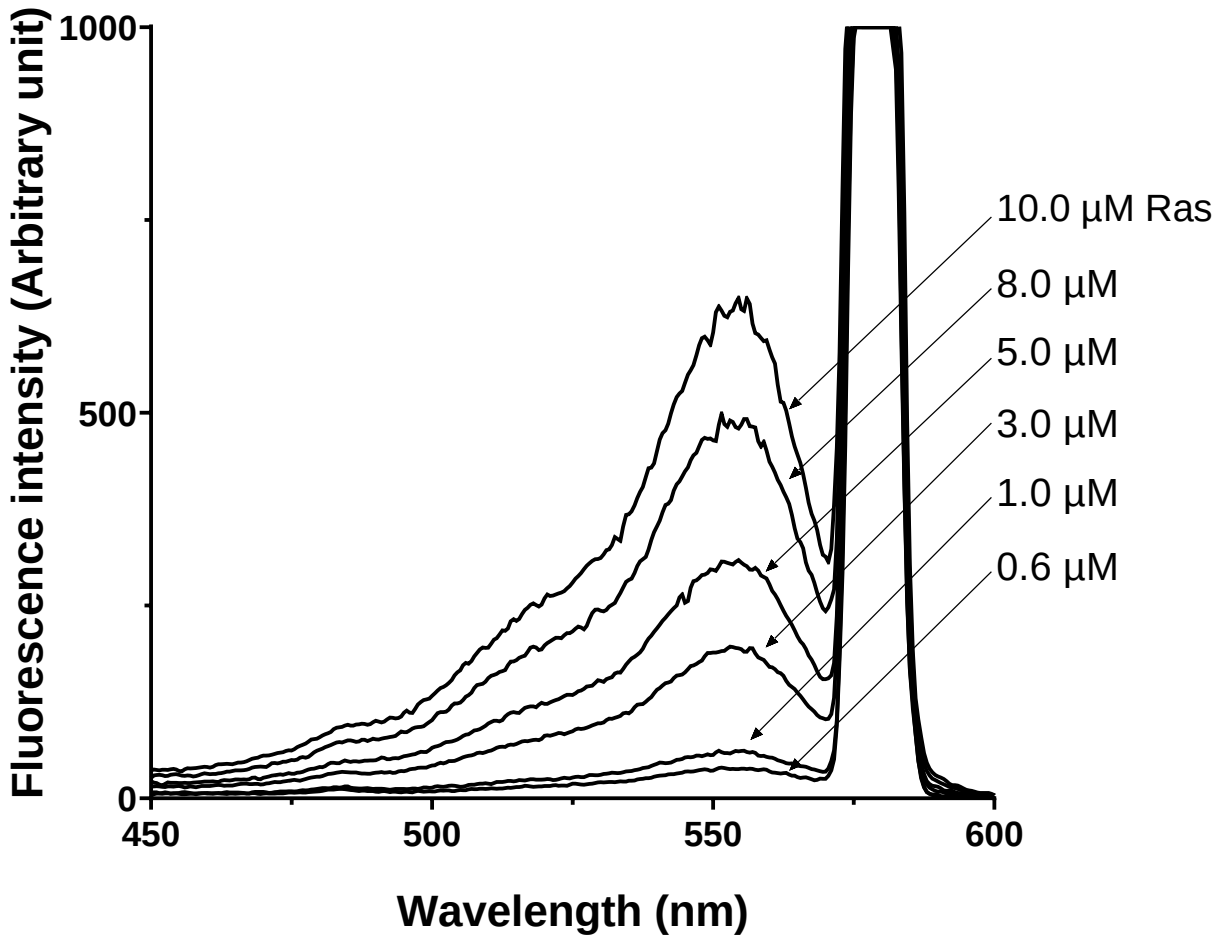

Figure C-6. RB fluorescence-based determination of association constant of the RasGRP1^{cat} for Ras to produce the Ras-RasGRP1^{cat} complex.

RasGRP1^{cat} (1.0 μM) was titrated with various amount of Ras (0.6-10.0 μM). The binding of Ras to RasGRP1^{cat} increases the Rhodamine B (RB) fluorescence intensity.

The increase in fluorescence intensities (∆FL) at 554 nm were determined by subtracting the measured fluorescence intensity of Ras mixed with RasGRP1^{cat} in the Tris buffer for the fluorescence intensity of control which contains only Ras in the Tris buffer. ∆FL at each concentration of Ras was then converted to the ligand bound (Ras:RasGRP1^{cat}) as follow:

Ligand bound (Ras:RasGRP1^{cat}) = $[Ras]_{bound}$ /$[E]_0$= (∆FL/slope)/$[E]_0$ (4)

Where ligand bound denotes the fraction of RasGRP1^{cat} that has Ras in binding site. $[E]_0$ denotes initial concentration of RasGRP1^{cat}.

The plot of Ligand bound (Ras:RasGRP1^{cat}) versus the initial concentration of Ras ([Ras]) was created and fitted to a simple hyperbola as shown in Figure 2.8. K_d, the dissociation constant for the complex, was equal to [Ras] at ½ Ligand bound.

Once the K_m, K_D, and k_{cat} were determined, the two constants k_1 and k_{-1} were calculated as follow:

$$K_m - K_D = \frac{k_{-1}+k_{cat}}{k_1} - \frac{k_{-1}}{k_1} = \frac{k_{cat}}{k_1} \quad (5)$$

$$K_D = \frac{k_{-1}}{k_1} \quad (6)$$